SENSITIVITY ANALYSIS OF 2-D FLOOD INUNDATION MODEL LISFLOOD-FP WITH RESPECT TO SPATIAL RESOLUTION AND ROUGHNESS PARAMETER

A THESIS SUBMITTED TO
THE GRADUATE SCHOOL OF NATURAL AND APPLIED SCIENCES
OF
MIDDLE EAST TECHNICAL UNIVERSITY

BY

EZGI KIYICI

IN PARTIAL FULFILLMENT OF THE REQUIREMENTS
FOR
THE DEGREE OF MASTER OF SCIENCE
IN
CIVIL ENGINEERING

APRIL 2019

Approval of the thesis:

SENSITIVITY ANALYSIS OF 2-D FLOOD INUNDATION MODEL LISFLOOD-FP WITH RESPECT TO SPATIAL RESOLUTION AND ROUGHNESS PARAMETER

submitted by **EZGI KIYICI** in partial fulfillment of the requirements for the degree of **Master of Science in Civil Engineering Department, Middle East Technical University** by,

Prof. Dr. Halil Kalıpçılar
Dean, Graduate School of **Natural and Applied Sciences** _____

Prof. Dr. Ahmet Türer
Head of Department, **Civil Engineering** _____

Prof. Dr. Sevda Zuhal Akyürek
Supervisor, **Civil Engineering, METU** _____

Examining Committee Members:

Prof. Dr. İsmail Yücel
Civil Engineering Dept, METU _____

Prof. Dr. Sevda Zuhal Akyürek
Civil Engineering, METU _____

Prof. Dr. Zafer Bozkuş
Civil Engineering Dept, METU _____

Assoc. Prof. Dr. Yakup Darama
Civil Engineering Dept, Atılım University _____

Dr. Müsteyde Baduna Koçyiğit
Civil Engineering Dept, Gazi University _____

Date: 25.04.2019

I hereby declare that all information in this document has been obtained and presented in accordance with academic rules and ethical conduct. I also declare that, as required by these rules and conduct, I have fully cited and referenced all material and results that are not original to this work.

Name, Surname: Ezgi Kıyıcı

Signature:

ABSTRACT

SENSITIVITY ANALYSIS OF 2-D FLOOD INUNDATION MODEL LISFLOOD-FP WITH RESPECT TO SPATIAL RESOLUTION AND ROUGHNESS PARAMETER

Kıyıcı, Ezgi
Master of Science, Civil Engineering
Supervisor: Prof. Dr. Sevda Zuhal Akyürek

April 2019, 130 pages

One of the most common disasters in the world is flooding and it's well known that it causes environmental, social and economic damages. Since these damages could be severe and destructive due to drivers such as climate change and humane factors, the necessity of flood management studies is revealed. Europe has recognized the need for creating flood risk maps and flood hazard maps. 1-D and 2-D hydraulic models have been used to obtain these maps.

This study is focused on the sensitivity of a 2-D hydraulic model, LISFLOOD-FP which uses simplified shallow water equations assuming convective acceleration term as negligible. The study area Terme City, which is located in the Middle Black Sea Region of Turkey was exposed to a storm event on July 2012 and the river water level reached the top of the levees. With the help of the available data, the effect of neglected convective acceleration term in hydraulic model is investigated in a benchmarking study where MIKE21 and LISFLOOD-FP hydraulic models are used. The results show that LISFLOOD-FP (Acceleration and Subgrid Channel Solver) is affected by spatial resolution in terms of the representation of flood propagation and computation time. In addition, roughness coefficient can be used to calibrate the model to obtain

better results. It's obtained that Subgrid Channel Solver gives better results compared to Acceleration Solver even for coarse resolutions since it allows the use of fine resolutions to define the channel, so that eliminates the negative effects of resampling, to a coarse resolution.

Keywords: LISFLOOD-FP, Subgrid Solver, Acceleration Solver, Flood Inundation, Shallow Water Equations

ÖZ

2-B BİR HİDROLİK MODEL OLAN LISFLOOD-FP'NİN MEKANSAL ÇÖZÜNÜRLÜĞE VE PÜRÜZLÜLÜK PARAMETRESİNE GÖRE DUYARLILIK ANALİZİ

Kıyıcı, Ezgi
Yüksek Lisans, İnşaat Mühendisliği
Tez Danışmanı: Prof. Dr. Sevda Zuhal Akyürek

Nisan 2019, 130 sayfa

Dünyadaki en yaygın doğal felaketlerden biri sel baskınlarıdır ve iyi bilindiği üzere çevresel, sosyal ve ekonomik zararlara sebep olmaktadır. Bu zararlar iklim değişikliği, beşeri faktörler gibi sebeplerden dolayı yıkıcı ve şiddetli olabileceğinden taşkın yönetimi gerekliliği ortaya çıkmıştır. Bu nedenle Avrupa, taşkın risk haritaları ve taşkın tehlike haritaları oluşturma ihtiyacını kabul etmiştir. Bu haritaları elde etmek için 1-Boyutlu ve 2-Boyutlu hidrolik modeller kullanılmaktadır.

Bu çalışma, basitleştirilmiş sığ su denklemlerini konvektif ivme terimini ihmal edilebilir varsayarak kullanan 2-Boyutlu bir hidrolik model olan LISFLOOD-FP'nin duyarlılığı üzerine odaklanmıştır. Türkiye'nin Orta Karadeniz Bölgesinde yer alan Terme Şehri çalışma sahası Temmuz 2012'de kuvvetli bir yağışa maruz kalmış ve nehir su seviyesi su setlerinin en üst seviyesine ulaşmıştır. Mevcut verilerin yardımıyla ihmal edilen konvektif ivme teriminin hidrolik modeldeki etkisi MIKE21 ve LISFLOOD-FP hidrolik modellerini kullanarak yapılan bir kıyaslama çalışmasıyla araştırılmıştır. Sonuçlar LISFLOOD-FP'nin (Acceleration Çözücüsü ve Subgrid Kanal Çözücüsü) taşkın yayılımının temsili ve hesaplama süresi açısından mekansal çözünürlükten etkilendiğini göstermektedir. Ayrıca, pürüzlülük katsayısı daha iyi

sonuçlar elde etmek için modeli kalibre etmede kullanılabilir. Subgrid Kanal Çözücü, kanalı tanımlamak için detay çözünürlüklerin kullanımına izin verdiği ve böylece kaba çözünürlüklere yeniden örneklemenin negatif etkilerini bertaraf ettiği için, kaba çözünürlüklerde bile Acceleration Çözücüsü'ne kıyasla daha iyi sonuçlar verdiği belirlenmiştir.

Anahtar Kelimeler: LISFLOOD-FP, Subgrid Çözücü, Acceleration Çözücü, Sel Baskını, Sığ Su Denklemleri

To My Family…

ACKNOWLEDGMENTS

I would like to express my deepest gratitude to my supervisor Prof. Dr. Sevda Zuhal Akyürek for her patient guidance and precious advices throughout the research.

I would like to thank my family for their endless support, love and understanding.

I would also like to thank my friends/colleagues Anıl Yıldırım Poyraz, Hacer Ocak, Şeyda Orhan, Ebru Seyfi, Tuba Gürgen and Giancarlo Dugatto for their support and motivation.

I owe thanks to DSI 7th Regional Directorate for providing the data I need to carry out this study.

TABLE OF CONTENTS

APPENDICES

LIST OF TABLES

TABLES

LIST OF FIGURES

FIGURES

CHAPTER 1

INTRODUCTION

1.1. Problem Statement

Floods are the most common natural disasters causing economic, environmental and social losses in all around the world. In Europe, river floods are considered as one of the most important natural disasters (De Moel et al., 2009).

Hall et al. (2014) stated that, Europe has experienced a series of major floods in the past years: extreme floods in central Europe in August 2002 (Ulbrich et al., 2003) and in England in 2007 summer (Marsh, 2008), unprecedented flash flooding in western Italy in 2011 autumn (Amponsah et al., 2014), and subsequently, extreme floods in central Europe in June 2013 (Blöschl et al., 2013). These and many other floods which exceeded past recorded levels in the last decade, caused a growing concern on flooding which has become more frequent and severe in Europe.

In Turkey, there is also an increase in the flash floods. According to "Natural Disasters with Meteorological Characteristic 2016 Evaluation Report" published by General Directorate of Meteorology (2017), China being in the first place, Macedonia, Germany and Pakistan were exposed to flash flood disasters which caused human loss and economical damages over the world in 2016. In the same report, the statistical data provided by General Directorate of Meteorology (2017) showed that, there have been a dramatic increase in flood disasters since 2000 for Turkey. In the last decade, almost over 50 flood events occurred. Şahin et al. (2013) listed some destructive floods occurred in recent years as follows: in Ankara, (25-26 August 1982), Trabzon (18-20 June 1990), Eastern Anatolia (16-17 May 1991), İzmir (4 November 1995), Western

Black Sea (21 May 1998), Hatay (28 May 1998), Batman (2 November 2006), and Antalya (9 October 2011).

Another report published by General Directorate of Meteorology (2018) pointed out that; among the observed meteorological disasters, precipitation/flood disasters were placed in the first lines with storms and hail events in 2017. In the last year, natural disasters due to severe meteorological events have been seen frequently in Marmara Region, the coastal zones of Aegean Region and Mediterranean Region and in the north and interior parts of Turkey.

There are two main reasons of flood occurring. The first reason is the abrupt and intense precipitation in urban areas which occurs quite often in recent years. These kinds of floods have an unregulated and destructive characteristic. The second reason is the river floods which take place because of the increasing water amount by snow melting in the streambed surpluses. Except from these, floods may occur because of spill of reservoirs or from coastal surges and high tides. Human factors also play a role for turning precipitation and snow melting into natural disasters by settling onto valleys and valley bottoms, destruction of vegetation, changing direction of the stream beds etc. Additional to these drivers, climate change is also a trigger for flood events. There is a general global augmentation on precipitation frequency due to climate change.

As a result of increase in flood frequency, flood forecasting and its effective control have gained more importance. Flood risk management came into prominence to reduce social, economic and environmental consequences of flood disasters especially in urban areas.

Socio-economic relevance of river flood studies has increased and this increase brought along the development of complex methodologies for the simulation of the hydraulic behavior of river systems and resulted in the development of different

innovative techniques. Detailed hydrological models are developed to parameterize the whole river basin by using both remote sensing materials and manually collected data.

In the last decade, there has been a remarkable advancement on computer-based flood inundation models as a response to the demand of improved flood forecasts. In flood plain mapping and flood risk assessment, one dimensional (1-D) and two dimensional (2-D) hydraulic models have been used.

Due to the insufficient data on fine scales, the use of two-dimensional flood modeling was limited especially in urban areas which requires 1 to 5 m grid resolution for flood propagation due to the representation of topographical features. Advancements in modern topographic digital data collection methods enabled the application of studies on two dimensional (2-D) hydraulic models. In the last decade, applicability of numerical models representing the complexities of shallow water equations is analyzed on a whole range of complicated urban problems (Hunter et al., 2008).

It is important to make reliable predictions since flood inundation models play an important role in flood forecasting. As a traditional method, direct observations of flooding from remote sources are used to validate the hydraulic models. However, in case of deficiency in this kind of gauged data, it is important to know about model sensitivity to obtain accurate results by using hydraulic model parameters.

1.2. Scope of the Study

The aim of this study is to analyze the use of simple inertial formulation of the shallow water equations in 2-D flood inundation modeling by neglecting the convective acceleration term. The sensitivity of the hydraulic model according to roughness parameter and spatial resolution of digital elevation model by using two different approaches to solve an inundation problem, is performed. While first approach applies

the calibration parameter (the roughness value) to whole domain as boundary conditions, second approach enables to separate the floodplain and the channel to solve the flood hydraulics. Thus, it is intended to obtain detailed information about the effects of these parameters on the solution to evaluate more accurate results. The comparison is done by using models –MIKE21 where full momentum equation is solved during modeling and LISFLOOD-FP where the convective acceleration is considered negligible in the solution of shallow water equations. The sensitivity of two-dimensional hydraulic model LISFLOOD-FP in relation to hydraulic parameters such as roughness coefficient and spatial resolution of the DEM is performed to see how these parameters affect the model outputs such as flood extent and water depth, besides whether these parameters can be used as calibration parameters.

The present study consists of six chapters. Chapter 1 introduces the research and describes the content of the study. Chapter 2 contains the literature inquiry. Chapter 3 presents methodology and the hydraulic model used in the study. Chapter 4 provides the analysis including benchmark and sensitivity analysis. Finally, Chapter 5 presents the discussion of the results and conclusions.

CHAPTER 2

LITERATURE REVIEW

The increasing possibility of flood frequency as a result of altered precipitation regime which is caused by climate change creates a demand for advanced flood inundation modeling thus more data. This is quite important for detecting inconsistencies between observations and predictions and for more reliable flood forecasting systems. For the last few decades, there has been a major improvement in flood inundation modeling and acquiring data. The researches have been substantially directed to the consequences of floods and the solutions to reduce the damages of floods.

De Moel et al. (2009) suggested a risk-based approach for flood management and stated that the European Parliament also adopted a new Flood Directive (2007/60/EC) on 23 October 2007 emphasizing the necessity to create flood hazard and risk maps for flood risk assessment. This research also indicated the importance of distinguishing these two general types of maps. It was specified that the flood hazard maps contain information about the probability and/or magnitude of an event yet risk maps contain additional information about the consequences such as economic damage, number of people affected.

In 2-D hydraulic modeling, it is quite important to make better predictions and making better predictions requires calibration. Horritt and Bates, (2001) stated that, the integration of hydrometric and flood extent data has been shown to be useful for discriminating the flood inundation models. For unconstrained parameters, the optimal parameters may be different for models calibrated against hydrometric data

and inundation data according to the adopted calibration methodology. Another complication which weakens the model's predictive power is the optimal parameter sets that may be differ from one flood event to another. Particularly, it is unclear that a parameter set calibrated against data from an event with a certain magnitude is valid for a more extreme event.

Fewtrell et al. (2008) stated that for urban flood modeling, the most common approach is calibrating friction parameters due to the observed data with a 2-D hydraulic model at high resolutions (Haider et al., 2003; Tarrant et al., 2005; Mignot et al., 2006). In many cases, obtained model friction values are higher than empirically derived values. Because, the friction factor is attempting to parameterize friction both on the sides of the flow besides bottom friction and incorporate the head loss associated with flow around structures. Fewtrell et al. (2008) suggested to set any value of friction parameter according to the model instead of empirically derived values because friction parameters tend to depend on model and scale together. Fewtrell et al. (2008), also claimed that in rural applications, the influence of the floodplain friction values is well understood. However, in urban areas the relevance of friction parameter and urban environments for different scales is less clear and it has been explored by Yu and Lane (2006) using a 2-D diffusive wave model.

The studies conducted for small areas with the use of floodplain solver of LISFLOOD-FP and the effects of spatial resolution and roughness coefficient of the model were investigated. Some of these researches are presented below and in a summary is given in Table 2-1.

Hunter et al. (2005) made a study on adaptive time step use in 2-D hydraulic models by adapting it to shallow water equations. Besides the effect of Δt, they also investigated the roughness coefficient and grid size influence on the outputs. They chose a 2,0X3,0 km^2 region of unvegetated beach from the Wrangle Flats area of The Wash, a large tidal embayment on the eastern coast of the UK, for simulation. For the

digital elevation models, four coarse resolutions were used (Δx=25, 50, 100, 200 m) and roughness parameters were taken between the range of 0,02-0,10 with 0,02 intervals. The results showed that, for every roughness value the lowest root mean square error (RMSE) was obtained for 25 m grid resolution.

Fewtrell et al. (2008) applied LISFLOOD-FP which uses an analytical flow equation calculating 1-D kinematic wave equation for channel flow that is linked to a 2-D representation of floodplain flows to a flooding scenario affecting a ≈0,5 km^2 area of Greenfield, a suburb of Glasgow, UK. To determine the effect of scale, Δx=2 m DEM was used to create coarser resolutions as Δx= 4, 8 and 16 m. A uniform roughness coefficient, n=0,035 was chosen as benchmark solution to test the sensitivity due to friction parameter and the simulations ran by altering this parameter between 0,01 to 0,10. The hydrograph they used had a peak discharge of Q_p≈10 m^3/s. Predicted water depths compared to the benchmark solution and the lowest RMSE was obtained for Δx= 4 m grid size. Regarding to the flood extents, the highest F-statistic value was calculated for Δx= 4 m. They also compared the time series of water depth predictions at four characteristic locations and the results showed that LISFLOOD-FP made better predictions in the models up to 8 m and model performance got worse for resolutions above these thresholds. In addition, the under/over estimations on these characteristic locations on the coarse resolution Δx= 16 m were explained. They claimed these estimations likely to stem from the blockages on the flow paths, overestimation of the building sizes and reduced definition of road network due to resampling procedures. As a consequence, they found out that the response surface to changes in the roughness coefficient across different scales was stationary with respect to changes in model resolution which reinforced the findings of Yu and Lane (2006). They also noted that what Yu and Lane (2006) suggested within the scope of spatially distributed friction parameters, recognizing the nature of friction values make possible to increase the dimensionality of any calibration or sensitivity analysis problem.

Table 2-1 Studies carried out with LISFLOOD-FP

Name of the article	Authors	Study Area (km^2)	Grid Size	Roughness
An adaptive time step resolution for raster-based storage cell modeling of floodplain inundation	Neil M. Hunter, Matthew S. Horrit, Paul D. Bates, Matthew D. Wilson, Micha G.F. Werner	2.0X3.0	25 m,50 m, 100 m, 200 m	0.02, 0.04, 0.06, 0.08, 0.1
Evaluating the effect of scale in flood inundation modeling in urban environments	T.j. Fewtrell, P.D. Bates, M. Horrit, N. M. Hunter	0.5	4 m,8 m,16 m	0.01 - 0.10
A simple inertial formulation of the shallow water equations for efficient two-dimensional flood inundation modeling	Paul D. Bates, Matthew S. Horrit, Timothy J. Fewtrell	1.0X0.4	5 m,10 m,25 m,50 m,100 m,200 m	0.01-0.09 with 0.03 increments
A subgrid channel model for simulating river hydraulics and floodplain inundation over large and data sparse areas	Jeffrey Neal, Guy Schumann and Paul Bates	800 km stretch of river	905 m	0.025-0.05
Low-cost inundation modeling at the reach scale with sparse data in the Lower Damodar River basin, India	Joy Sanyal, Patrice Carbonneau and Alexandre L. Densmore	110 km channel reach	3 m,4 m,8 m,16 m	0.024-0.038 for channel 0.03-0.038 for the floodplain
Testing the skill of numerical hydraulic modeling to simulate spatiotemporal flooding patterns in the Logone floodplain, Cameroon	Alfonzo Fernandez, Mohammad Reza Najafi, Michael Durand, Bryan G. Mark, Mark Moritz, Hahn Chul Jung, Jeffrey Neal, Apoorva Shasty, Sarah Laborde, Sui Chian Phang	8000	250 m, 500 m, 1000 m	0.10 for floodplaim 0.025 for channel roughness
Quantifying the importance of spatial resolution and other factors through global sensitivity analysis of a flood inundation model	James Thomas Steven Savage, Francesca Pianosi, Paul Bates, Jim Freer, and Thorsten Wagener	2000	10 m, 20 m, 30 m, 40 m, 50 m	0.025-0.04 for channel 0.025-0.05 for the floodplain
Calibration of channel depth and friction parameters in the Lisflood-Fp hydraulic model using medium-resolution SAR data and identifiability techniques	Melissa Wood, Renaud Hostache, Jeffrey Neal, Thorsten Wagener, Laura Giustarini, Marco Chini, Giovani Corato, Patrick Matgen, Paul Bates	30.5X52.4	75 m	0.015-0.1 for channel 0.06 for entire domain

Bates et al. (2010) used 1,0X0,4 km^2 domain in the Greenfields area of Glasgow, UK to compare the adaptive time step diffusive model with the adaptive time step inertial model which was developed hereafter. They chose this area because there had been an observed flood in response to heavy rainfall in the small upstream catchment. To test the sensitivity against grid resolution Δx=5, 10, 25, 100 and 200 m DEMs were selected for identical simulations using both inertial and diffusive models. The inflow hydrograph given to the system had $Q_p \approx 10$ m^3/s peak discharge. As a result, they found out that while inertial solver is giving better results for Δx=50, 100 and 200 m, diffusive solver gave better results for Δx=5, 10 and 25 m grid resolutions. Using constant roughness coefficient n=0,03, Δx=25 m grid resolution gave the lowest RMSE. Also, altering the roughness coefficient between 0,01-0,09 with 0,03 increments made no significant effect on RMSE.

Following these studies, channel flow solvers of LISFLOOD-FP were used for the solution of inundation problems of large areas. The accuracy of the model was investigated by setting different roughness coefficients and spatial resolutions to floodplain and channel separately. Some of these studies are mentioned below:

Sanyal et al. (2014) compared TELEMAC-2D model and LISFLOOD-FP in their study. Lower Damodar Basin which suffers from chronic flooding in India was selected as study site. Three types of satellite images were used for calibration and validation of the flood inundation models. As LISFLOOD-FP input, a raster with a uniform 8 m grid size was used. To prepare the observed data and calibration, the images belonging to flood events were employed. Two different roughness coefficients were set for the channel and floodplain after consulting the published typical roughness values from Chow (1959). The calibration was run for the roughness values n=0,024-0,03 for the channel and n=0,030-0,038 for the floodplain. They claimed that while the TELEMAC-2D performed best with value of n=0,037 for the channel, LISFLOOD-FP did not show much sensitivity to the n values in the context of improving accuracy in comparison with observed flood extent.

Fernández et al. (2016), made a study in an annually flooded site, the Logone floodplain which is a part of the Lake Chad Basin and covers approximately 8000 km^2 in the Far North Region of Cameroon. For LISFLOOD-FP simulations the topographical data was derived from an original 90 m SRTM resolution as 250 m, 500 m and 1000 m spatial resolution. The optimal values for the floodplain and channel roughness values were set separately as 0,10 and 0,025 respectively due to the calibration of the model based on flow discharge at Logone Gana. For benchmarking study with the observational data, different versions of simulations were run by setting spatial resolution to 1000 m and roughness coefficient between the range of 0,08-0,14. Afterwards, RMSE was calculated and the obtained values showed that the model was not very sensitive to roughness parameter. They also claimed that varying grid cell resolution for the model from 250 m to 1000 m did not make a significant change in the outputs but resulted in very small differences between simulated flood volume, discharge and flooded area.

Savage et al. (2016) performed their study in Imera basin in Sicily, which covers an area of approximately 2000 km^2. The available data for Southern region of the basin was taken from a flood event including a 2 m DEM obtained from LIDAR covering an area of 50 km^2 and the hydrograph of the event was obtained. The study focused on model predictions and behavior rather than performance against observed data. Although models could be run at finer resolution, since the given domain was predominantly rural, they found unnecessary to resolve the length scales finer than 10 m, so that 10, 20, 30, 40 and 50 m spatial resolutions were set for digital elevation models. They noted that the previous studies applied on LISFLOOD-FP for this site performed reasonably well at resolutions up to 50 m where the flood observations were compared (Horritt and Bates, 2001; Aronica et al., 2002; Savage et al., 2016). The chosen approach for roughness coefficient was spatially disaggregating into two values for floodplain and channel separately. Thus, the plausible ranges for friction parameters were chosen as n= 0,025-0,040 for the channel and 0,025-0,050 for floodplain. Consequently, they found that spatial resolution and DEM were not

influential on their own on flood extent for their magnitude of event. Also, it is stated that the choice of spatial resolution and DEM were quite important for local scale predictions of water depth. They noted that, the spatial and temporal variability of the model's sensitivity to each of these factors, except for floodplain friction, reflects the complexity of predicting water depths. So that, they suggested to use a finer resolution if decision maker was interested in local-scale inundation predictions. As for the friction parameter, they found that the boundary conditions and channel friction were more influential than floodplain friction taking into account comparing predictions of water depth against observed data. While evaluating spatially distributed predictions of water depth, a modeler therefore should consider the uncertainty when degrading topographic data to coarser resolutions.

Wood et al. (2016) carried out their study on a 30,5X52,4 km^2 area of Tewkesbury (UK), which is located at the junction of the Rivers Severn and Avon. The study stated that calibration of the hydraulic models is quite essential to obtain accurate results and emphasized that recent studies were considerably focused on calibration studies. Therefore, the study is determined to calibrate the channel roughness and depth simultaneously and is broadened to estimate channel friction and geometry parameters by using medium resolution SAR data. For the hydraulic model 150 m ENVISAT SAR-derived flood extent maps were used. The width of the river was set as constant along the reach and the depth of the tributaries was assumed insignificant on flooding. Two different LISFLOOD-FP models which had 75 m spatial resolution were used. The same inflows were performed to the same rectangular shaped channels. The first model was created as "observed" model to specify the channel width and depth with a fixed roughness parameter (n=0,038). The second model was created as "test" model which includes the determination of the depth parameter and channel roughness parameter. Roughness parameter was altered in the range of n=0,015-0,10 for the channel and for the entire domain it was set to n=0,060. Manning values were assumed spatially and temporarily invariant for both the channel and floodplain. The results showed that the observed model gave the best estimate of domain-average channel

roughness parameter even though the test model had 1000 parameters having various depth and roughness values. Consequently, Wood et al. (2016) found out that the channel roughness was less sensitive to the variations in flood extent and failed to locate a representative value for this parameter especially when the depth parameter was also varied. However, keeping roughness parameter in a plausible range it was possible to advance the calibration method and a better estimate of the depth parameter.

Neal et al. (2012) conducted their study on a 800 km stretch of the river Niger Inland Delta in Mali by using the Subgrid Channel Solver of LISFLOOD-FP. Since the available SRTM DEM had a ground resolution of approximately 90 m over the test site and the computational cost increased in fine resolutions, a DEM of 905 m resolution was used. A total of 588 simulations were run for each model by setting the roughness coefficient in a range of 0,025-0,05 with 0,005 sampling interval. The optimal subgrid model runtime was 106 min on a quad core 2.8 GHz Intel E5462 processor. They concluded that including subgrid channels on the floodplain altered inundation patterns over the delta and increased model accuracy in terms of water level simulation, wave propagation speed and inundation extent.

Özdemir et al. (2018) conducted their study in the urban area of Alcester (Warwickshire, UK) with a 10 cm resolution DEM generated from LIDAR data and it was stated that despite the advancements in river and coastal flooding studies, the researches on the progress of the methods to accurately model and mitigate the consequences of the flood inundation and its dynamics were still in the beginning phase. The prevention and mitigation of urban flooding have been limited in scope and strongly depended on the sewerage system. Also, the effect of topography on the urban flooding was underestimated. Relatively high flow depths occurred in large parts of the urban areas as a result of heavy rainfall mostly caused by accumulation of the water previously routed from the urban catchment along the roads and other flow paths. This kind of surface flow is a phenomenon of shallow water which can move at

relatively high velocities. Özdemir et al. (2018) conducted 4 different scenarios involving small topographical changes on a DEM which had a submeter scale with 2 different discharge values to show the influence of topography on shallow water modeling. As a consequence, he found out even small changes in topography may alter the flood inundation contrastingly. The results prove that the model is highly sensitive to this kind of changes especially in fine scales. Therefore, it would be beneficial to consider the influence of even small changes in topography for future flood mitigation studies.

Flood modeling studies in Turkey are conducted by the General Directorate of Water Management where most of them are carried out by tendering. Small scale modeling is conducted by using some flood modeling indices. For the sites showing high vulnerability, hydraulic modeling is performed. Flood risk management plans for the basins have been done by creating flood risk maps and flood hazard maps by hydrological and hydraulic modeling (1-D and 2-D) in the context of EU Flood Directive. Yeşilırmak and Antalya basins flood management plans are completed. Sakarya, Susurluk, Ceyhan, West Blacksea, Euphrates-Tigris, East Mediterranean and Kızılırmak basins flood management studies are ongoing by the time this study is conducted (Ministry of Agriculture of Forestry General Directorate of Water Management).

Some 1-D and 2-D flood modeling studies have been done in Turkey. A flood event occurred in Ayamama River (İstanbul, Turkey) in 2009 because of intensive rainfall and dam-breaching of Ata Pond. 1-D and 2-D flood model studies were conducted for this region. For Ata Pond breaching, both HEC-RAS and LISFLOOD-FP-Roe were used as hydraulic models and results were compared with the real flood extent (Özdemir et al., 2013). The benchmark results showed that LISFLOOD-FP-Roe model which resolves 2-D shallow water equations using Saint Venant formulation gave more than 80% fit to the real event.

Another study was conducted on Ürkmez Dam break using HEC-RAS to represent the dam break and FLO-2D for wave propagation model (Haltaş et al., 2013). Since the physical model of the study was also constructed, a comparison study was made between the results of numerical and physical models. The 25 m grid size numerical model results were compatible with the physical model results. Despite the representation of 25 m grid size DEM of the numeric model, physical model could not represent the area with sufficient resolution. Therefore, a combination of the physical and numerical model was suggested for the optimum solution.

Nimaev (2015) made a hypothetical study on a small area in Terme town, Samsun. In that study it was aimed to present the effect of spatial resolution of DEM in shallow water solutions with 25 cm, 50 cm and 1 m digital elevation models which were obtained from LIDAR data. The study contained an analysis of floodplain solvers in LISFLOOD-FP, a benchmark study with LISFLOOD-FP-Acceleration Solver and MIKE21 hydrodynamic model and a sensitivity analysis with respect to roughness and spatial resolution. Uniform Manning's roughness coefficient of n=0,035 was used in all models and a discharge of Q=0,50 m^3/s was given to the system. The results showed that both the diffusive and acceleration solvers gave similar results. But Roe solver made an over estimation in flooded areas by almost 35% compared to Acceleration solver. As for the benchmark study between LISFLOOD-FP and MIKE21 flood models, MIKE21 predicted the inundated area almost 10% more than LISFLOOD-FP. Sensitivity analysis in terms of spatial resolution was carried out with n=0,013 representing asphalt conditions with DEM having 25 cm, 50 cm, 1 m spatial resolutions. The results showed that increasing the resolution enabled and improved representation of the topography. The effect of roughness parameter was investigated for a 25 cm model resolution, where the roughness coefficient was set to four values as 0,013-0,025-0,030-0,035. The results indicated that smaller roughness coefficients caused varying water depths due to more rapid propagation flow and higher velocities at control points. As for the flood extent, the difference between the models were determined as negligible.

Bozoğlu (2015) also conducted a study in the Terme District of Samsun City. Some of the outputs and evaluations of that study are used as input for the current study. Bozoğlu (2015) investigated the flooding problem in Terme District and discussed the upstream solutions by using a 1-D and 2-D hydraulic model MIKE (MIKE11 and MIKE21). He calculated the peak discharge hydrographs with the help of the data obtained from gauging stations. 2-D simulations of MIKE21 were run with different scenarios including/excluding the flows coming from the four sub basins in the upstream part of the river while considering the contribution of a dam and control structures. As a result, the possible upstream solutions for the flooding problem in this area were presented according to the scenarios conducted in the study area.

CHAPTER 3

METHODOLOGY

In this part of the study, the hydraulic model and the analyses performed were presented.

First of all, the accuracy of the LISFLOOD-FP model is evaluated by benchmarking with previous studies. To make this comparison, flood extent of MIKE21 simulation result obtained from a previous study is used as base map (Bozoğlu, 2015). The aim is to find consistent results with LISFLOOD-FP by considering spatial resolution and roughness coefficient. Secondly, benchmarking simulation of LISFLOOD-FP which gives the convenient outputs with MIKE21 is selected as base map in attempt to investigate the effect of changing spatial resolution and roughness coefficient to understand if these parameters can be used for model calibration. RMSE and F-statistic values of water depth and flood extent are used as statistical measures.

MIKE 21 is a commercial hydraulic model which is used for flood modeling in all over the world. The modeling system of MIKE 21 bases on the numerical solution of the two/three dimensional incompressible Reynolds Averaged Navier-Stokes equations subject to the assumption of Boussinesq and hydrostatic pressure. LISFLOOD-FP is a raster-based hydraulic model which can simultaneously simulate 1-D river and 2-D overland hydrodynamics while using the 1-D Saint Venant and 2-D shallow water equations neglecting convective acceleration term. LISFLOOD-FP is chosen since it is not a commercial software and it is aimed to explore capabilities in 2-D flood modeling. The reason to use these two hydraulic models is to understand

the effects of neglecting convective acceleration term while solving the flood hydraulics.

3.1. Study Site

For this study, Samsun Terme City is chosen due to the availability of data.

Location of Terme City is in the Middle Black Sea Region of Turkey between about 40°32′- 40º41′ North and 29º29′- 30º08′ East. The river named "Terme" passes through the city center by dividing the city into two parts. The study site contains the Terme River and its four tributaries extending from Black Sea to the Salıpazarı Bridge (Figure 3-1).

Terme City Center was exposed to a storm created approximately 510 m^3/s peak flood discharge, resulting water level reach in the river to the top of the levees in July 2012. According to the hydrological report (11.07.2012) of DSI 7^{th} Regional Directorate, this discharge almost equals to 6-year return period of flood discharge. The hydrologic model studies performed in this area by 7^{th} Regional Directorate showed that higher return periods could cause a flood disaster in Terme City. Based on this information, studies carried on to understand the flow characteristics of the sub-basins for the upstream part including the effect of meanders and ongoing dam project (Bozoğlu, 2015). With the contribution of these previous study results, this study aims to investigate the sensitivity of a hydraulic model LISFLOOD-FP (two-dimensional hydraulic model) by changing roughness coefficient and spatial resolution and show the effects on flood extent considering the upstream tributaries of Terme River.

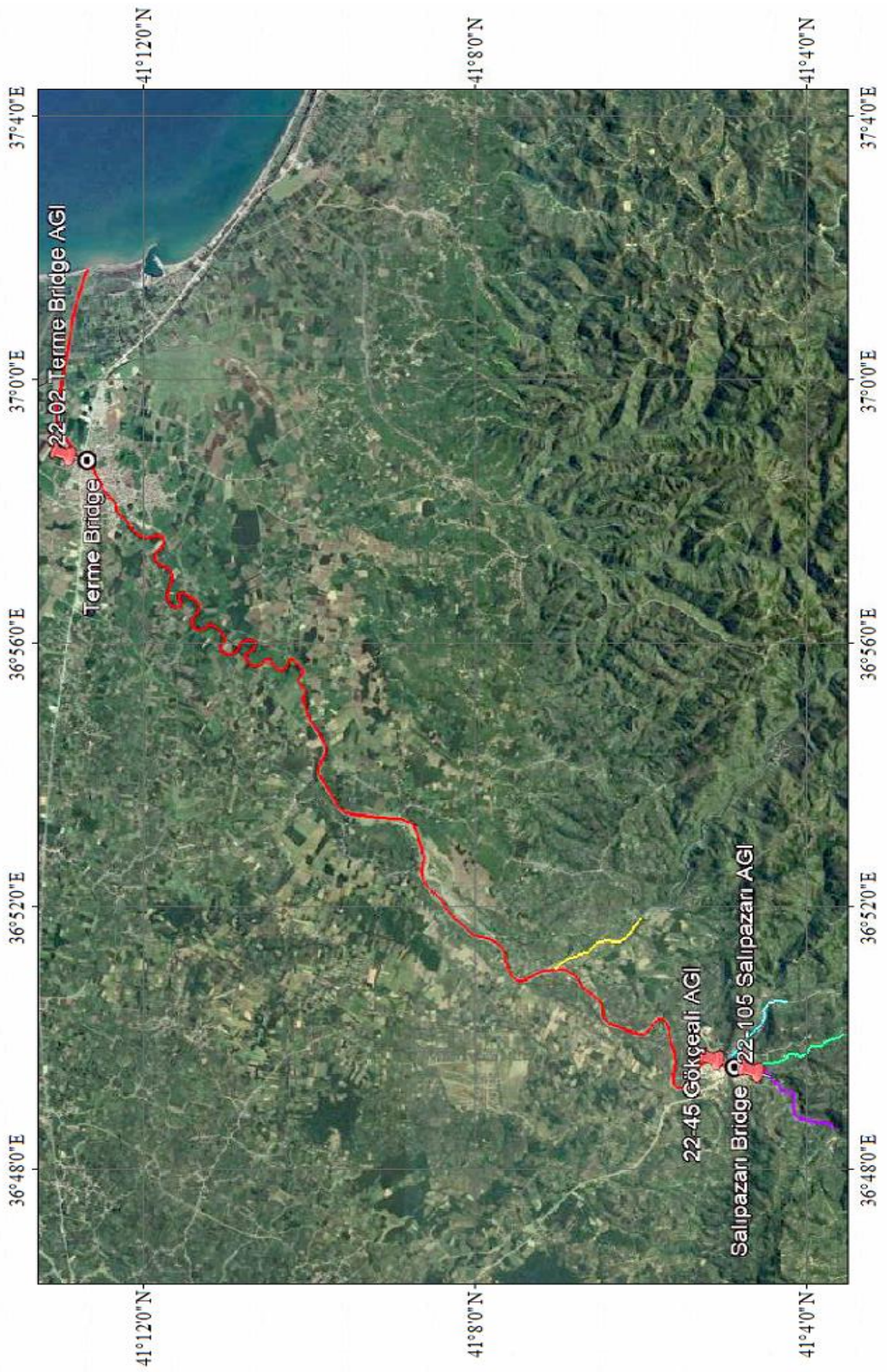

Figure 3-1 Project Area

3.2. Project Data and Software

Topographic data collection is a crucial part of hydraulic modeling. The digital elevation data was acquired from associated governmental organization, DSI 7th Regional Directorate, and from previous studies. Study area is composed of the river and its four tributaries.

Two types of digital elevation model are used in this study. The first one, used as base map for benchmark study, is obtained from Bozoğlu (2015). It is composed of the point data obtained from 1/5000 scaled orthophotographs and 1/1000 scaled elevation values of the x-sections obtained at the site. The DEM area starts from Salıpazarı Bridge and extends to Black Sea and has 5 m spatial resolution (Figure 3-2).

The second digital elevation model having 1/1000 scale is obtained from DSI 7th Regional Directorate. The DEM consists of river bathymetry data measured with tachometer and grid size of the elevation point data is resampled to 1 m. DEM contains the tributaries of the Terme River which are located at upstream part of Salıpazarı Bridge and also the area nearby Terme Bridge. This DEM is used as base to create rasters/layers with different spatial resolutions (Figure 3-3).

In this study, to solve the flood hydraulics LISFLOOD-FP (two-dimensional) hydraulic model; for resampling of the digital elevation models and further data analyses, ArcGIS software of Environmental Systems Research Institute (ESRI) and for performing LISFLOOD-FP simulations Intel(R) Xeon(R) CPU X5650-2.67 GHz (2 processors) computer are used.

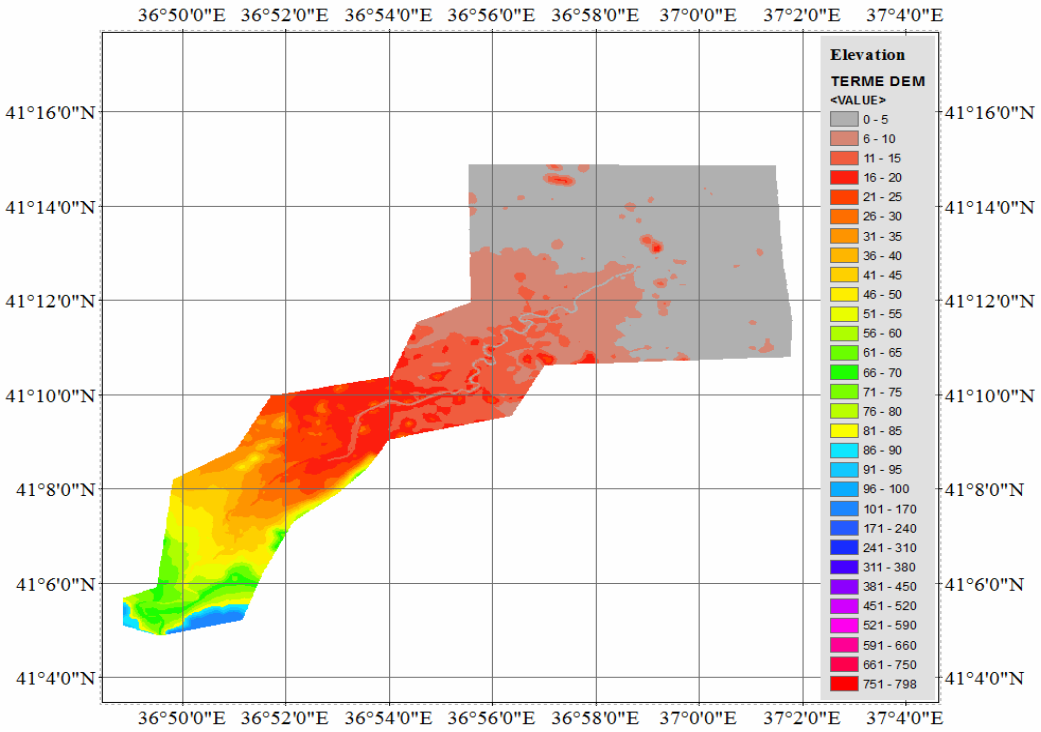

Figure 3-2 1/5000 Scaled DEM

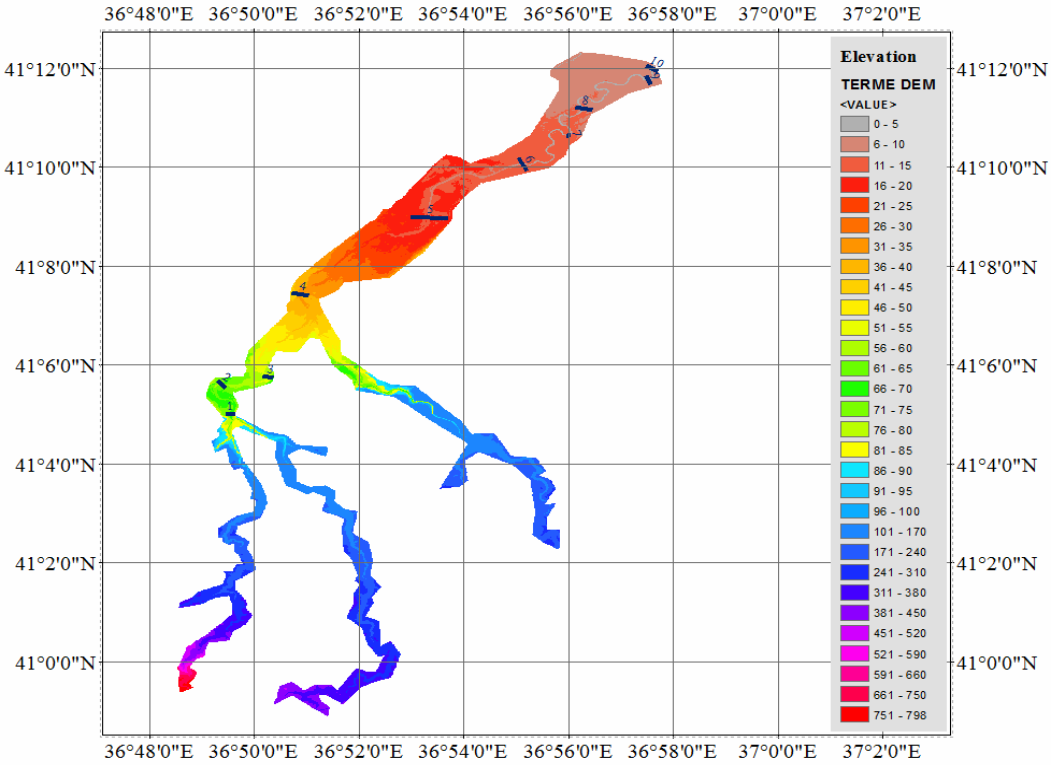

Figure 3-3 1/1000 Scaled DEM with Bathymetry Data

3.3. Hydraulic Model

LISFLOOD-FP is developed in the University of Bristol as a raster-based flood inundation model for research purposes (Bates et al., 2010; De Almeida et al., 2013). The model has several numerical schemes to simulate the propagation of flood waves along channels and across floodplains using simplified derivations of the shallow water equations (Bates et al., 2013).

In this study, LISFLOOD-FP 2-D hydraulic model is used to simulate flood flows. LISFLOOD-FP model is simplified form of the shallow water equations which neglects the convective acceleration term. Flows between cells are evaluated as a function of the friction, water slopes, and local water acceleration. The time step used by the solver varies throughout the simulation according to the Courant-Friedrichs-Lewy condition and is related to the cell size and water depth. The stable time step scales with 1/Δt, thus it can significantly decrease computational time. The simplified versions of shallow water equations are described below (Bates et al., 2013). The Saint-Venant Equations are as follows:

$$\frac{\partial Q}{\partial x} + \frac{\partial A}{\partial t} = 0 \tag{3.1}$$

$$\frac{1}{A}\frac{\partial Q}{\partial t} + \frac{1}{A}\frac{\partial}{\partial x}\left(\frac{Q^2}{A}\right) + g\frac{\partial h}{\partial x} - g\left(S_0 - S_f\right) = 0 \tag{3.2}$$

(a) (b) (c) (d) (e)

where

Q – flow discharge in x-direction (m^3/s)
A – cross-section flow area (m^2)
g - gravitational acceleration (m/s^2)
h – cross-section average flow depth (m)

Equation (3.1) and Equation (3.2) represent continuity equation and momentum conservation equation, respectively. Other terms included within the momentum conversation equation are;

(a) - local acceleration term
(b) -convective acceleration term
(c) -pressure term
(d) -bed slope term
(e) -friction term

3.3.1. Floodplain Flow Solvers

3.3.1.1. Flow-limited Solver

Flow-limited model is the least complex solver of LISFLOOD-FP based on the shallow water equations. The diffusion wave equations used by this model are being founded on Manning's equation. In this model both local and convective acceleration terms are assumed negligible and the flow between cells during a time step is calculated as a function of free surface, bed gradients (the water slope) and friction slope. Time step for this model remains fixed during simulation and it is defined by user. However, in case of time step being not small enough, it allows all the water to drain from one cell to the next one over a single step which causes instabilities in the model. To eliminate this error a "flow limiter" was incorporated into the model to set a limit on the volume of water which can flow between cells during a single time step as a function of flow depth, grid size and time step. Due to its poor accuracy, this flux limited scheme is rarely used (Bates et al., 2013).

3.3.1.2. Adaptive Solver

Adaptive model is a uniform flow formula which is based on one dimensional approximation and is decoupled in x and y directions to allow 2D flow simulations. The difference between adaptive model and flow limited model is that the adaptive model uses a varying time step throughout the simulation. Thus, the stability problem caused by the flow between cells during a time step is eliminated without using a flow limiter. However, this solution leads an increase in computation time for fine grid resolutions since the stable time step scales with $(1/\Delta x)^2$ where Δx is the cell size. Therefore, this model is rarely used for the simulations with high resolutions (Bates et al., 2013).

3.3.1.3. Acceleration Solver

Acceleration model is a simplified form of the shallow water equations. In this model, convective acceleration term is assumed negligible and flow between cells is calculated as a function of friction and water slopes, and local water acceleration. The method uses a semi-implicit treatment for the friction term to aid stability. The time step used by acceleration solver varies throughout the simulation according to the Courant-Friedrichs-Levy (CFL) condition and is related to the cell size and water depth. This model decreases the computation time in contrast to the adaptive model although it is more complex than other solvers by setting the stable time scale to $1/\Delta t$ (Bates et al., 2013).

3.3.1.4. Roe Solver

Roe model introduces all the terms of the shallow water equations based on Godunov approach. The explicit discretization is first-order in space on a raster-grid. Full shallow water equations are solved by a shock capturing scheme and the model uses a point-wise friction based on the Manning's equation while the domain boundary

uses a ghost shell approach. The stability of this approach is approximated by the CFL condition for the shallow water models. Since this solver has only been tested on a limited number of scenarios, it is not considered to be as robust as other solvers (Bates et al., 2013).

3.3.2. Channel Flow Solvers

3.3.2.1. Kinematic Solver

Kinematic model is the simplest of the channel flow models which is a 1-D kinematic wave approximation of shallow water equations. This model assumes the friction and bed gradient terms as negligible (Bates et al., 2013).

3.3.2.2. Diffusive Solver

Diffusive model uses the 1-D diffusive wave equation including the water slope terms in contrast to kinematic model. Thus, this model can predict the backwater effects. Once channel water reaches the bankfull height, the water is routed onto the adjacent floodplain cells to be distributed to the selected floodplain solver while using 1-D channel solvers (Bates et al., 2013).

3.3.2.3. Subgrid Solver

Subgrid solver is the most recently developed method in channel flow solvers of LISFLOOD-FP. This method represents rivers as sub-grid channels, embedded with the two-dimensional (2-D) domain. Flow between channel segments is calculated based on the friction and water slopes, and local water acceleration by using the acceleration model equations. This solver also assumes convective acceleration term negligible. For any cell containing a sub-grid channel segment, the solver calculates the combined water flow within the cell, including both the channel located in that cell

and across the adjacent floodplain. Subgrid model is designed to employ large data sparse areas where limited channel section data are available.

The two-dimensional base model LISFLOOD-FP uses an explicit forward difference scheme on a staggered grid as can be seen in Figure 3-4a. To use the base model for large areas two important changes are implemented in the model. The first one is bringing in a sub-grid procedure to represent channel networks. Thus, the representation of river channels of any size below that of the grid resolution is provided. Second one is inserting hydraulic geometry theory in the model to estimate the unknown channel depth from observable variables such as channel width and bank elevation. So, these variables introduced to the base model as can be seen in Figure 3-4b (Neal et al., 2012) The subgrid section is given in Figure 3-4c.

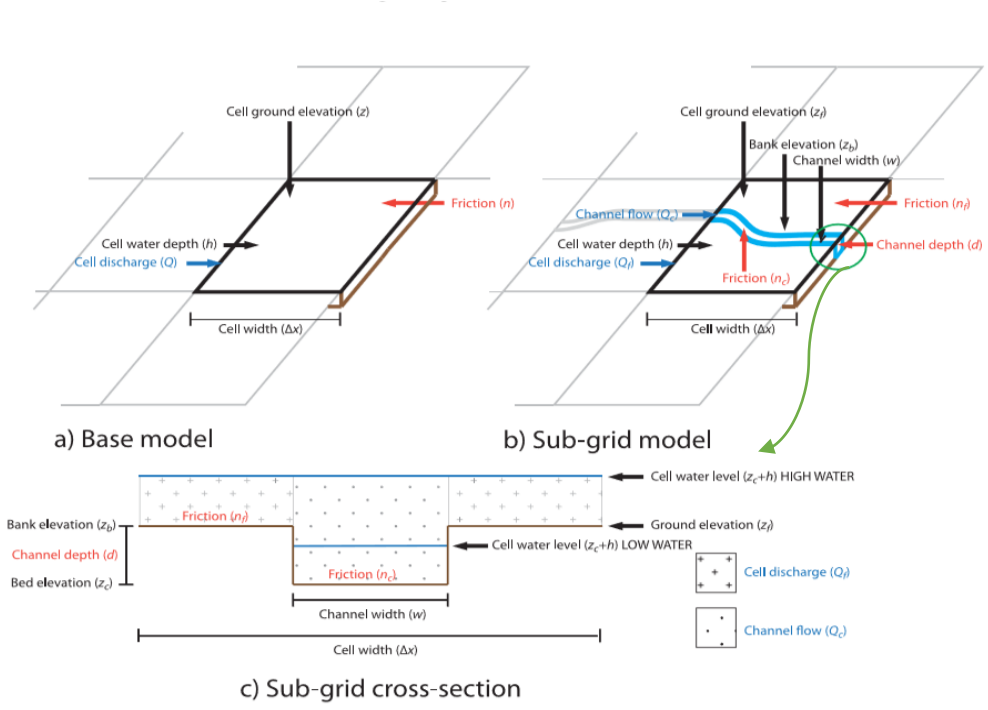

Figure 3-4 Conceptual Diagram of LISFLOOD-FP a) base model, b) subgrid channel model, and c) subgrid section (Neal et al., 2012)

3.3.3. Data Requirements for LISFLOOD-FP Solvers

- Raster Digital Elevation Model
- Boundary Conditions
  - Inflow hydrograph
  - Point sources within the domain
  - Flow across the domain edge
- Channel geometry
  - Channel slope
  - Channel width
  - Bankfull depth
- Model Time Step
  - Fixed Time Step Version
  - Adaptive Time Step Version (Bates et al., 2013)

3.4. Performance Measures

3.4.1. F-Statistic Value

To compare the output maps derived from LISFLOOD-FP on the flood extent basis, F-statistic value is used, because of its easy applicability. The aim is to evaluate how spatial resolution and roughness coefficient affect the obtained flooded area with respect to the chosen base map. While calculating F-statistic, the pixels are assessed according to their wet and dry conditions as can be seen in the Table 3-1 and Equation (3.3).

Table 3-1 F-Statistic Pixel Conditions

	Observed=Dry	Observed=Wet
Model=Dry	A=-Dry/Dry	B=Predicted dry but observed wet
Model=Wet	C=Predicted wet but observed dry	D=Wet/Wet

$$F=\frac{D}{B+C+D} \tag{3.3}$$

This divides the number of pixels correctly predicted as wet by the total number of floodplain pixels. It doesn't account for the pixels correctly predicted as dry as this might bias the measure according to domain size (e.g. it is easy to predict a small flood in a large domain as most pixels will be dry). The value of F goes from 0 for a model with no overlap between observed and modelled data, to 1 for a model with perfect overlap.

3.4.2. Root Mean Square Error (RMSE)

To make a benchmark study between the predicted water depths, Root Mean Square Error (RMSE) is used. RMSE measures the error between two datasets. In other words, it compares predicted value and observed value.

$$RMSE = \sqrt{\frac{\sum_i^n (\hat{y}_i - y_i)}{n}} \tag{3.4}$$

where

$\hat{y}_i$ → expected value (unknown results)

y_i → observed values (known results)

n → sample size

The flowchart of the methodology is presented in Figure 3-5.

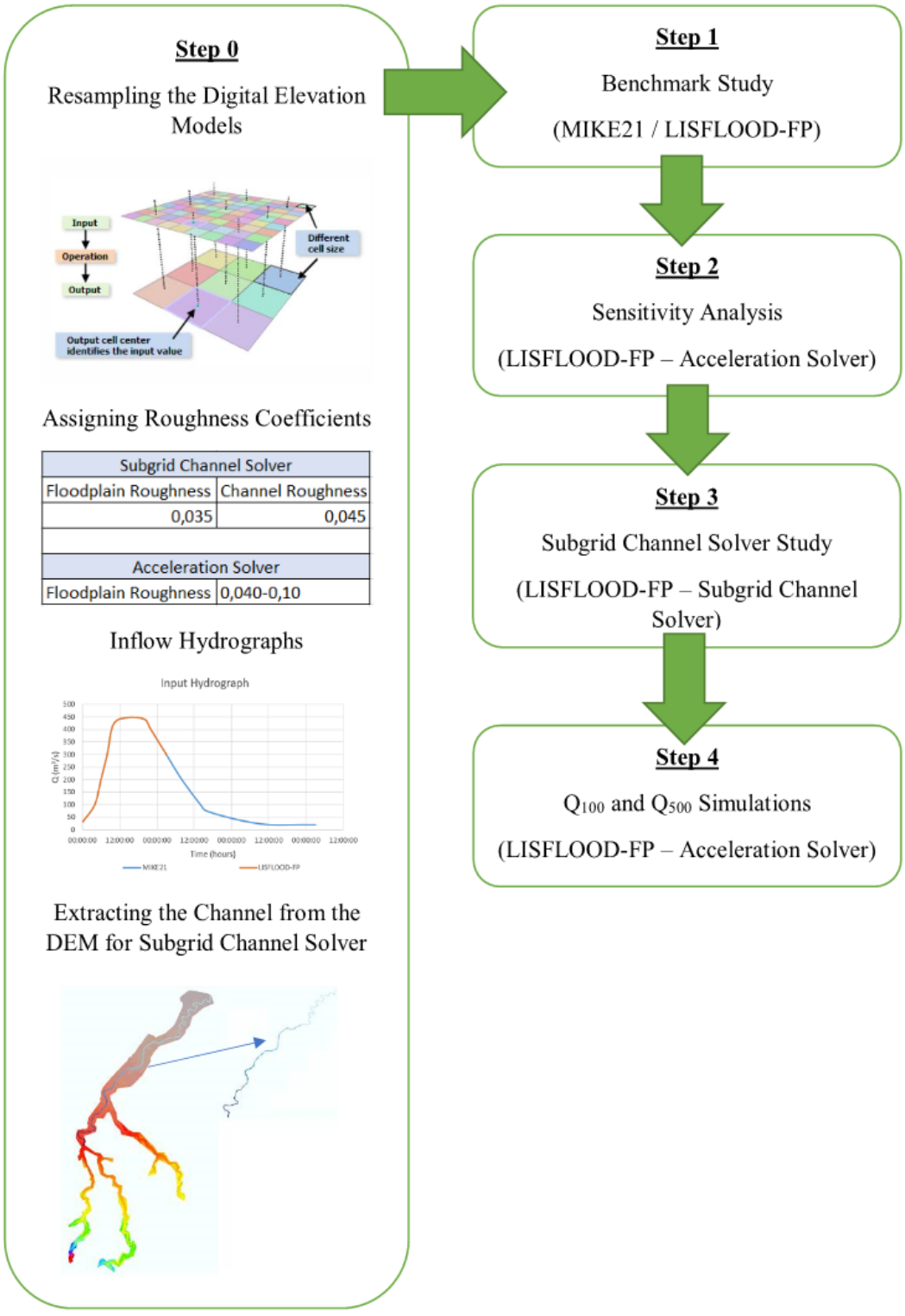

Figure 3-5 Flowchart of Methodology of the Study

3.5. Boundary Conditions

3.5.1. Resampling Process for Digital Elevation Model

Since LISFLOOD-FP uses digital elevation models as parameter files and extracts the resolution from them, for every simulation a different digital elevation model which has a different spatial resolution is used. Thus, it is aimed to see how the simulation is affected by altering the DEM resolution based on channel and floodplain.

The digital elevation model available for LISFLOOD-FP simulation has 1 m resolution (Figure 3-3). Since the model requires long computation times for fine resolutions, spatial resolution is altered to coarser resolutions by resampling technique which uses nearest neighbor with the help of ArcGIS (Figure 3-6). In resampling process while cell size is changed, the extent of raster dataset remains the same. However, the process leads to a loss of information regarding the sub-grid scale topographic variability by altering the representation of the channel. To understand this information loss and see how the channel is represented after resampling process on the digital elevation model, x-sections are extracted from the DEM. The locations of these sections are shown in Figure 3-3. The difference between the x-sections due to the change in grid resolution is also presented as follows (Figure 3-7 to Figure 3-16):

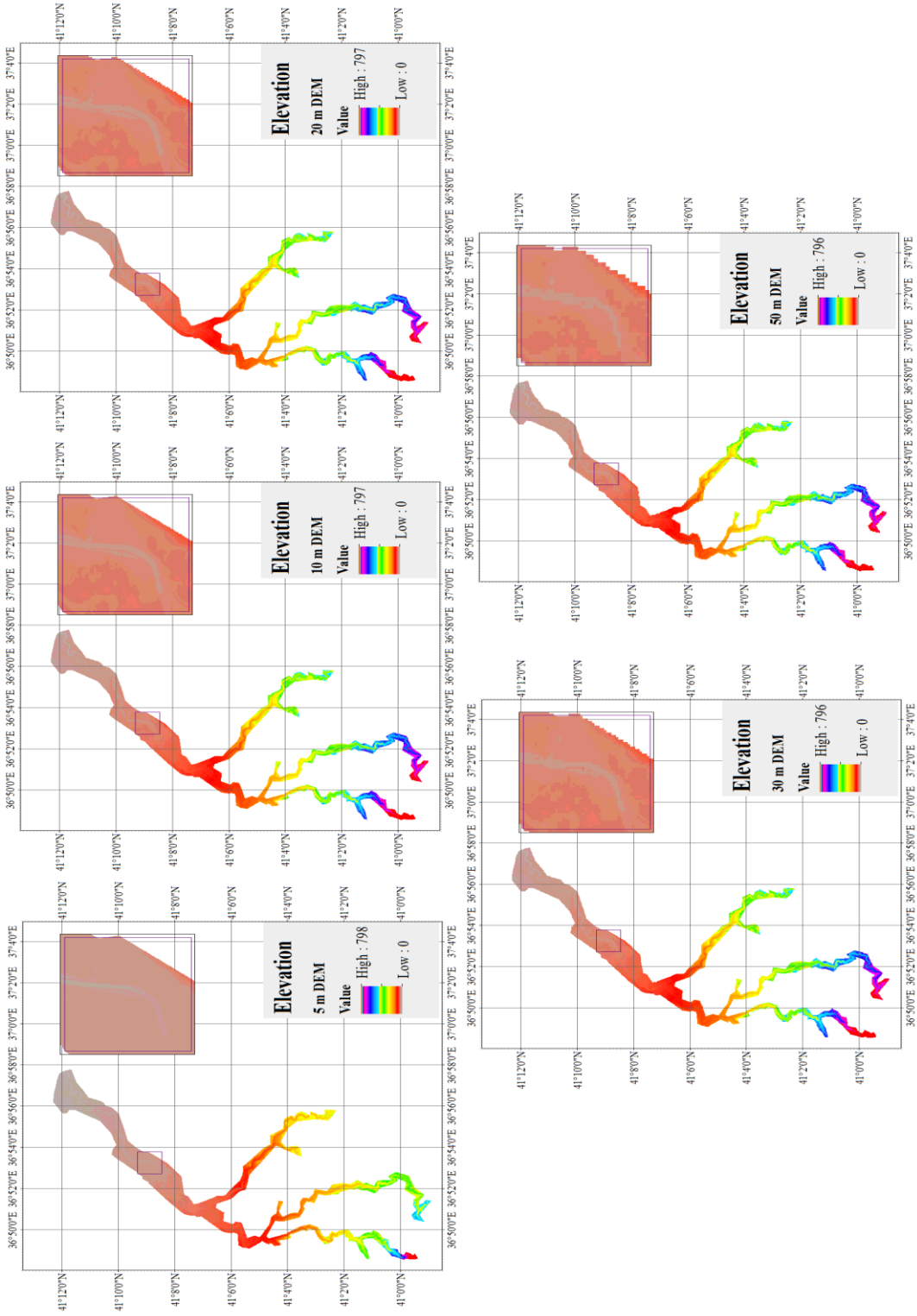

Figure 3-6 DEMs having different spatial resolution

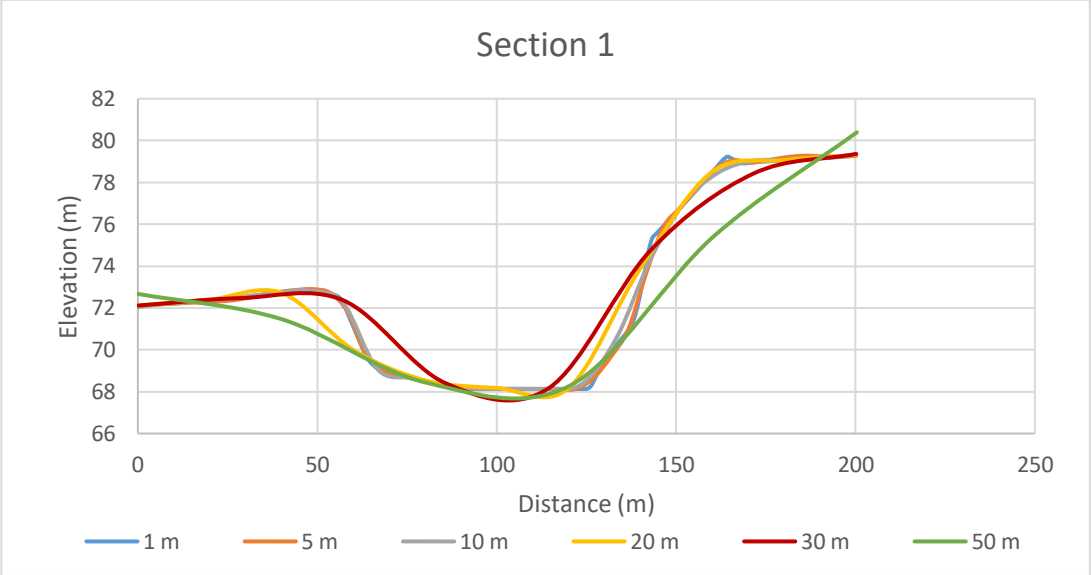

a)

b)

Figure 3-7 a) X-section of Section 1 for different spatial resolutions **b)** Google Earth image of Section 1

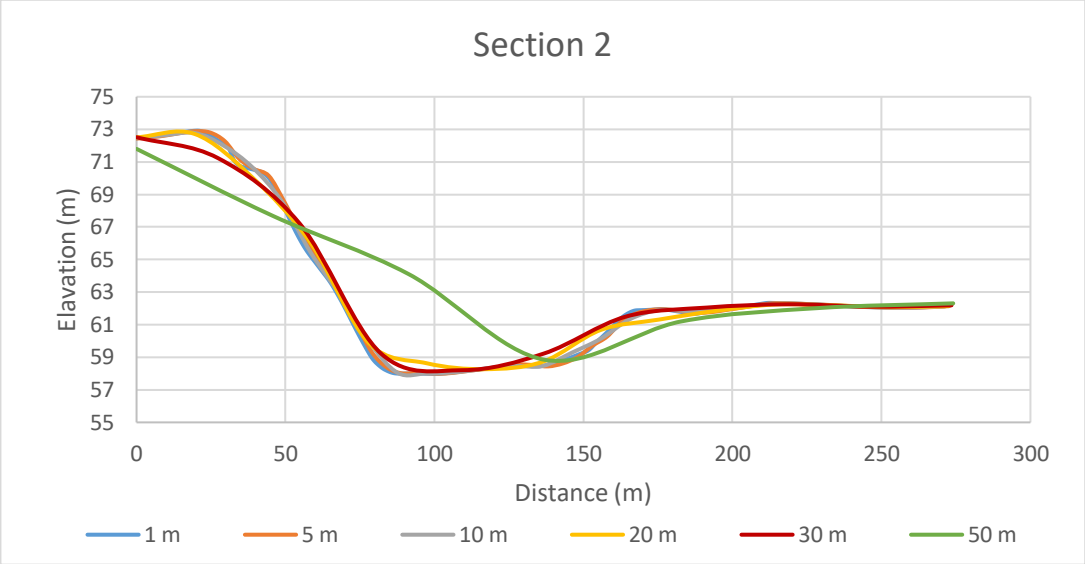

a)

b)

Figure 3-8 a) X-section of Section 2 for different spatial resolutions **b)** Google Earth image of Section 2

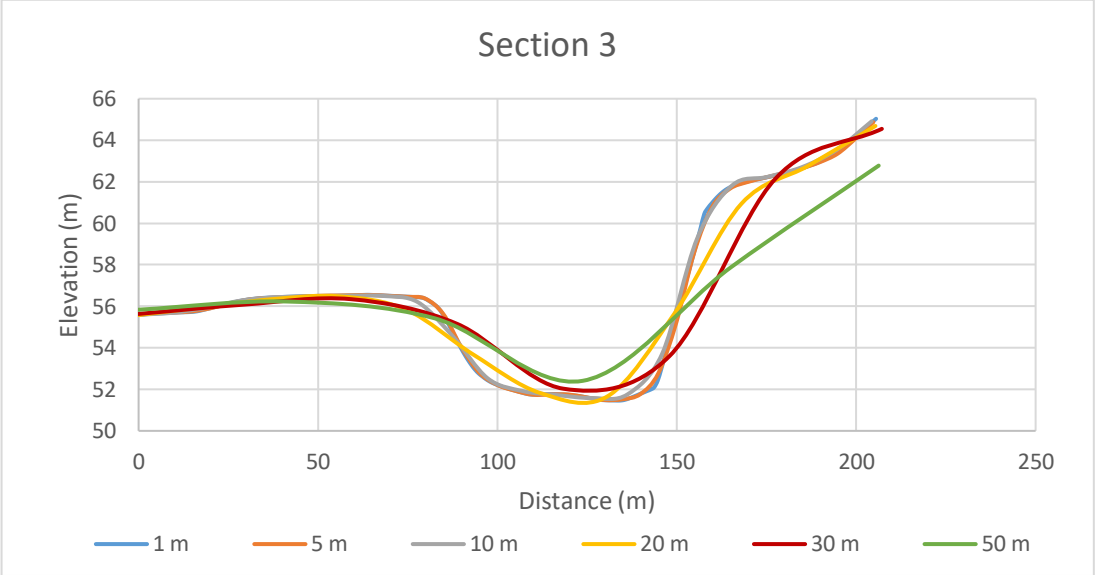

a)

b)

Figure 3-9 a) X-section of Section 3 for different spatial resolutions **b)** Google Earth image of Section 3

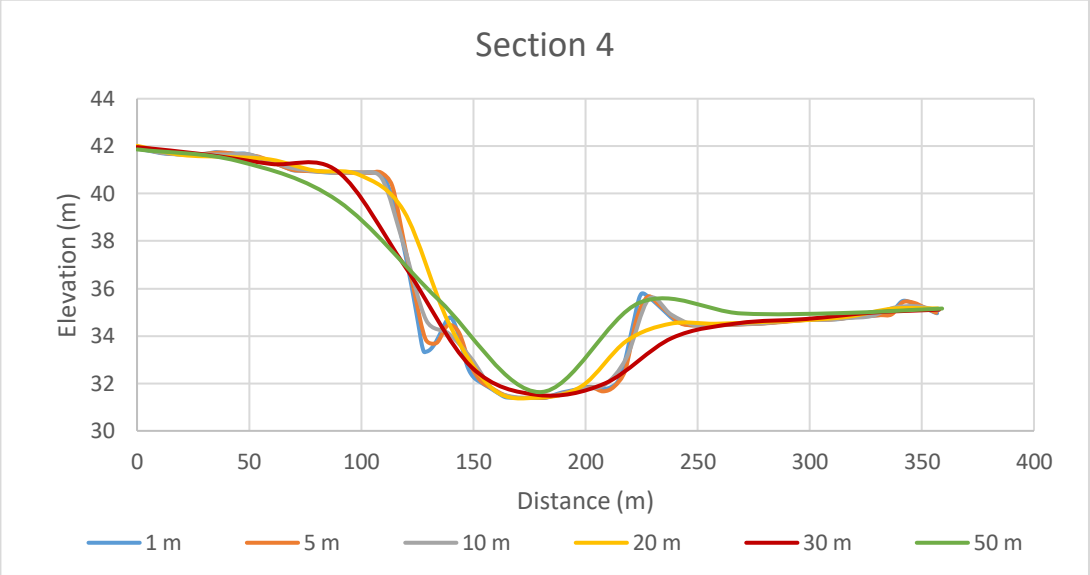

a)

b)

Figure 3-10 a) X-section of Section 4 for different spatial resolutions **b)** Google Earth image of Section 4

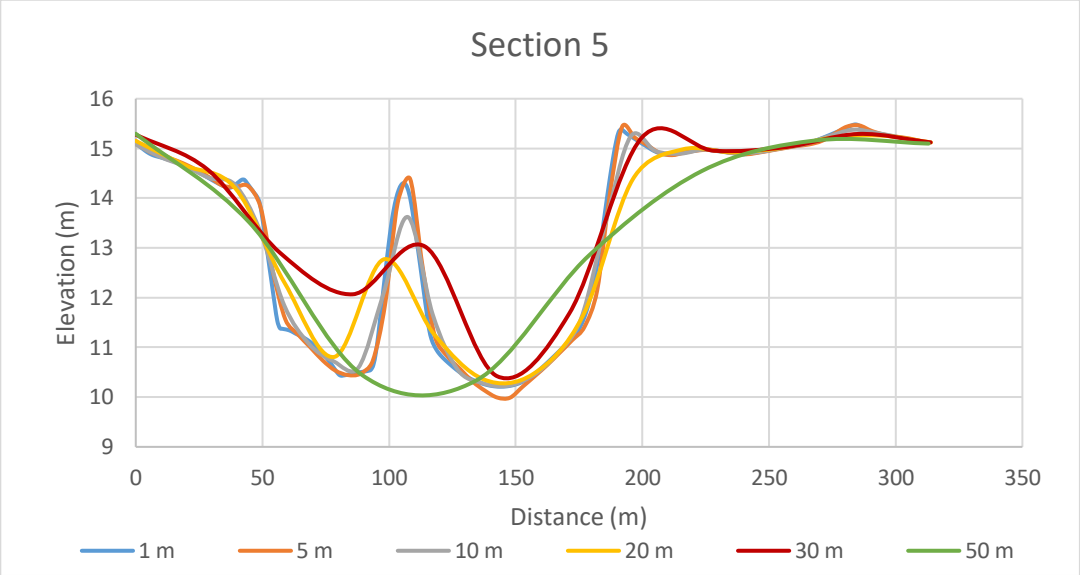

a)

b)

Figure 3-11 a) X-section of Section 5 for different spatial resolutions **b)** Google Earth image of Section 5

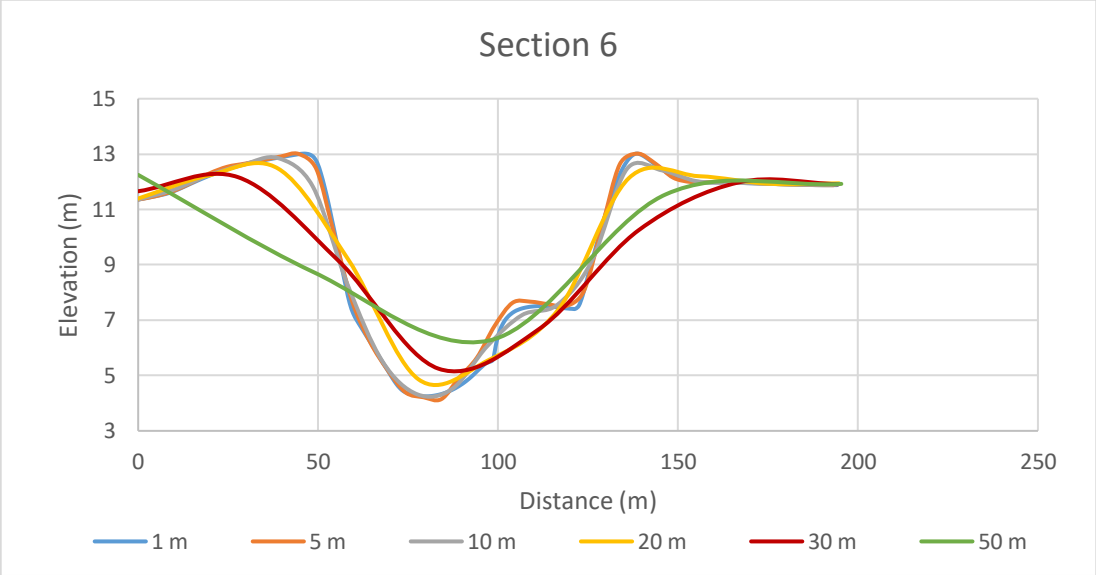

a)

b)

Figure 3-12 a) X-section of Section 6 for different spatial resolutions **b)** Google Earth image of Section 6

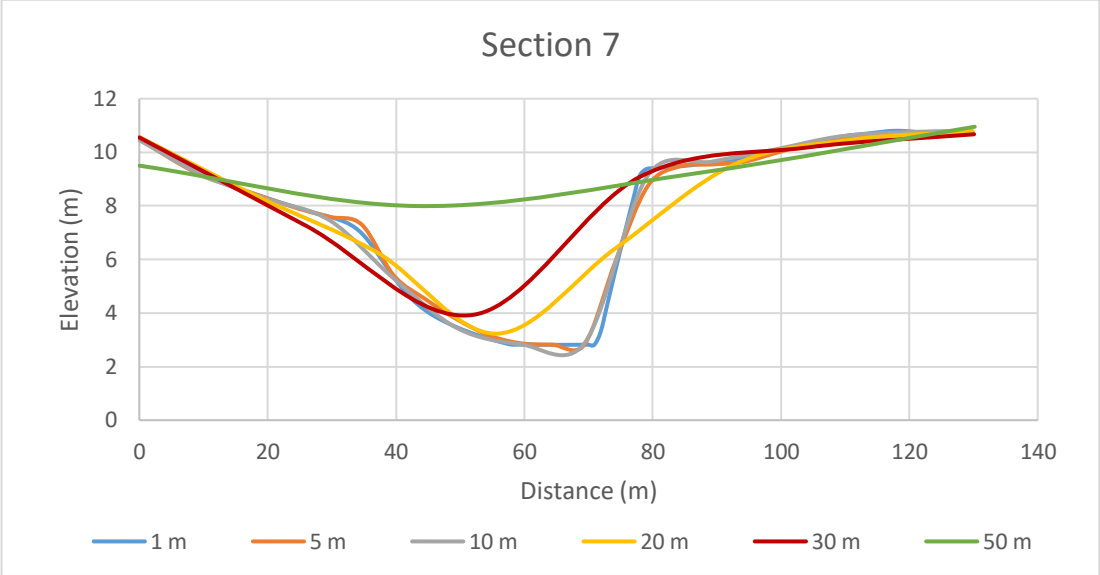

a)

b)

Figure 3-13 a) X-section of Section 7 for different spatial resolutions **b)** Google Earth image of Section 7

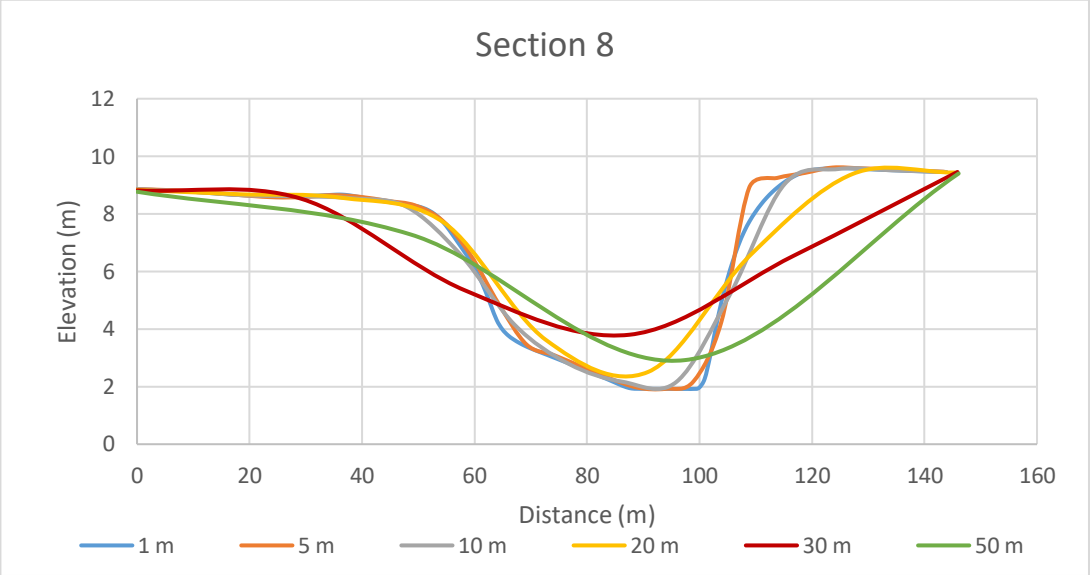

a)

b)

Figure 3-14 a) X-section of Section 8 for different spatial resolutions **b)** Google Earth image of Section 8

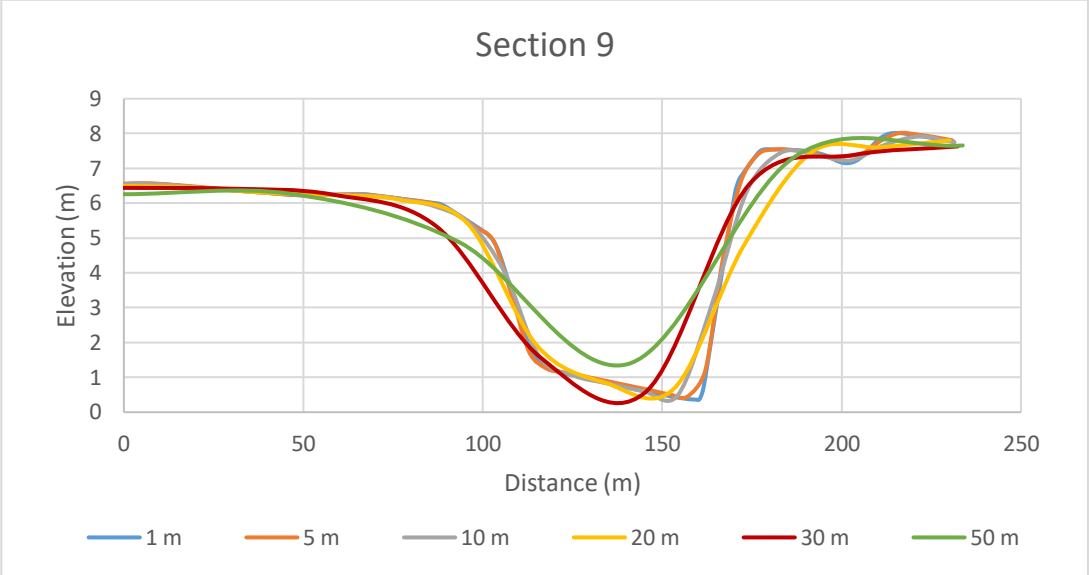

a)

b)

Figure 3-15 a) X-section of Section 9 for different spatial resolutions **b)** Google Earth image of Section 9

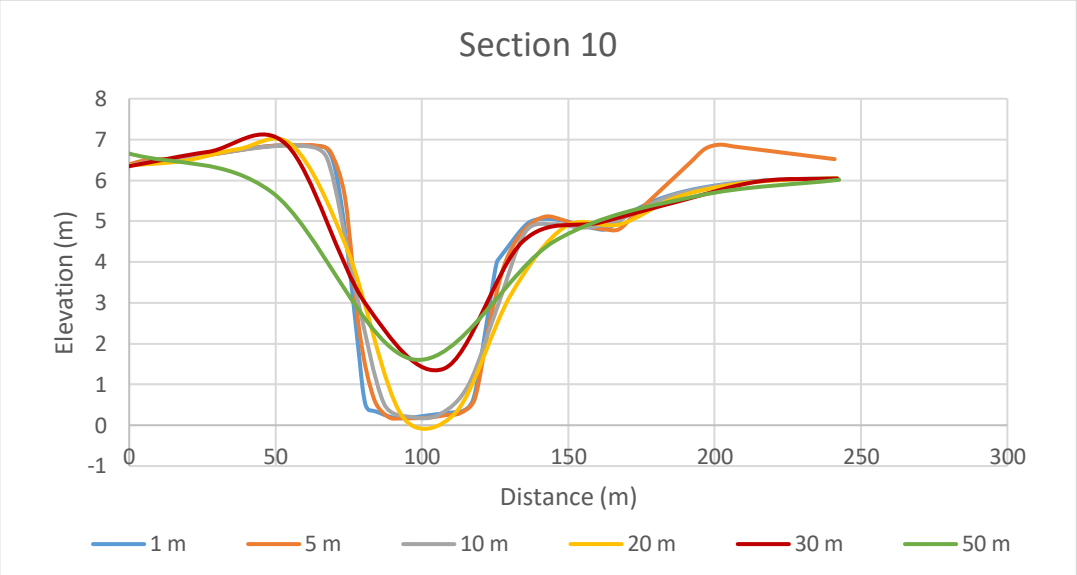

a)

b)

Figure 3-16 a) X-section of Section 10 for different spatial resolutions **b)** Google Earth image of Section 10

3.5.2. Altering the DEM Borders

Since LISFLOOD-FP reads only the DEM as boundary condition, it is not possible to define a different structure in or around the DEM by the parameter file. All the changes must be done on the DEM in .ascii format. Since backwatering effects occurred in the results, the cells around the DEM are set as "0" to provide the water to leave the area to prevent any backwatering problem.

3.5.3. Input Hydrograph

The input hydrograph taken from previous study (Bozoğlu, 2015) was obtained with DSI Synthetic method by using three main gauging stations in the basin which are 22-45 Gökçeali AGI, 22-02 Terme Bridge AGI and 22-105 Salıpazarı AGI (Figure 3-1).

Hydrographs for 2, 5, 10, 25, 50, 100 and 500-year return periods were obtained from Bozoğlu (2015). These hydrographs were calculated from the observations at 22-45 Gökçeali AGI. The peak discharges for 22-45 Gökçeali AGI are shown in Table 3-2. (Bozoğlu, 2015).

Table 3-2 Peak Flood Discharge Hydrographs (Bozoğlu, 2015)

Years	**2**	**5**	**10**	**25**	**50**	**100**	**500**
$Q_{22\text{-}45}$ m^3/s	219,71	350,43	446,74	578,27	682,83	792,41	1041,34

The flood discharges for sub-basins were obtained by using area ratio method, and they are presented in Table 3-3 (Bozoğlu, 2015).

Table 3-3 Distributed peak flood discharges to sub-basins (Bozoğlu, 2015)

Area (km^2)	Q_2	Q_5	Q_{10}	Q_{25}	Q_{50}	Q_{100}	Q_{500}
Basin 1	70,92	113,11	144,19	186,64	220,39	255,76	366,11
Basin 2	44,04	70,24	89,54	115,90	136,86	158,82	208,71
Basin 3	103,78	165,52	211,01	273,14	322,53	374,28	491,86
Basin 4	127,30	203,03	258,83	335,04	395,62	459,11	603,33

In this study, hydrograph Q_{10} having a peak value of 446,74 m^3/s is used for the benchmark and sensitivity analyses. Due to runtime limitations the hydrograph used for LISFLOOD-FP has terminated at 27^{th} hour, after the peak discharge is reached in the benchmark part of this study (Figure 3-17). As for the sensitivity part, the hydrograph is terminated when the peak discharge is reached because the water has already arrived to the end of the DEM as well as having a benefit from computation time (Figure 3-18).

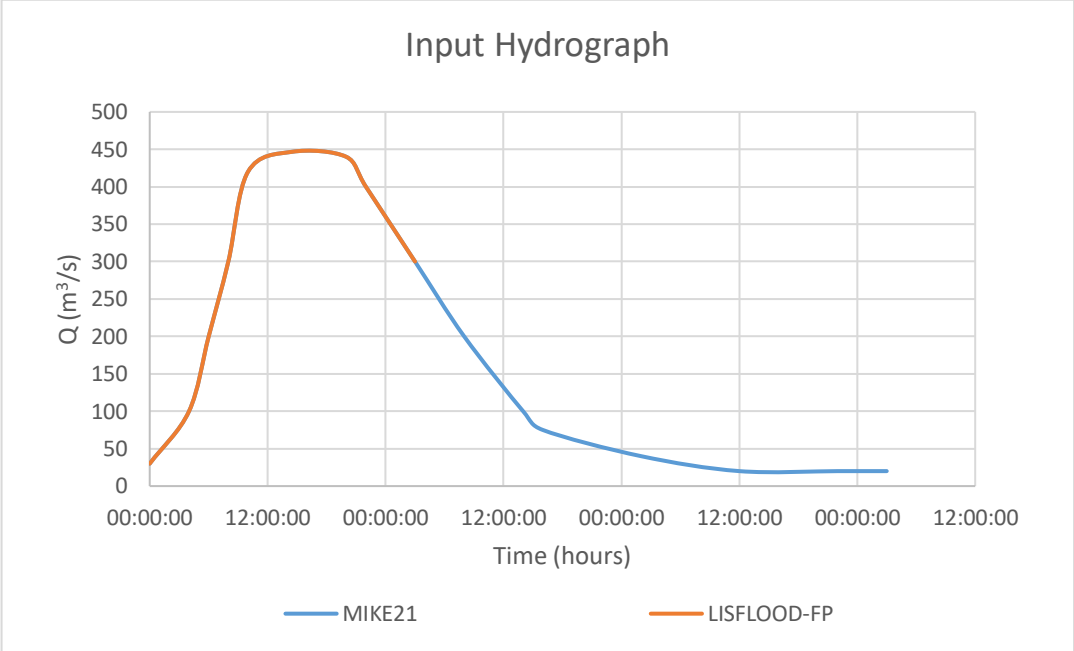

Figure 3-17 Input Hydrograph for Benchmark Study (Demir, 2016)

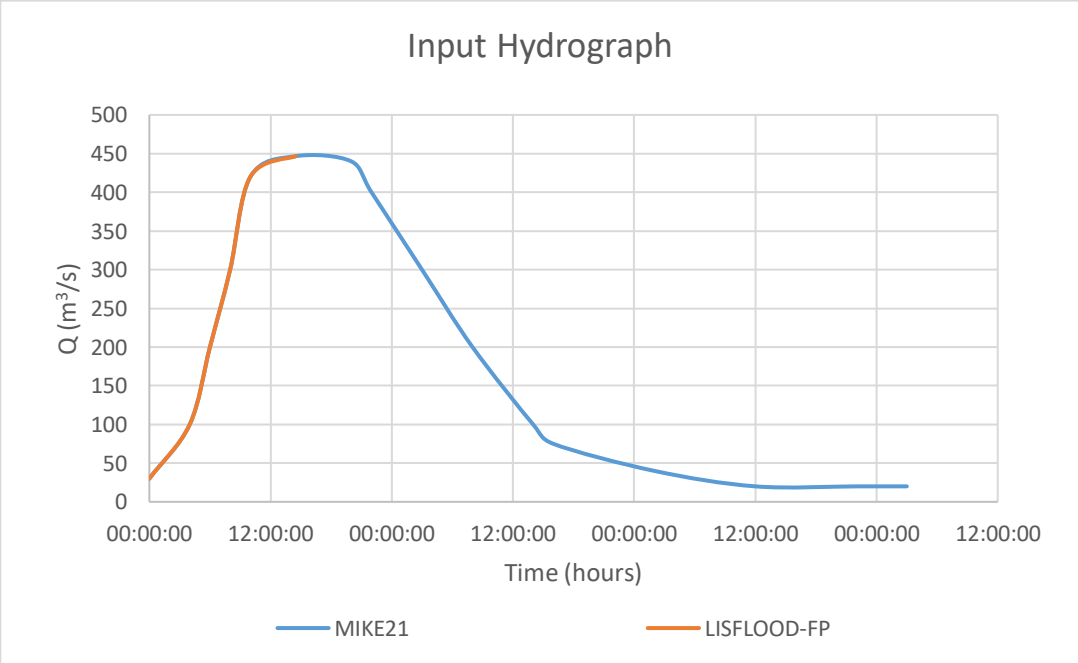

Figure 3-18 Input Hydrograph for the Sensitivity Analysis

3.5.4. Point Source Locations

In this study, input hydrographs are given to the system as point sources. Two different scenarios are conducted and summarized as follows:

The project area was divided into four sub-basins as in the previous study (Bozoğlu, 2015) and the flood discharges for each sub-basin were used (Bozoğlu, 2015). For the comparison part of the current study, the total discharge of these four basins are given to the system as one input hydrograph from one location, 22-45 Gökçeali AGI (Figure 3-19).

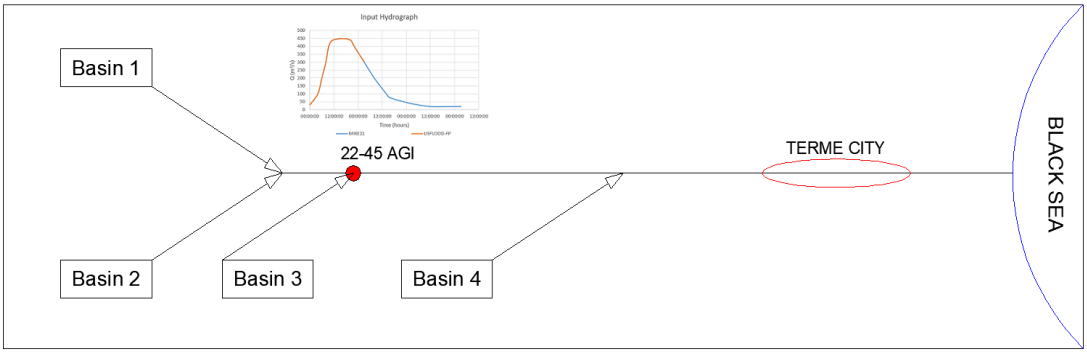

Figure 3-19 Input hydrograph locations

For sensitivity analysis, the discharge hydrograph is divided into two components. The first component is defined as the total discharge of three basins on the upstream and given to the system from the location of 22-45 Gökçeali AGI. Hydrograph given for sub basin 4 is inserted into the system from the intersection point of the Basin 4 contribution and main channel (Figure 3-20).

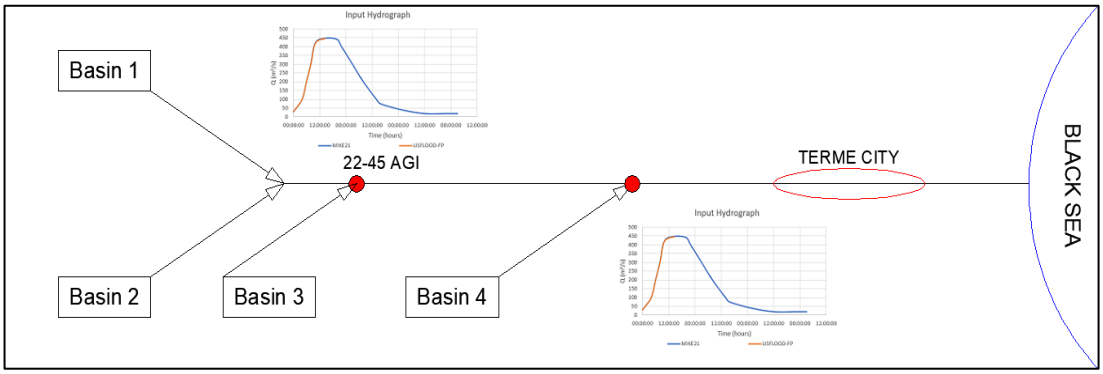

Figure 3-20 Input hydrograph locations

3.5.5. Roughness Coefficients and Spatial Resolutions

Calibration is an important part of hydraulic modeling to obtain more accurate results. In this study, the use of roughness coefficient and spatial resolution as calibration parameters for the LISFLOOD-FP hydraulic model is investigated. For the study site, the Manning's n value is presented in "Samsun Terme District, Terme River Hazard Map Designation" report (DSI, 2013) with Cowan's method. In this report, roughness value for Terme Bridge is calculated as 0,029 and for upstream part of the river, the average value is computed as 0,045.

In the comparison part of the study, the aim is to find the closest simulation results on the flood extent basis with MIKE21 results by altering the roughness values considering the previous roughness information.

For sensitivity analysis part DEM's having 5 m, 10 m, 50 m and 100 m spatial resolutions are used and roughness coefficient is altered between the range of 0,040 – 0,10 to understand how LISFLOOD-FP reacts to these changes.

CHAPTER 4

ANALYSES

4.1. Benchmark Study

MIKE21 simulation result is obtained from the previous study (Bozoğlu, 2015) LISFLOOD-FP simulations are done on DEM having 5 m resolution which is presented in Figure 3-2.

In MIKE21 simulation roughness coefficient values vary in and around the stream bed to prevent the stability problems for 5 m spatial resolution DEM (Demir and Akyürek, 2016). The hydrograph duration was chosen as 75 hours for Q_{10}=446,74 m^3/s.

For LISFLOOD-FP simulation, the Acceleration Solver which solves the flood hydraulics by assigning the same roughness coefficient to whole floodplain is used to see if the result is resembling the MIKE21 simulation result. The input hydrograph is given to the system from 22-45 Salıpazarı AGI and DEM border is prepared as it is explained in section 3.5.2. Since computation times last too long for fine spatial resolutions (e.g. 5 m), the hydrograph duration is set to time to peak of hydrograph, which is 14.5 hours. When the hydrograph is set to peak discharge the water could not reach to the sea therefore, the hydrograph is terminated at 27^{th} hour to ensure the water reaches to the edge of the DEM and leaves the floodplain to the sea. Even though the input hydrograph is shortened to 27 hour, runtime lasted for 1476,50 minutes.

The roughness coefficient is selected by trial and error approach. Since the roughness coefficient is calculated as n=0,029 for Terme Bridge and n=0,045 for the upstream part of the river, firstly n=0,030 is assigned to apply the Terme Bridge area

characteristics on whole floodplain for the simulation. But stabilization errors occurred in water depth outputs. Therefore, roughness coefficient is increased to n=0,035 which eliminates the oscillations in water depth outputs however, the flood extents do not match with the results of MIKE21 simulation. Finally, when the roughness coefficient set to n=0,040 obtained flood extent is resembled with MIKE21 results.

As can be seen in the Figure 4-1 and Figure 4-2, MIKE21 and LISFLOOD-FP simulation results are close, but the calculated area of the flood extent has difference. The inundated areas of MIKE21 and LISFLOOD-FP simulations are calculated to compare, and results are presented in Table 4-1.

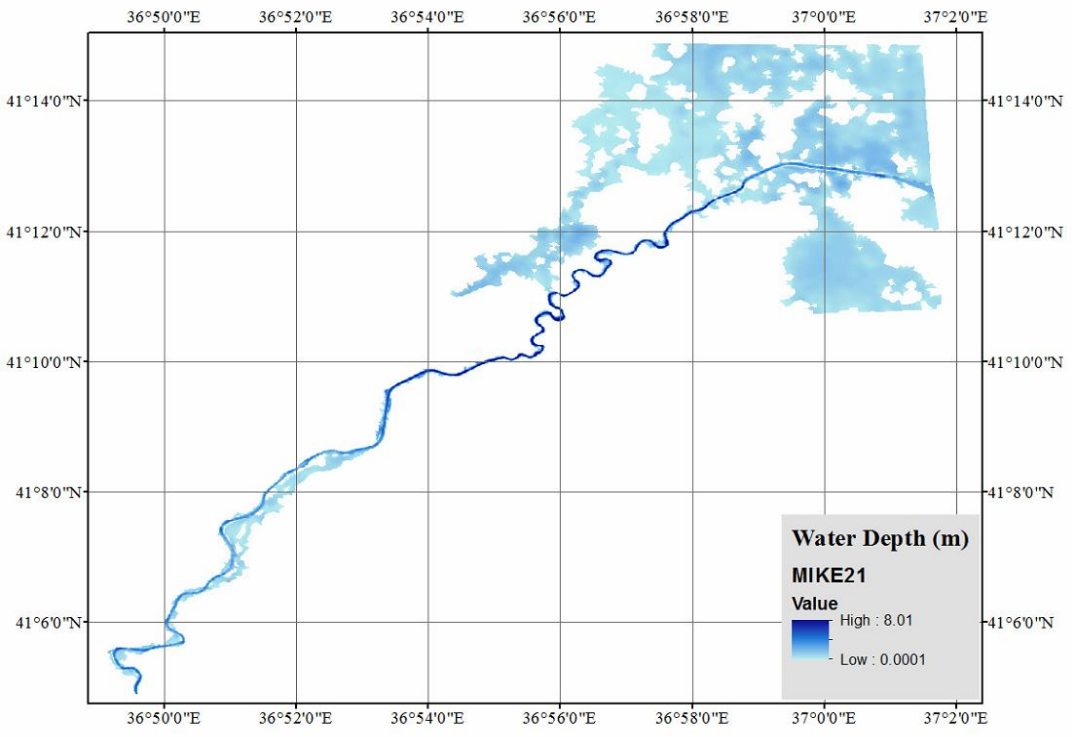

Figure 4-1 Flood extent result of MIKE21 (Demir, 2016)

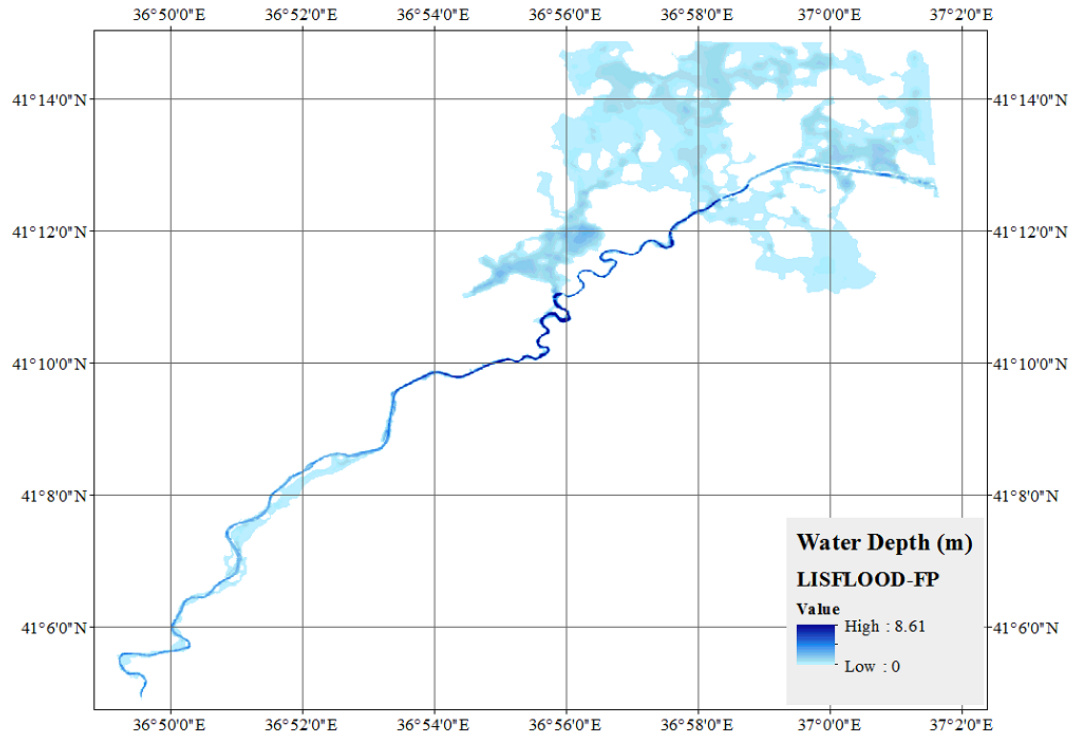

Figure 4-2 Flood Extent Result of LISFLOOD-FP

Table 4-1 Flooded area comparison of LISFLOOD-FP and MIKE21

Simulations	Total Area (km^2)	Flooded Area (km^2)	Percentage over Total Area (%)
Mike 21	112,035	32,839	29,31
LISFLOOD-FP	112,035	29,944	26,73

The effect of meandered and braided parts of the stream is investigated to make a further explanation about the difference between LISFLOOD-FP and MIKE21 results. To provide this information, sections are taken from these parts of the DEM and the hydrograph at these sections is obtained. The location of the sections and the obtained output discharge hydrographs are presented as follows: (Figure 4-3 to 4-6).

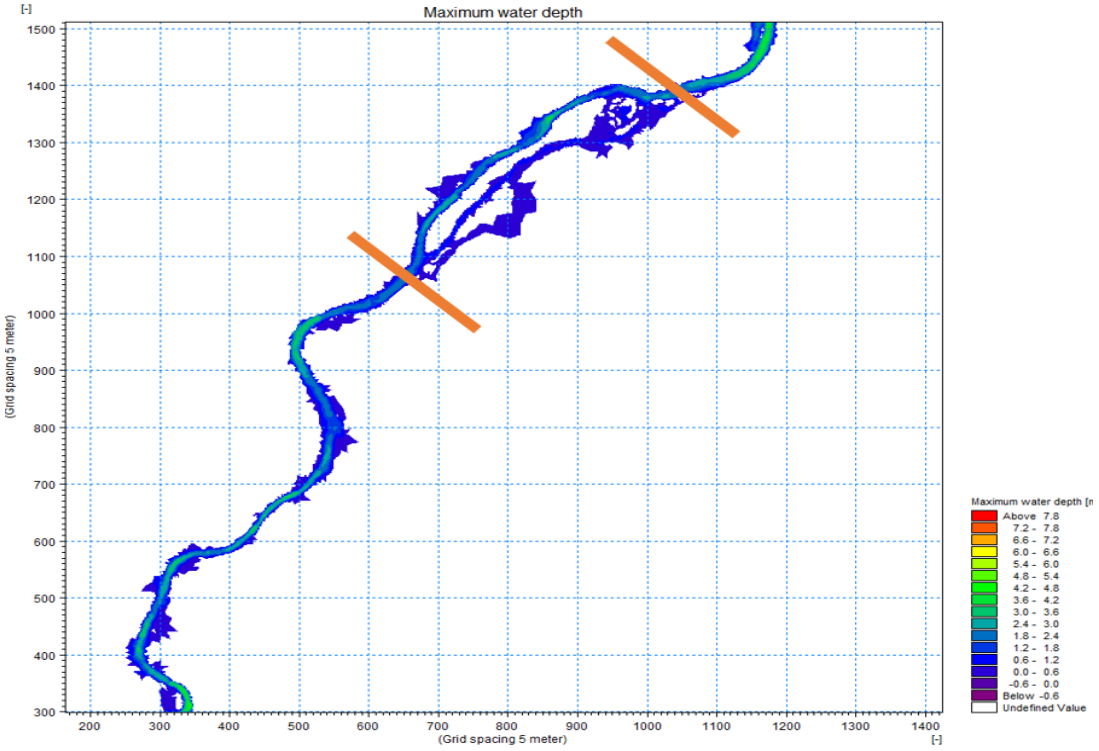

Figure 4-3 Discharge locations for braided part of the DEM (Demir, 2016)

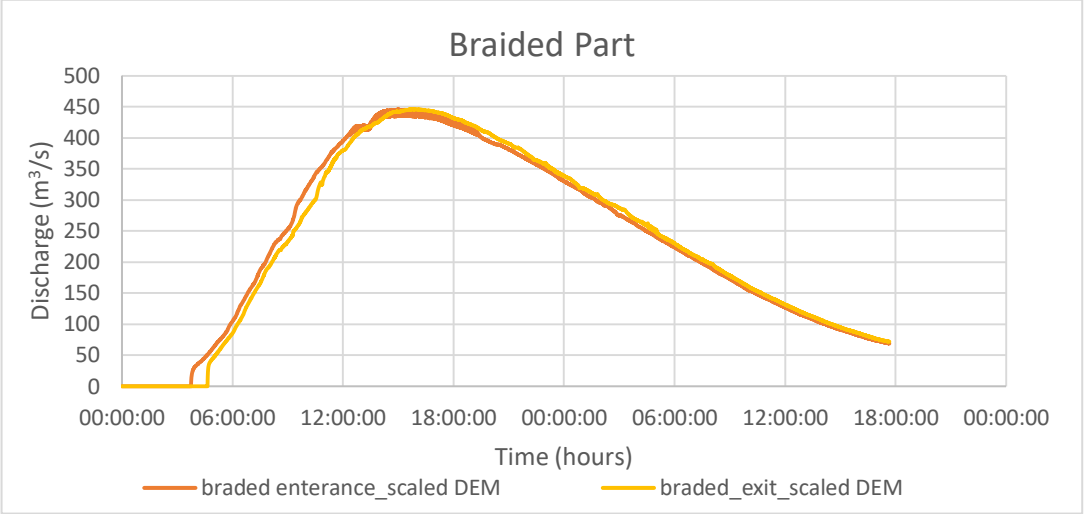

Figure 4-4 Resulting Discharge hydrograph for entrance and exit of the braided part on MIKE21 (Demir, 2016)

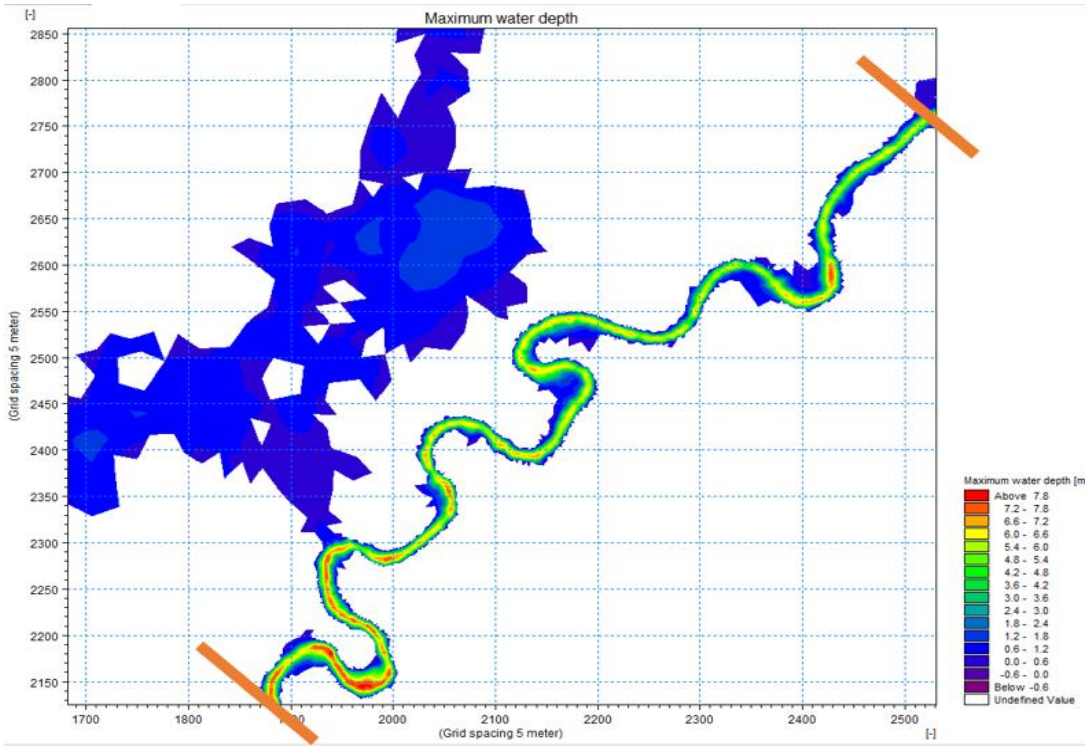

Figure 4-5 Discharge locations for meandered part of the DEM (Demir, 2016)

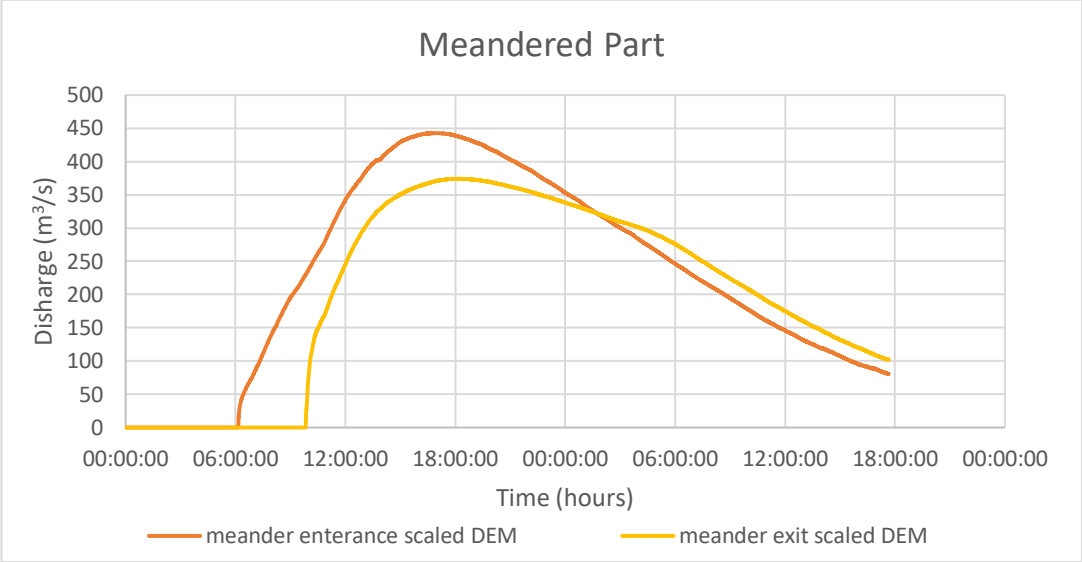

Figure 4-6 Resulting Discharge hydrograph for entrance and exit of the meandered part on MIKE21 (Demir, 2016)

These graphs show that meandered part of the DEM stores more discharge than braided part due to the ponding in that region. For braided part, lag time between entrance and exit discharge is considerably small which means meandering formations are holding the water longer than braided formations as it can be expected.

To make a detailed investigation about the differences between the two hydraulic models, local effects are examined. MIKE21 results indicated that topographical formations also have an influence on water propagation therefore, x-sections are taken from the meandered and braided parts of the DEM. The obtained output hydrographs are given as follows: (Figure 4-7 and Figure 4-8).

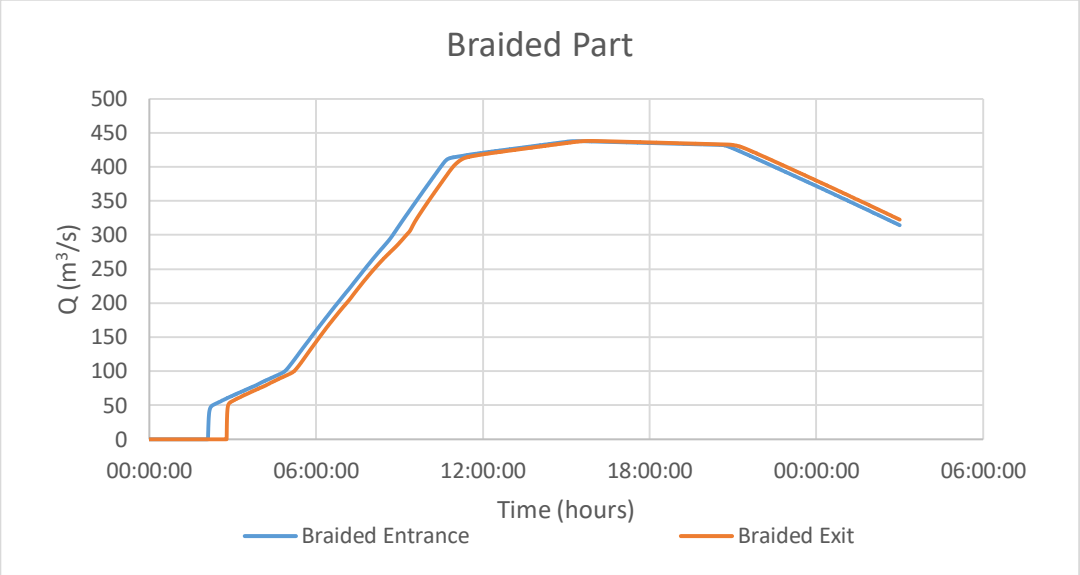

Figure 4-7 Resulting Discharge hydrograph of braided part entrance and exit on LISFLOOD-FP

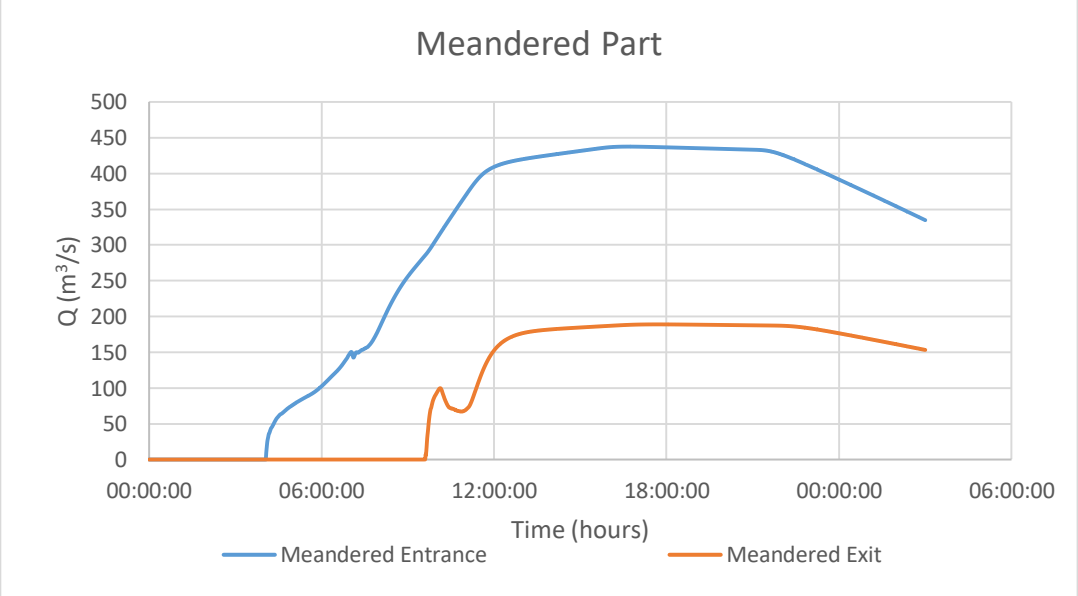

Figure 4-8 Resulting Discharge hydrograph of meandered part entrance and exit on LISFLOOD-FP

The resulting hydrographs of MIKE21 and LISFLOOD-FP for braided part of the DEM are almost similar except for the time of water entrance and the duration until the water leaves the section. As for the meandered part besides the difference of the time of water entrance and exit at the section, LISFLOOD-FP model shows an instability in the routing through the section.

4.2. Sensitivity Analysis for Acceleration Solver

In the previous part, the differences/similarities between MIKE21 and LISFLOOD-FP simulation results are investigated. Resulting flood extents are similar but to ensure this similarity, the distribution of roughness parameter is rearranged. While the system stability of MIKE21 is provided by distributing different roughness coefficients to whole domain, uniform distribution is adequate for LISFLOOD-FP-Acceleration Solver. Under a certain value of roughness coefficient (n=0,035), LISFLOOD-FP gives stabilization errors and to obtain compatible flood extents, calibration by trial and error is required. Therefore, the necessity to understand the response of the hydraulic model due to the change of roughness parameter arises.

Since it is well known that model sensitivity is crucial to obtain accurate results, model calibration according to certain hydraulic parameters is the main focus of this study. In this part of the thesis, model sensitivity due to the change of roughness besides spatial resolution is investigated.

In general, aerial photographs are used for validating and calibrating the hydraulic model. In this case, it is only known that "Q=510 m^3/s has passed through the Terme Bridge without overflow" during the event occurred in July 2012 therefore, this study is built on this information and Q_{10}= 446,74 m^3/s peak discharge is used for the sensitivity studies. Since fine resolutions increase the computation time in LISFLOOD-FP, and the DEM based on tachometer has a smaller size which causes the water reaches to the edge of the DEM earlier, the hydrograph is terminated when

the peak value is reached (Figure 3-18). As the input hydrograph locations, 22-45 Salıpazarı AGI and Basin 4 contribution to the main channel are chosen (Figure 3-20). The roughness coefficients are uniformly distributed and altered in the range between 0,040-0,10 because the use of lower values create stabilization errors in local water depth measures. As for the spatial resolutions; 5 m, 10 m, 50 m and 100 m grid resolutions derived by resampling of 1 m DEM, which was given in Figure 3-3 are used. For the finest spatial resolution 5 m is selected due to the computational costs and the challenges while removing the DEM boundaries from the large matrix of ascii files for finer resolutions.

The analysis is composed of two parts. In the first part the spatial resolution effect on flood extent is investigated. The simulations are run with constant roughness coefficient n=0,040 (chosen to prevent stabilization errors) while changing the spatial resolution. In the second part, the effect of roughness coefficient is checked. For the second part, for 5 m spatial resolution, roughness coefficient is altered. To understand the local effects, sections are taken from locations of the DEM and water depth change graphs are obtained at the selected x-sections (Figure 4-9).

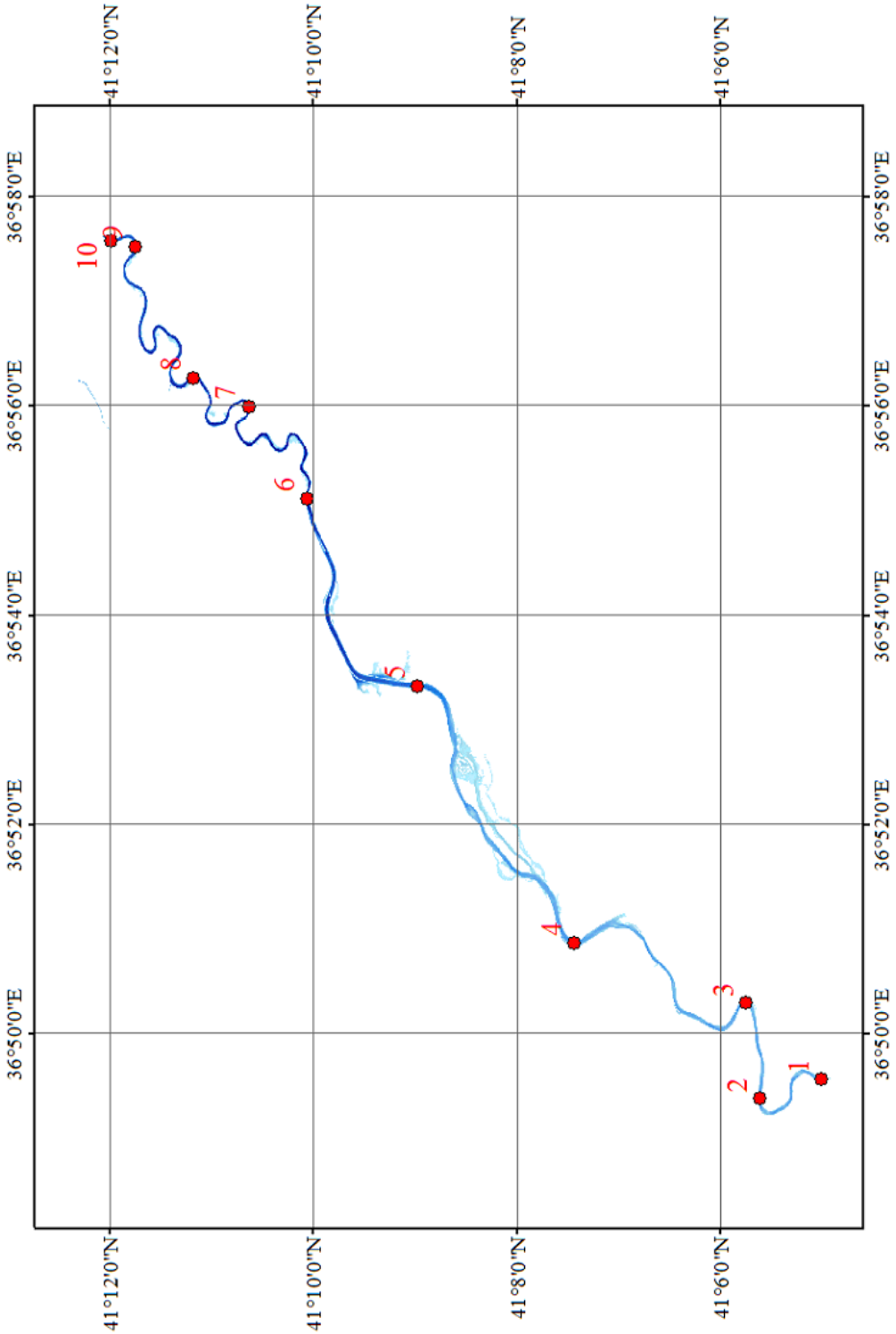

Figure 4-9 Water Depth Measurement Locations

4.2.1. Effect of Spatial Resolution on the Floodplain

For this part of the analysis, the simulations are run with n= 0,040 roughness value and simulation time is set to 14.5 hours at the time hydrograph reaches the peak discharge. Also, DEM boundaries are removed to prevent backwatering effects and allow the water to reach the sea. Resulting flood extents are obtained for 5 m, 10 m, 50 m and 100 m spatial resolutions (Figure 4-10) and the detailed outputs are given in the Appendix A. For comparison, F-statistic values are calculated to find out how flood extent changes due to the spatial resolution change by taking 5 m simulation result as base map. To understand the local effects of the change in spatial resolution, RMSE values of water depths are calculated by taking the 5 m map as base map.

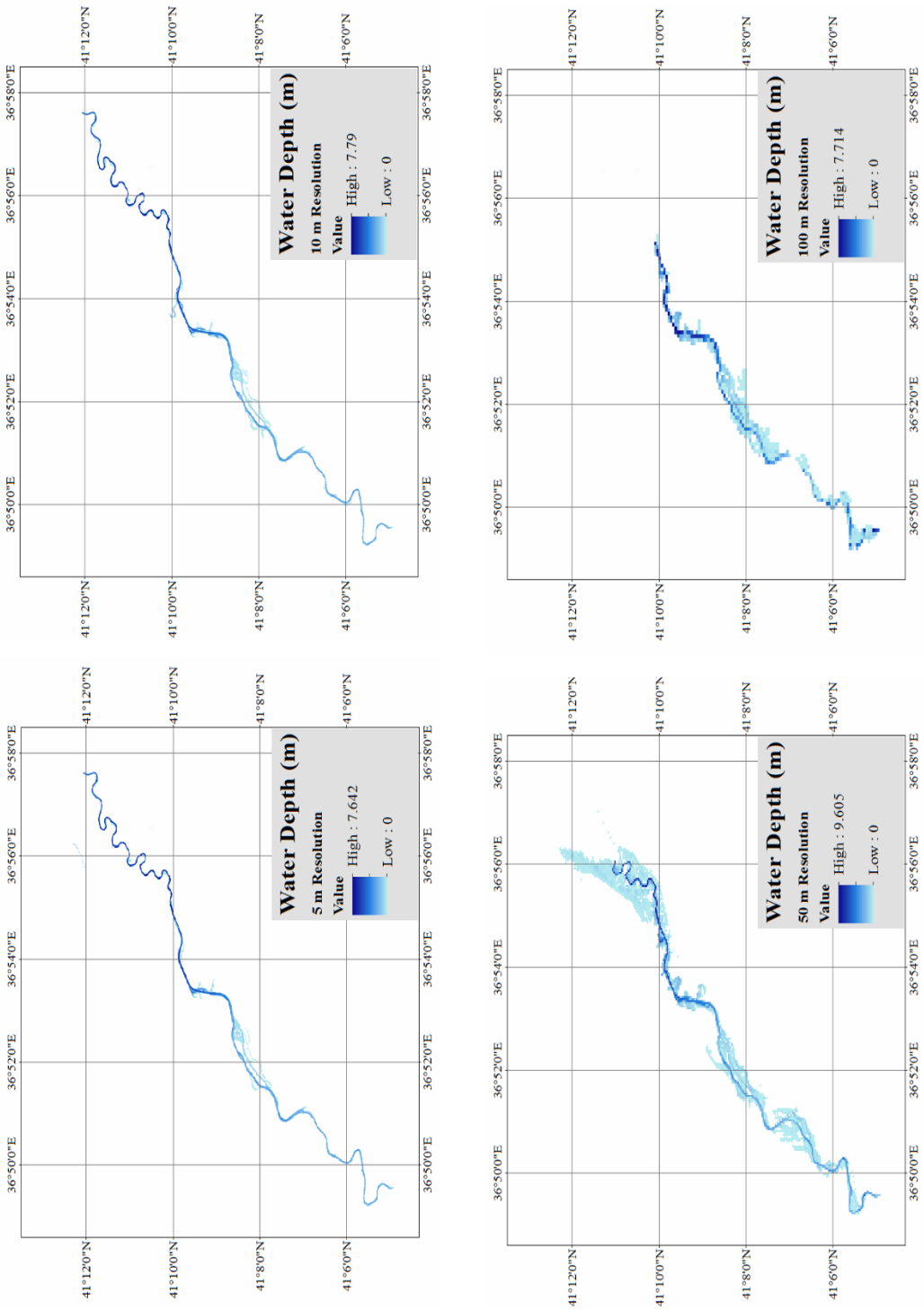

Figure 4-10 Flood extent for n=0,040 and 14,5 hours simulation time for 5, 10, 50 and 100 m resolutions

As can be seen in Figure 4-10, while the resolution getting coarser, representation of the flood becomes insufficient. Flood propagation gets slower for the coarse resolutions even though simulation time is set as the same for each run. To make a further look to these inferences, F-statistic values of flood extents (Table 4-2) and RMSE of local water depths are calculated for chosen sections (Table 4-3) by taking the results of 5 m DEM as benchmark map.

Table 4-2 F-statistic results in terms of flood extent and runtimes

Spatial Resolution	F-statistic (base 5 m)	Runtime (min)
5 m	-	286,77
10 m	0,938	39,07
50 m	0,289	1,18
100 m	0,053	0,58

Table 4-3 Local water depth RMSE for each section taking the base map as n=0,040 and 5 m resolution

Sections	Water Depth RMSE			
	5 m DEM	10 m DEM	50 m DEM	100 m DEM
Section 1	-	0,034	0,321	2,903
Section 2	-	0,102	0,284	1,656
Section 3	-	0,042	2,486	1,203
Section 4	-	0,026	0,408	0,432
Section 5	-	0,272	0,885	1,791
Section 6	-	0,761	2,854	3,944
Section 7	-	0,464	3,161	4,211
Section 8	-	0,211	3,688	3,688
Section 9	-	0,196	2,649	2,649
Section 10	-	0,188	2,577	2,577

According to the tables above, the lowest RMSE is found for 10 m resolution for local water depths and the highest F-statistic value is obtained for 10 m grid size which shows that fine resolutions give compatible results with each other. The computation cost changes according to spatial resolution the results are presented in Table 4-2.

The table shows that, grid resolution also influences computation time along with the representation of flood propagation. For that reason, it can be useful to consider appropriate grid size while establishing a hydraulic model to reduce computational cost as well as the representation of flood propagation. Additional to this information, water depth change with respect to spatial resolution is presented with graphs (Figure 4-11 to 4-20).

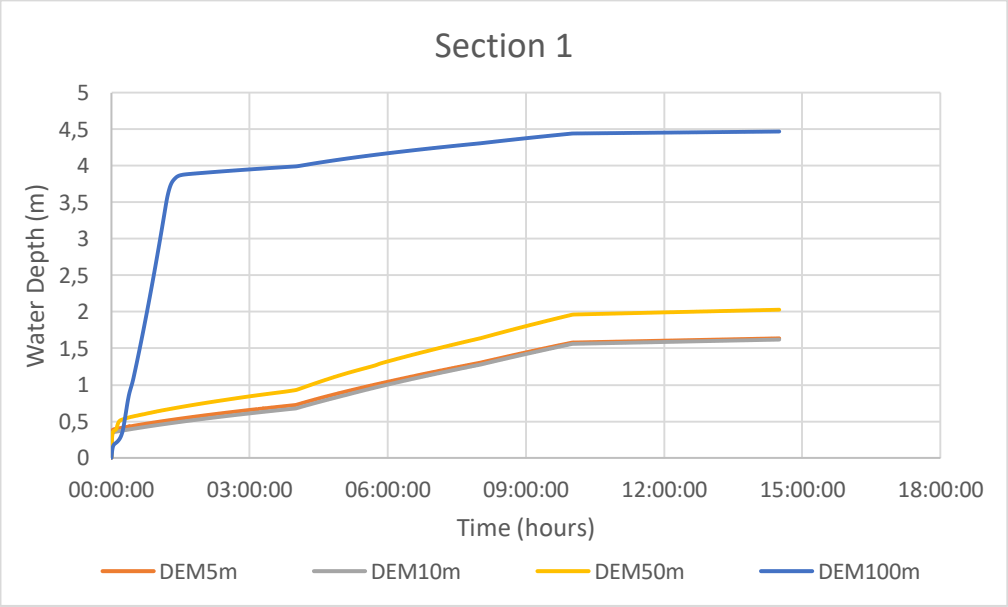

Figure 4-11 Water depth change at Section 1 due to different spatial resolutions

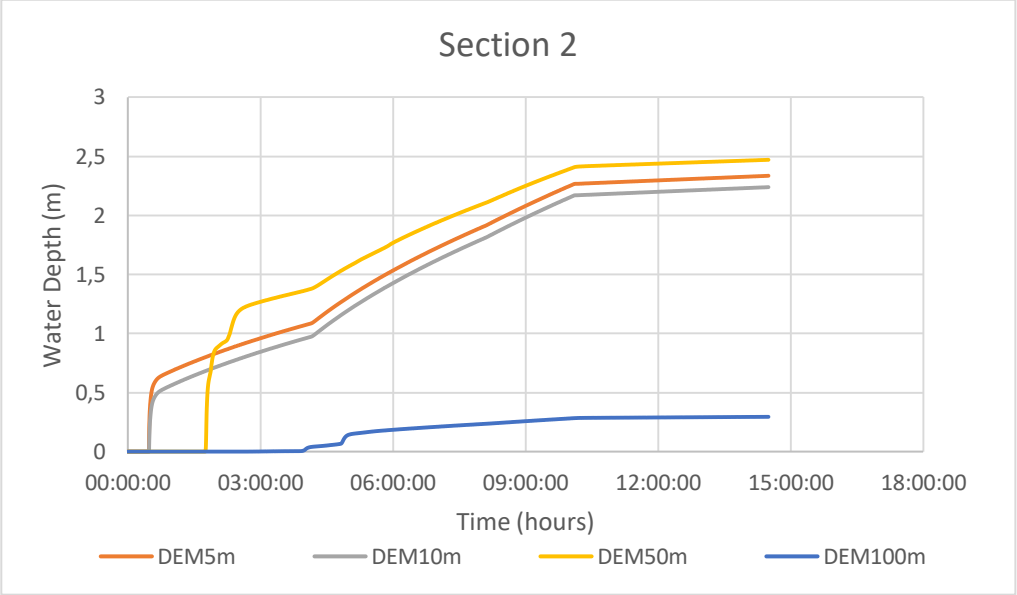

Figure 4-12 Water depth change at Section 2 due to different spatial resolutions

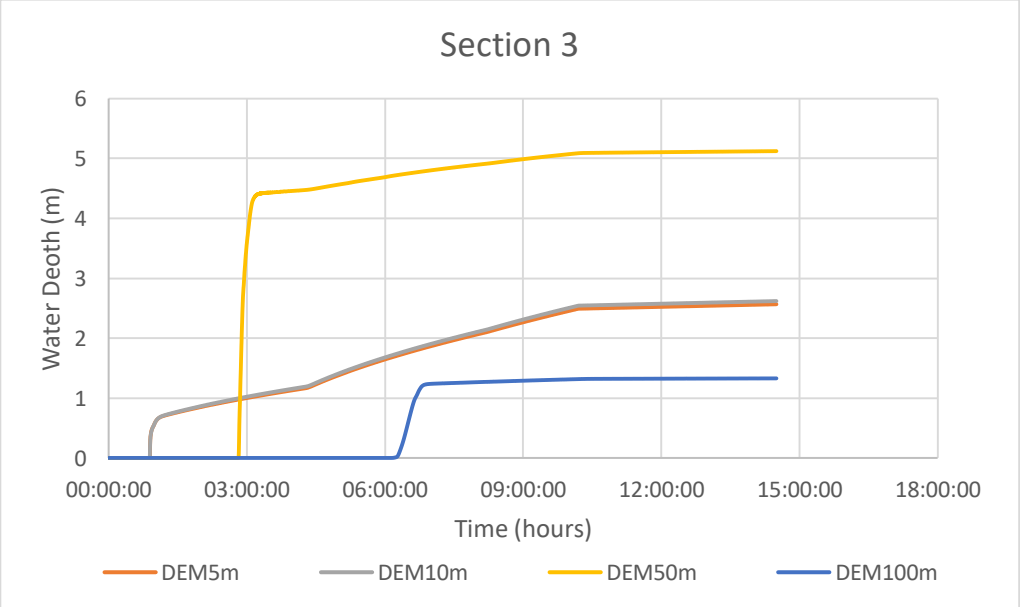

Figure 4-13 Water depth change at Section 3 due to different spatial resolutions

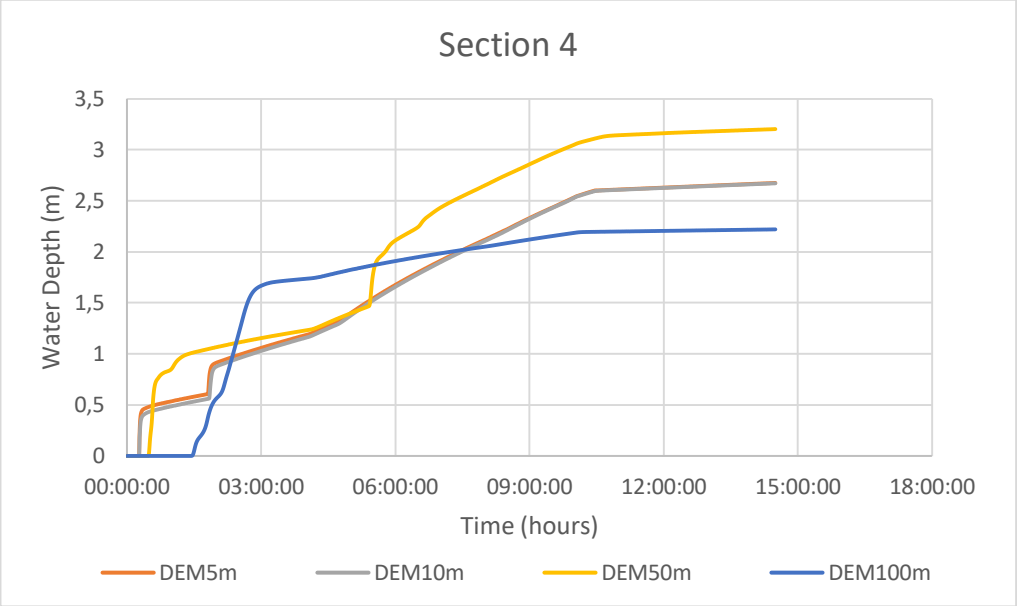

Figure 4-14 Water depth change at Section 4 due to different spatial resolution

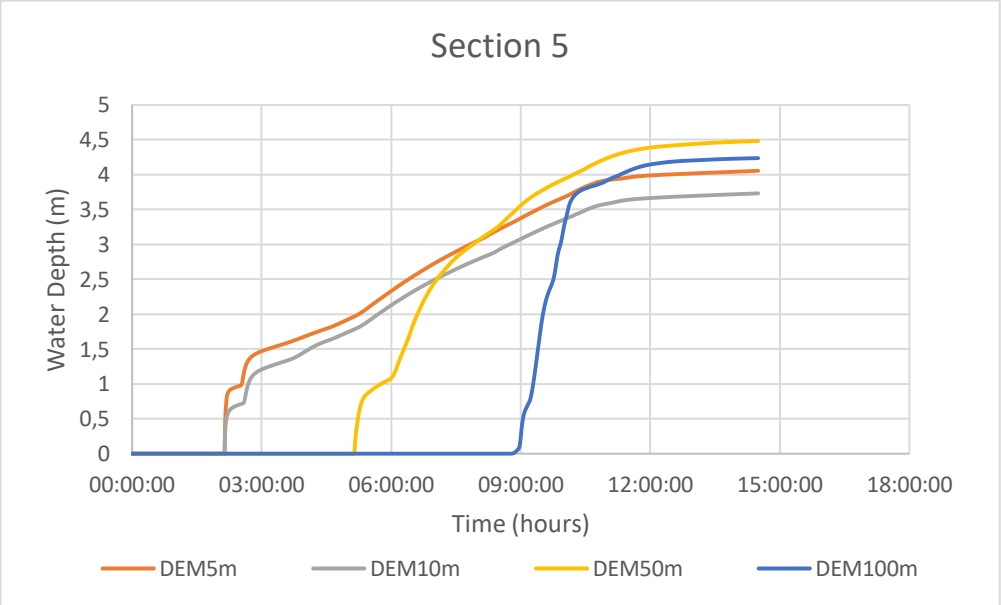

Figure 4-15 Water depth change at Section 5 due to different spatial resolutions

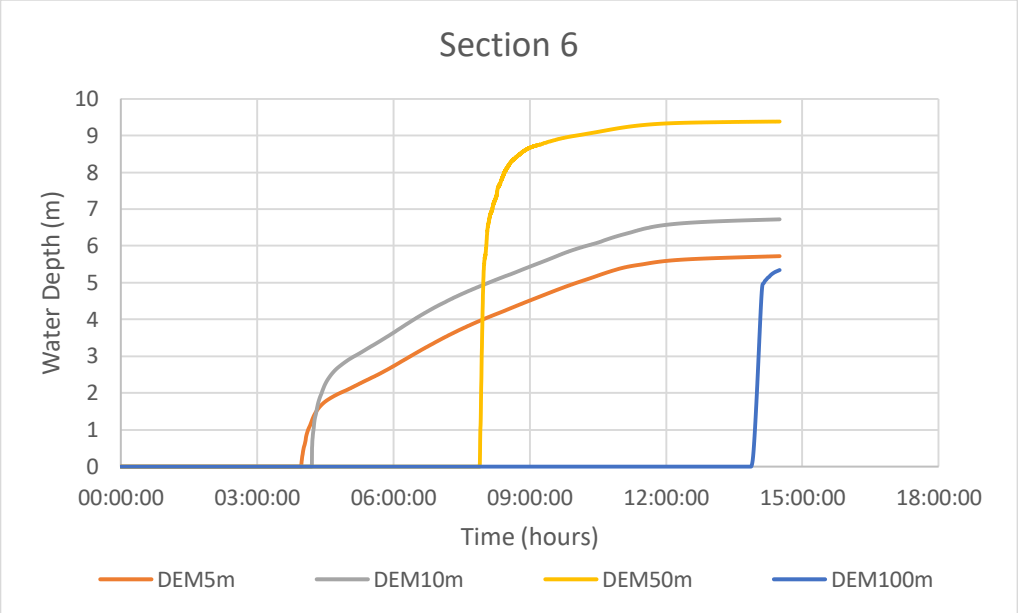

Figure 4-16 Water depth change at Section 6 due to different spatial resolutions

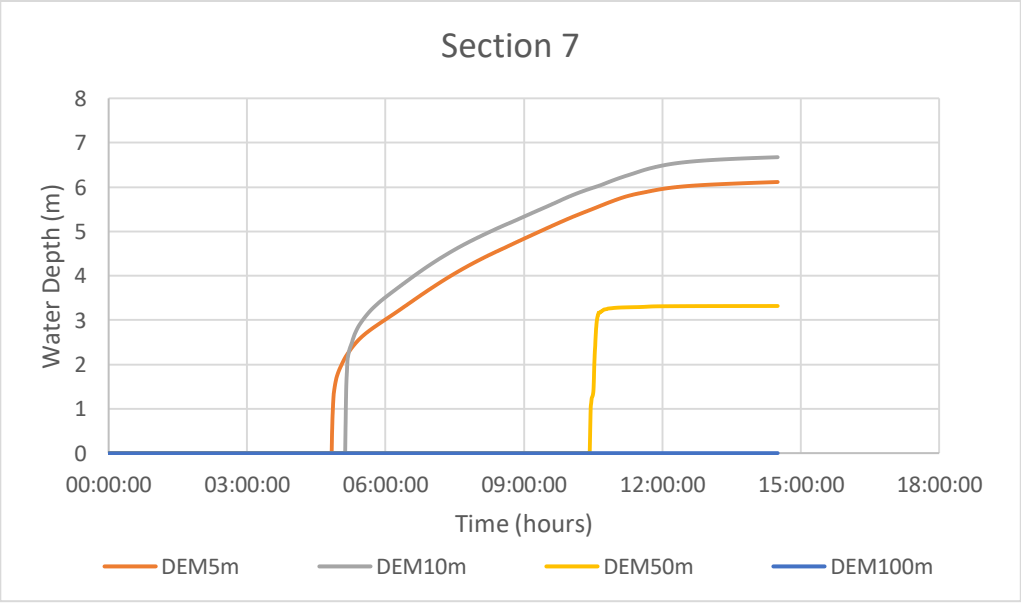

Figure 4-17 Water depth change at Section 7 due to different spatial resolutions

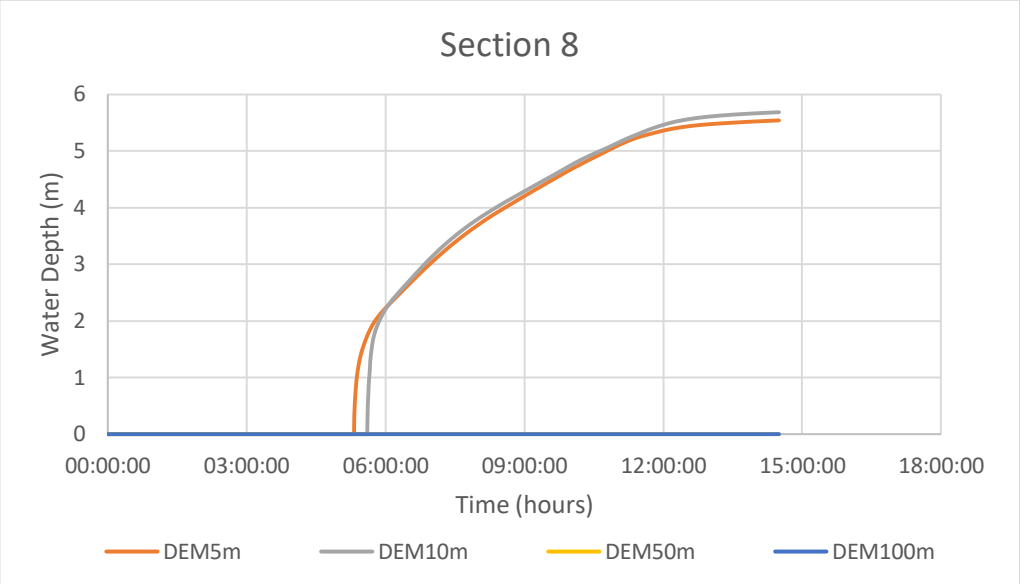

Figure 4-18 Water depth change at Section 8 due to different spatial resolutions

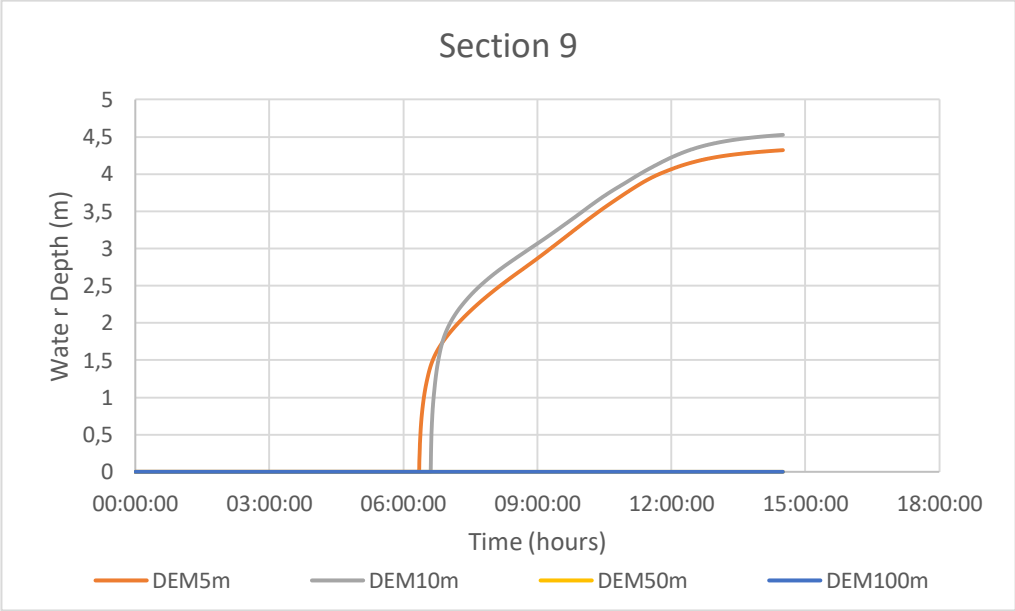

Figure 4-19 Water depth change at Section 9 due to different spatial resolutions

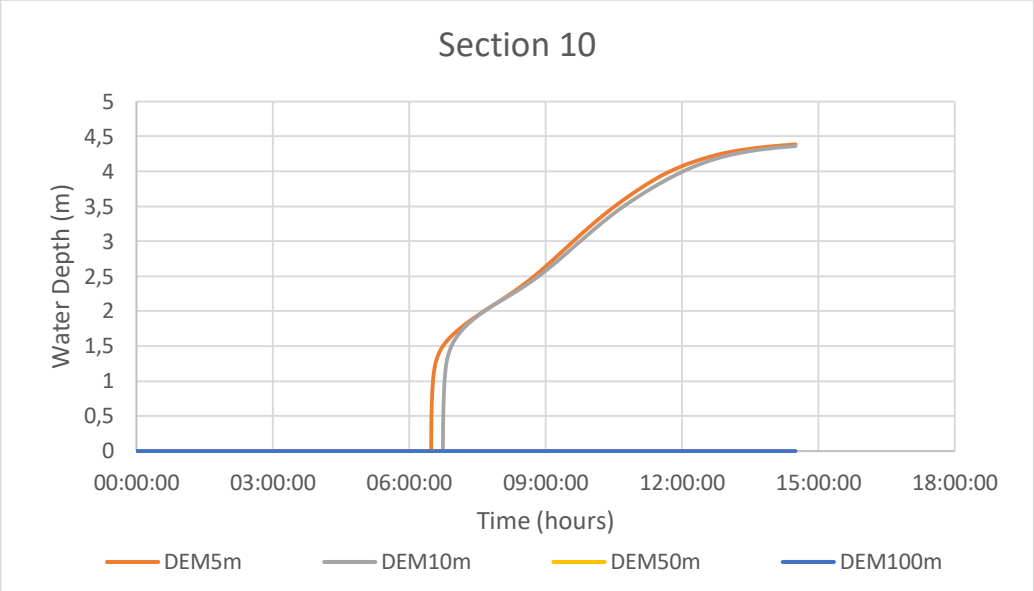

Figure 4-20 Water depth change at Section 10 due to different spatial resolutions

The resulting graphs show a consistency between fine resolutions. However, small differences occurred due to the local topographical characteristics. As for the coarse resolutions, calculated water depths are not consistent. There is no compatibility between the calculated water depths for each section and a significant difference in water depths is observed.

4.2.2. Effect of Roughness Coefficient for Floodplain

In this part of the analysis, simulations are run with the 5 m spatial resolution DEM. Simulation time is set to 14,5 hours and roughness coefficient is altered in the range of 0,040-0,10. The resulting flood extents (Figure 4-21) and local water depths are calculated by taking n=0,040 as base map. The benchmark study is made by comparing F-statistic and RMSE values for every roughness coefficient.

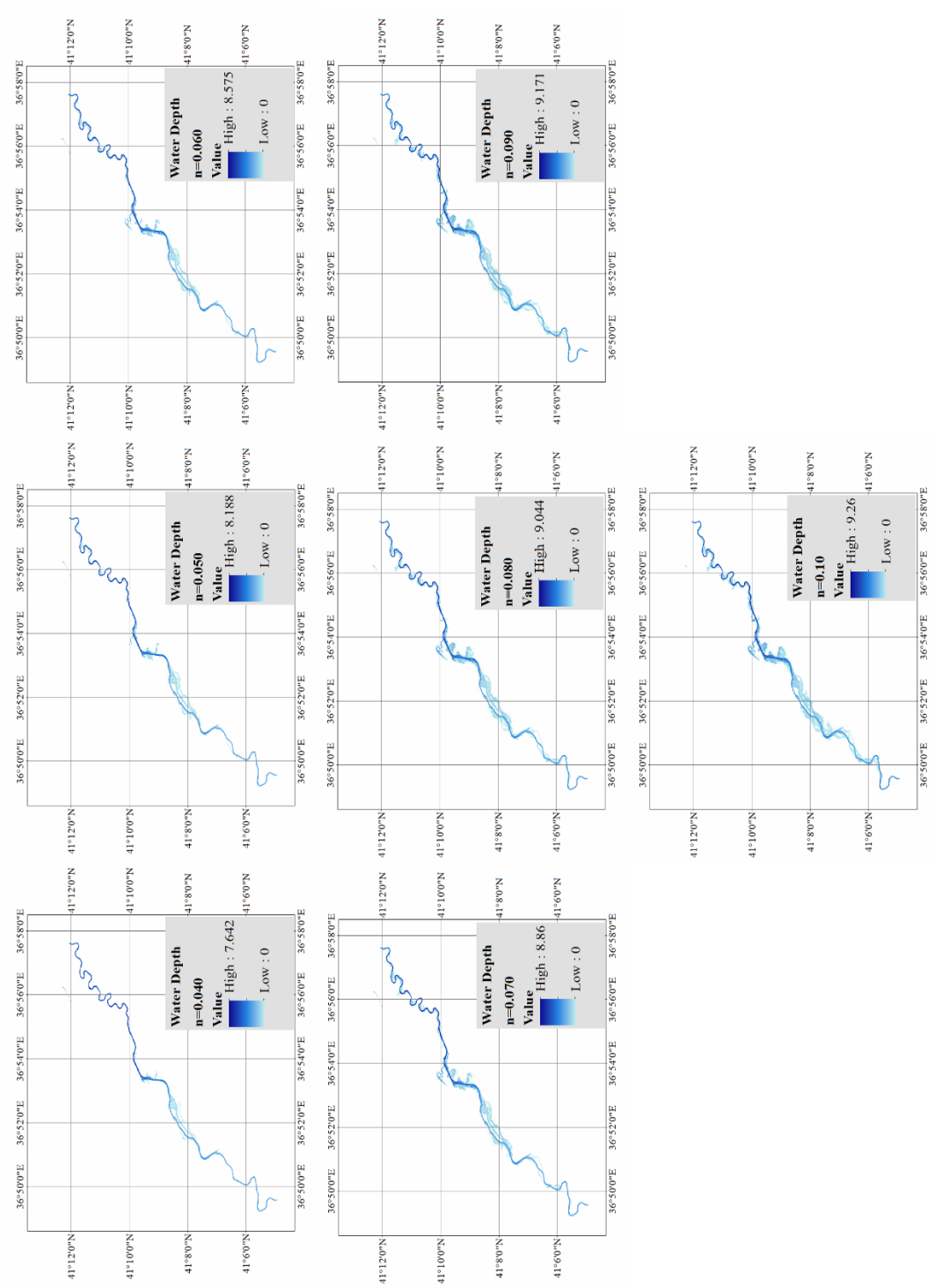

Figure 4-21 Flood extent for 5 m resolution and 14.5 hours simulation time by changing roughness coefficient in the range of 0,04-0,10

As it can be seen in the figures, increase in roughness coefficient affects the flood propagation by slowing it down for the constant simulation time. Water depth is calculated higher as the roughness coefficient increases because the roughness prevents the water propagation. Detailed simulation results are given in Appendix B. To make a detailed research F-statistic values are calculated for each roughness coefficient for and highest value is obtained for n=0,050 (Table 4-4), which means the closest result on flood propagation for base map n=0,040. These results show that, it is important to keep roughness value in a plausible range to obtain accurate results.

Table 4-4 F-static values of flood extents for different roughness coefficients

Spatial Resolution (m)	Roughness (base map n=0,040)	F-Statistic (flood extent)
5 m	0,040	-
	0,050	0,748
	0,060	0,583
	0,070	0,461
	0,080	0,370
	0,090	0,302
	0,100	0,253

Besides the flood propagation process, it is also important to understand local effects of roughness coefficient change. Therefore, water depth results of specified sections are obtained (Figure 4-22 to 4-31).

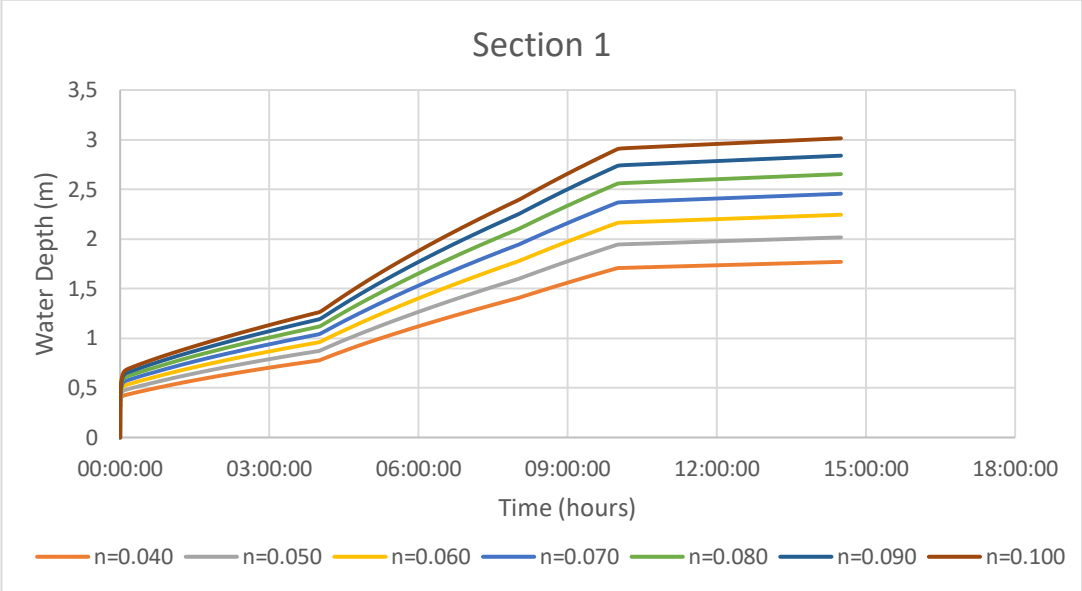

Figure 4-22 Water depth change at Section 1 due to roughness coefficient for 5 m resolution

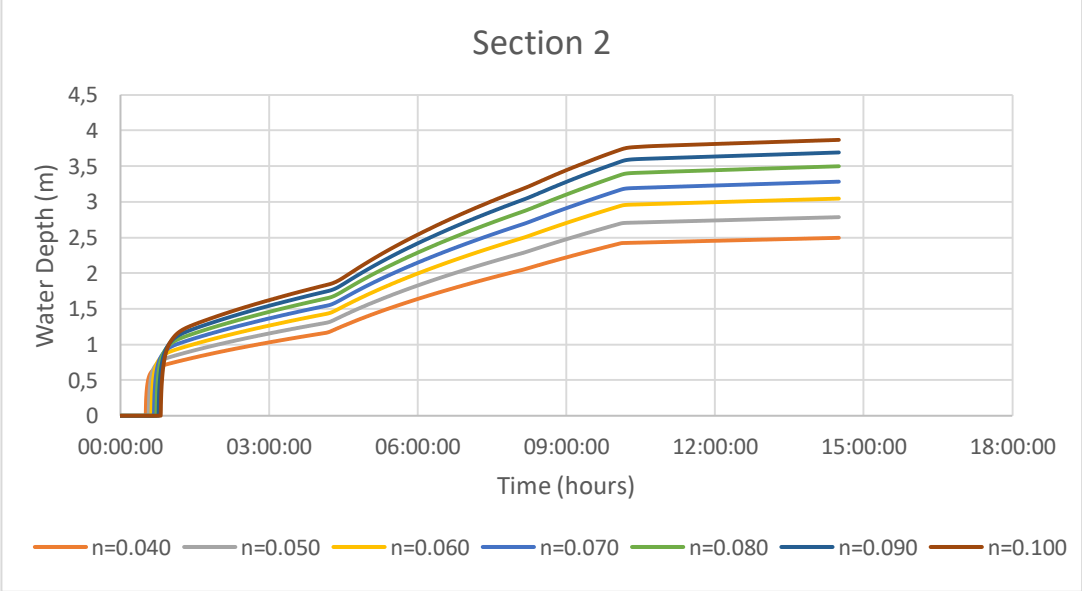

Figure 4-23 Water depth change at Section 2 due to roughness coefficient for 5 m resolution

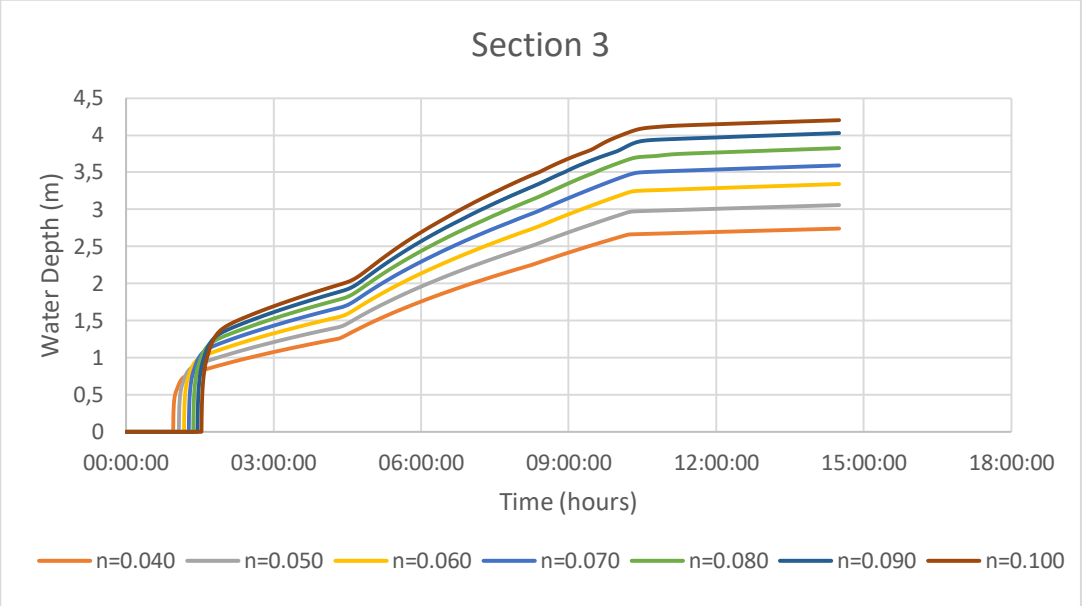

Figure 4-24 Water depth change at Section 3 due to roughness coefficient for 5 m resolution

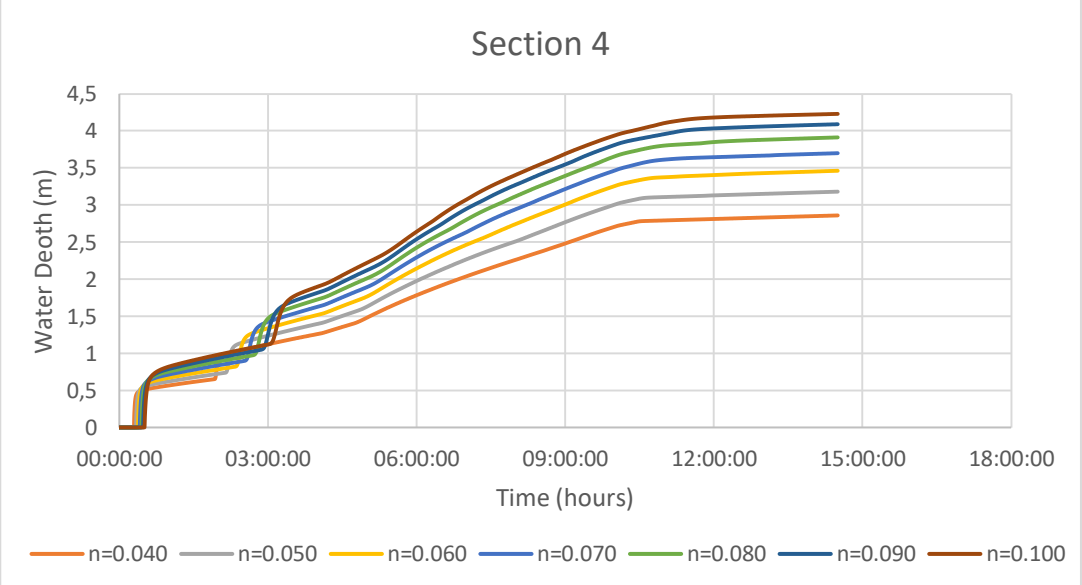

Figure 4-25 Water depth change at Section 4 due to roughness coefficient for 5 m resolution

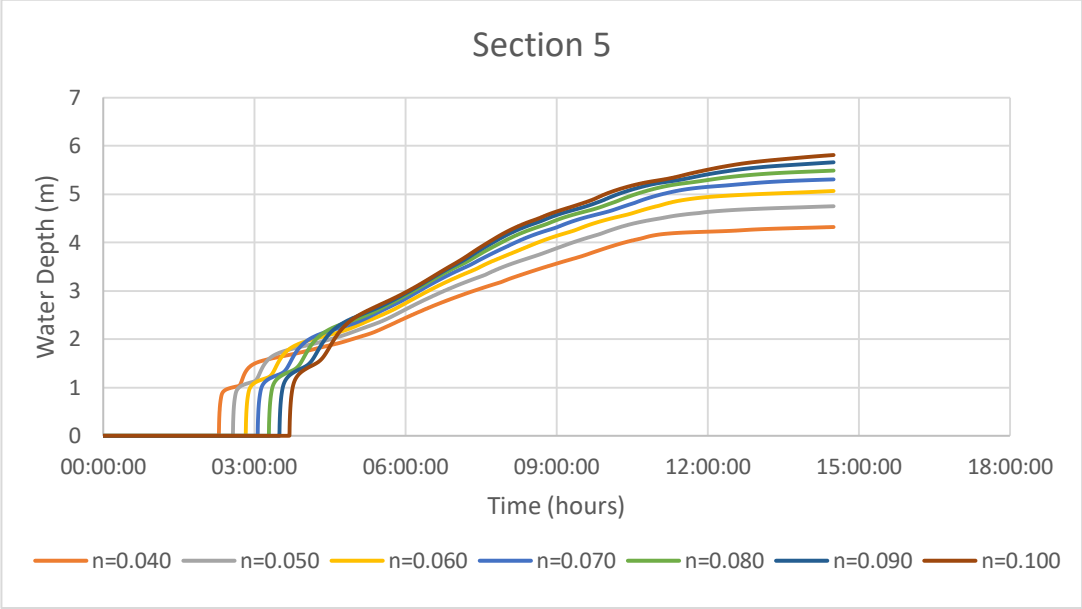

Figure 4-26 Water depth change at Section 5 due to roughness coefficient for 5 m resolution

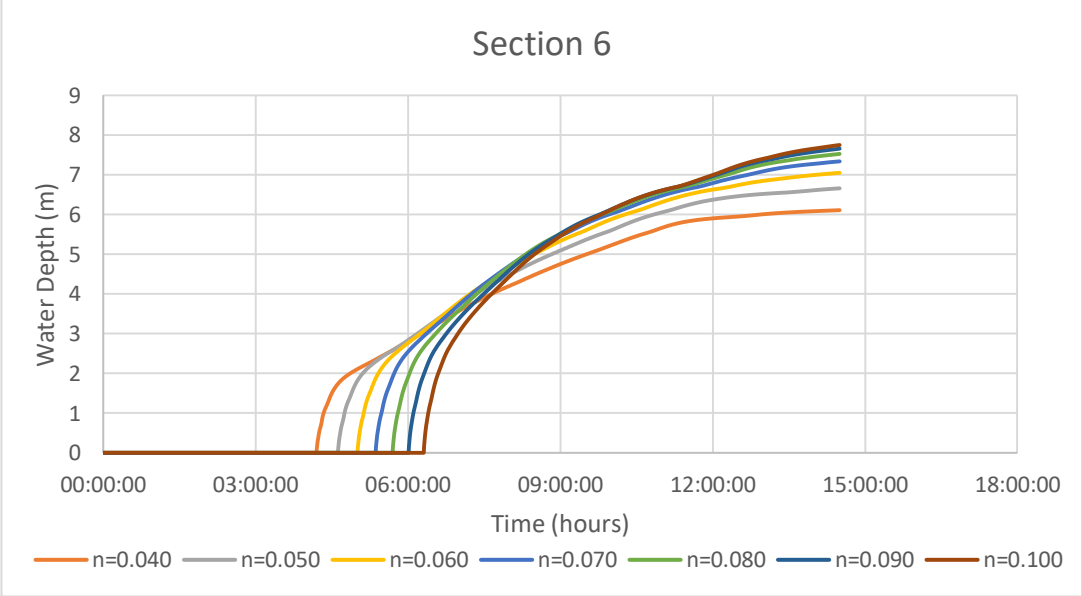

Figure 4-27 Water depth change at Section 6 due to roughness coefficient for 5 m resolution

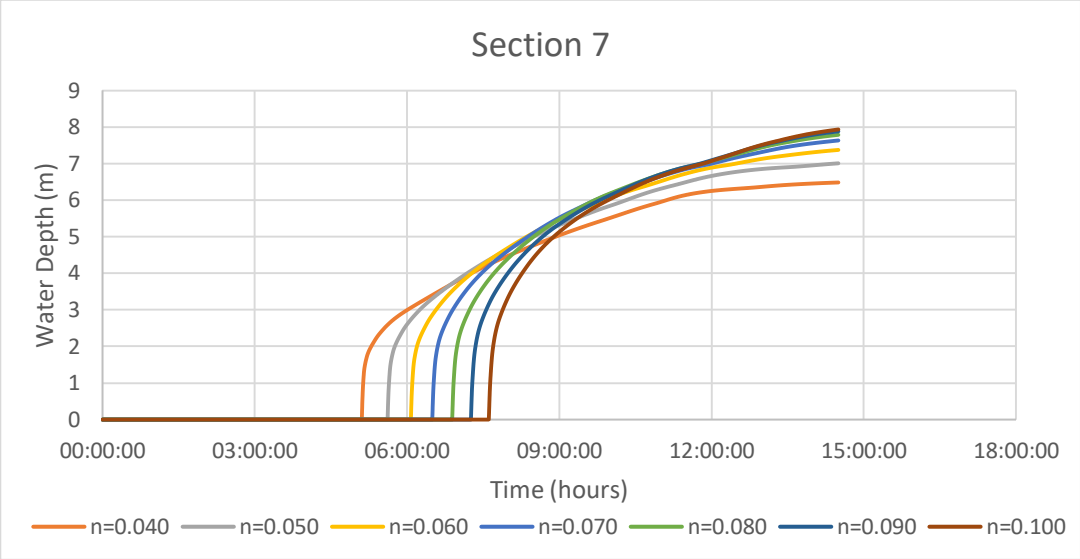

Figure 4-28 Water depth change at Section 7 due to roughness coefficient for 5 m resolution

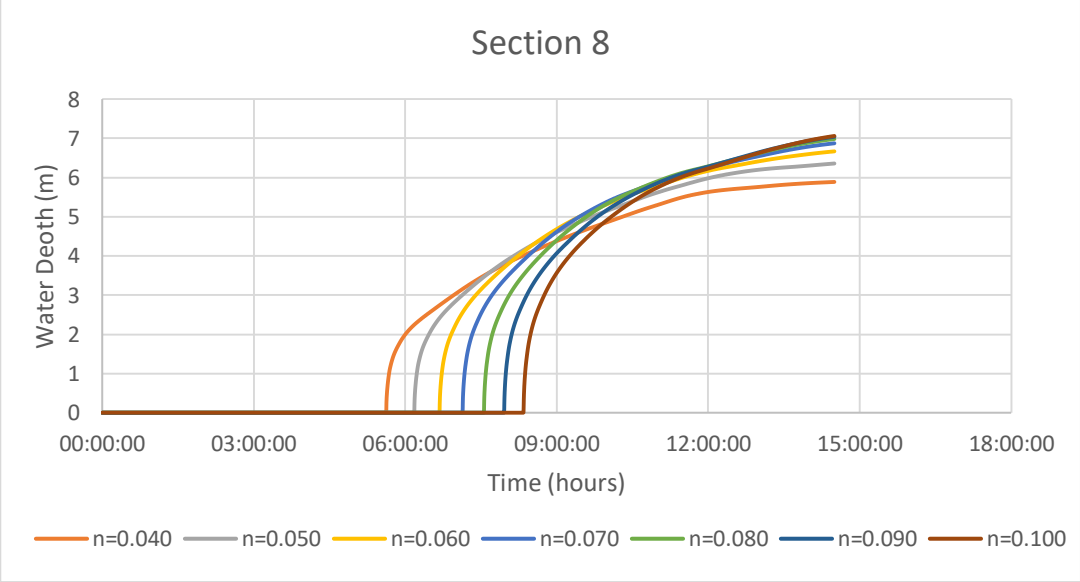

Figure 4-29 Water depth change at Section 8 due to roughness coefficient for 5 m resolution

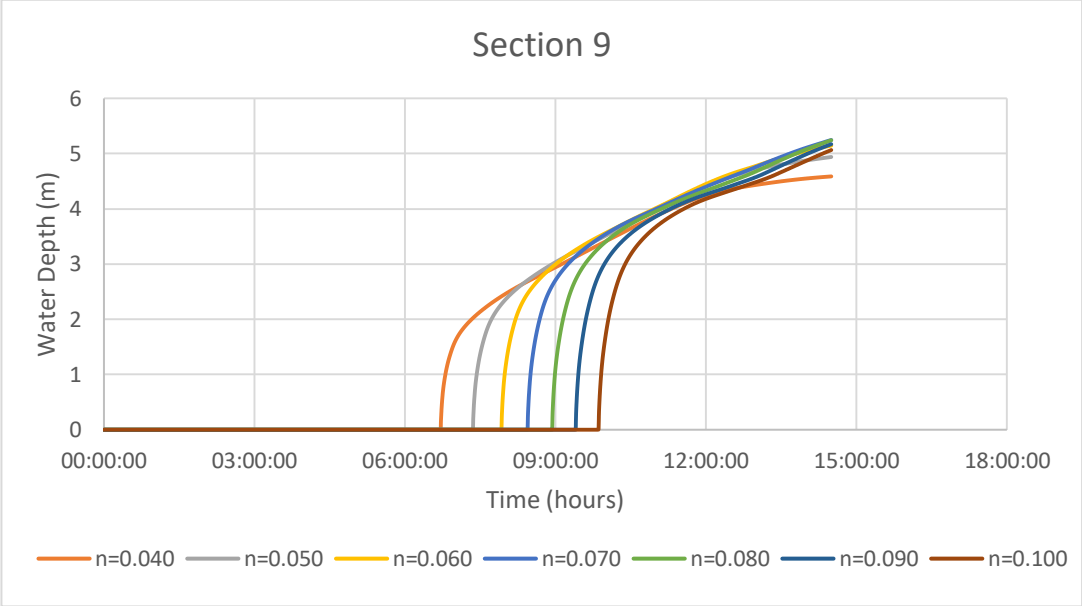

Figure 4-30 Water depth change at Section 9 due to roughness coefficient for 5 m resolution

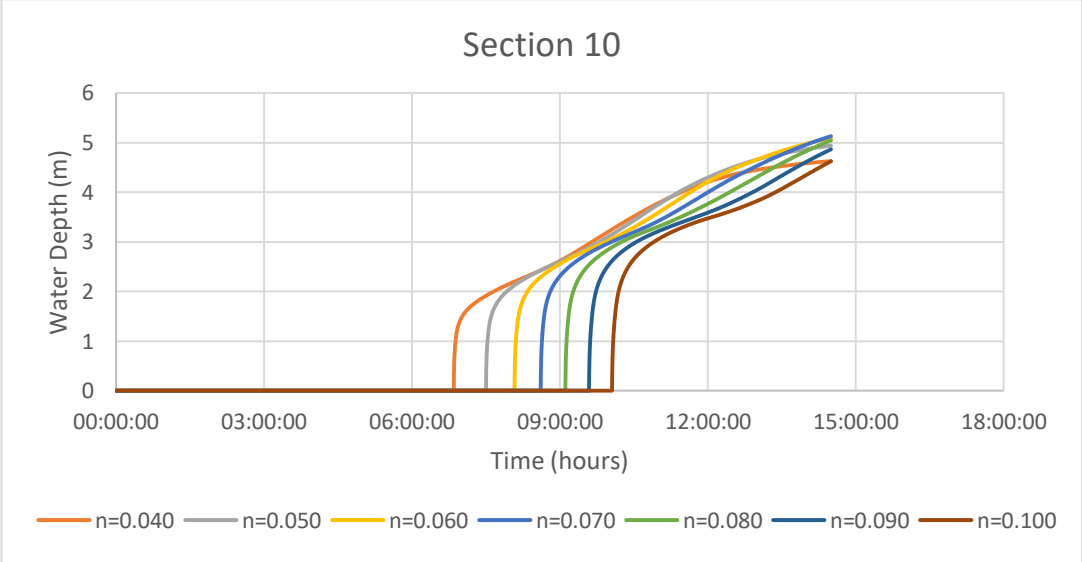

Figure 4-31 Water depth change at Section 10 due to roughness coefficient for 5 m resolution

The results show that assigning different roughness parameter (n) as boundary condition affects water depth. Increasing roughness parameter slows down the water due to the roughness as can be seen in the graphs time axis. These results prove that roughness parameter can be used as a calibration parameter and it would give better predictions if it is selected in an appropriate range (Table 4-5). Lowest RMSE value is obtained for n=0,05 which also gives the closest result on flood propagation compared to the result of base map with n=0,040.

Table 4-5 Water depth RMSE values for 5 m resolution due to roughness change compared to the result of base n=0,040

Water Depth RMSE						
Sections / Roughness	0,05	0,06	0,07	0,08	0,09	0,1
Section 1	0,179	0,345	0,499	0,645	0,782	0,912
Section 2	0,219	0,413	0,590	0,752	0,899	1,036
Section 3	0,239	0,448	0,635	0,804	0,956	1,091
Section 4	0,236	0,437	0,611	0,762	0,892	1,003
Section 5	0,304	0,517	0,685	0,810	0,909	0,989
Section 6	0,391	0,645	0,831	0,969	1,081	1,177
Section 7	0,496	0,794	1,022	1,207	1,368	1,515
Section 8	0,441	0,713	0,927	1,108	1,270	1,422
Section 9	0,384	0,608	0,784	0,940	1,088	1,236
Section 10	0,369	0,565	0,727	0,882	1,039	1,202

As the last step of this analysis, RMSE variation for the x-sections is obtained to have a further look on the changes due to spatial resolution (Figure 4-32).

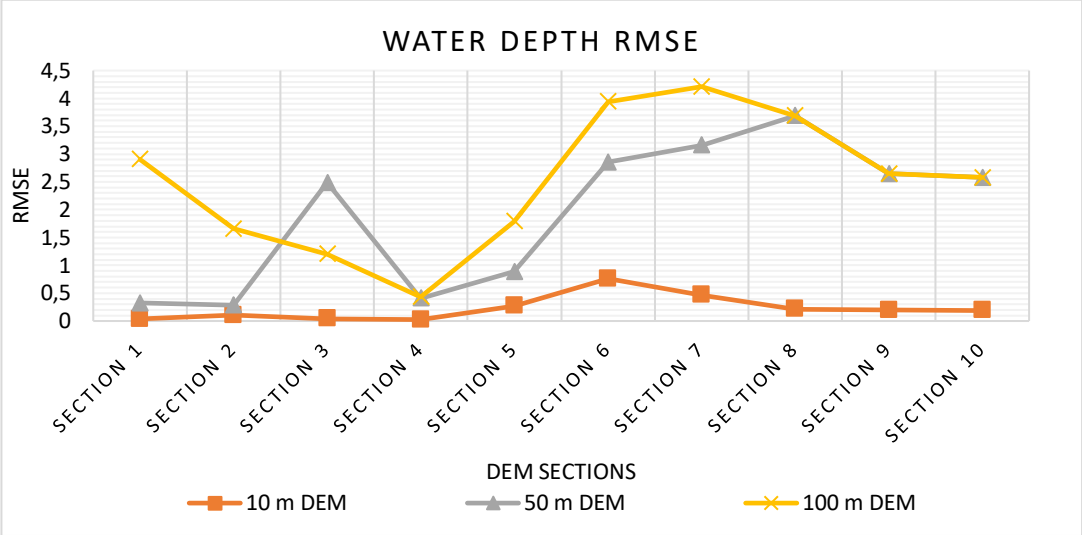

Figure 4-32 Water depth RMSE for all sections and spatial resolutions

Section 1 is located in the urbanized area at the beginning of the DEM. The channel is wide, and irregular sedimentation exists around the river channel besides the structures such as buildings (Figure 3-7b). The distortion in the section is not so significant for 50 m resolution (Figure 3-7a). Section 2 is located at the end of a meandered part of the DEM. Irregular sedimentation around the river channel is quite noticeable and a slight vegetation exists (Figure 3-8b). The distortion of the Section 2 is more distinct in comparison to Section 1 for 50 m resolution (Figure 3-8a). Figure 4-32 shows that RMSE value calculated for Section 1 is greater than Section 2 for 100 m resolution. Therefore, it can be said that sedimentation itself has no significant effect in the results however, when it is combined with the structures such as buildings around the channel the results are biased more due to the resampling. Namely, as the elevation variation increases in the terrain the bias in the results also increase.

Section 3 is in the meandered part of the DEM. This section includes both vegetation and sedimentation (Figure 3-9b). The distortion for that section is as significant as Section 1 (Figure 3-9a). As can be seen in Figure 4-32 the resulting RMSE values are incompatible with each other for 50 m and 100 spatial resolutions. This difference

shows that the combination of the topographical features such as meandering, braiding and the change in roughness coefficient such as sedimentation, vegetation, buildings have a significant effect in results.

Section 4 is in the meandering part of the DEM, yet the river channel looks quite smooth in spite of the sedimentation and vegetation in the side of the riverbed (Figure 3-10b). The details of the channel are dissolved significantly for 50 m resolution (Figure 3-10a). As can be seen in Figure 4-32 the calculated RMSE values are almost the same for 50 m and 100 m spatial resolutions. Accordingly, it can be said that the results are not biased by the meandering feature of the terrain due to the uniform roughness coefficient in the section.

Section 5 is located in an aligned path of the terrain. Except for the slightly irregular sedimentation around the riverbed, no disturbance is observed (Figure 3-11b). The details of this section is disappeared significantly for the 50 m resolution (Figure 3-11a). Also, Section 6 is located in an aligned path just before a meandering part begins. The river channel looks narrow with vegetation in the sides of the riverbed (Figure 3-12b). The channel section is distorted due to resampling (Figure 3-12a). Section 7 is in the meandering part of the terrain with an intense vegetation around the narrow river channel (Figure 3-13b). The riverbed section looks almost flat due the loss of information throughout the resampling process (Figure 3-13a). Section 8 is also in the meandering part of the terrain with sedimentation on one side of the river channel and vegetation formations on both sides (Figure 3-14b). The channel details are still meaningful even though some slight losses due to the resampling (Figure 3-14a).

Section 9 is also located in the meandering part of the terrain with sedimentation on one side besides vegetation and some buildings exist on the other side of the riverbed (Figure 3-15b). The channel section is slightly distorted due to the resampling (Figure 3-15a). Section 10 is at the end of the DEM with an intense vegetation on both sides of the riverbed (Figure 3-16b). The depth of the river channel is dissolved throughout

the resampling process (Figure 3-16a). Since the water could not reach to these sections for the simulations run by coarse resolutions, similar RMSE values are calculated for these sections.

As can be seen in Figure 4-32 the change in calculated RMSE values are compatible for Section 5, Section 6, Section 7 and Section 8 even though the information loss in terms of topographical features throughout the resampling process or vegetation/sedimentation formations effecting roughness coefficient of the terrain. Considering the results in all sections, it can be said that roughness change and topographical features do not make any significant bias in the results but the combination of these two parameters affects the results of water depths.

4.3. Subgrid Channel Solver

In the previous section (section 4.2) the aim was to understand the sensitivity of the model by defining only the floodplain with respect to roughness parameter and spatial resolution. Subgrid solver is the most recent solver provided by LISFLOOD-FP which enables to define the channel characteristics as bankfull depth, channel width and channel slope. The advantage of Subgrid Channel Solver is to define the river channel characteristics as well as providing the identification of the roughness parameter for the channel and floodplain separately. In this study, these characteristics are extracted from the bathymetry data given in Figure 3-3. The river channel is extracted from the DEM with the x-sections containing the bankfull depth, slope and channel width data by using ArcGIS.

Since the roughness coefficient for upstream part of the study area is calculated as n=0,04 for subgrid channel solver simulation, the same value was assigned to the floodplain. As for the channel roughness, roughness coefficient n=0,035 was assigned since it is the value which eliminates the stabilization errors of the system.

Another advantage of Subgrid Channel Solver is the ability to define the channel and floodplain characteristics in terms of different spatial resolutions. Thus, it is provided to choose the representation of the details for the channel and floodplain separately. In this study, it is aimed to investigate how the model overcomes the information loss caused by resampling process by applying different spatial resolutions to the channel and floodplain. Since the hydraulic model allows using different spatial resolutions for the channel and the floodplain, a 5 m fine resolution is selected to preserve the channel details. However, 20 m, 30 m and 50 m spatial resolutions are assigned by compromising the representation of the floodplain characteristics due to the computational cost of the model. When fine resolutions such as 5 m is set for the floodplain, the runtime continues days to weeks. Even for 20 m resolution, the runtime reached to 1496,70 minutes which is almost more than one day. The runtime durations are also provided to show the computational cost (Table 4-6). For large areas, to run flood modeling run time is important. Therefore, the choice of the DEM resolution and strength of the computer processor should be considered while using Subgrid Channel Solver.

Since the Subgrid Channel Solver also uses the same formula with the Acceleration Solver while calculating the flood hydraulics, these two solvers are compared to see the effect of using different spatial resolutions and roughness parameters for the channel and floodplain. To make the comparison, roughness coefficient is taken as n=0,035 while using the Acceleration Solver, since it is set as n=0,035 for the Subgrid Channel Solver.

For the Subgrid Channel Solver simulations, the same hydrograph which is used for the Acceleration Solver in sensitivity analysis part is assigned (Figure 3-18). The simulation duration is shortened to 14,5 hours and the hydrograph is terminated when the peak discharge is reached. To prevent the backwatering effects, DEM boundaries are removed also for these simulations. As point source locations 22-45 Gökçeali AGI and the Basin 4 contribution to the main channel is selected and discharge hydrograph

is given to the system from these locations (Figure 3-20). To calculate the local water depth change, the same locations given in Figure 4-9 are selected. The resulting flood extents are presented in Figure 4-33 and detailed simulation results are given in Appendix C.

Table 4-6 Runtime of the Simulations

LISFLOOD-FP Solver	Spatial Resolution	Runtime (mins)
Acceleration Solver	5 m	284,17
	5 m (only channel)	161,85
Subgrid Channel Solver	20 m	1496,7
	30 m	392,53
	50 m	58,68

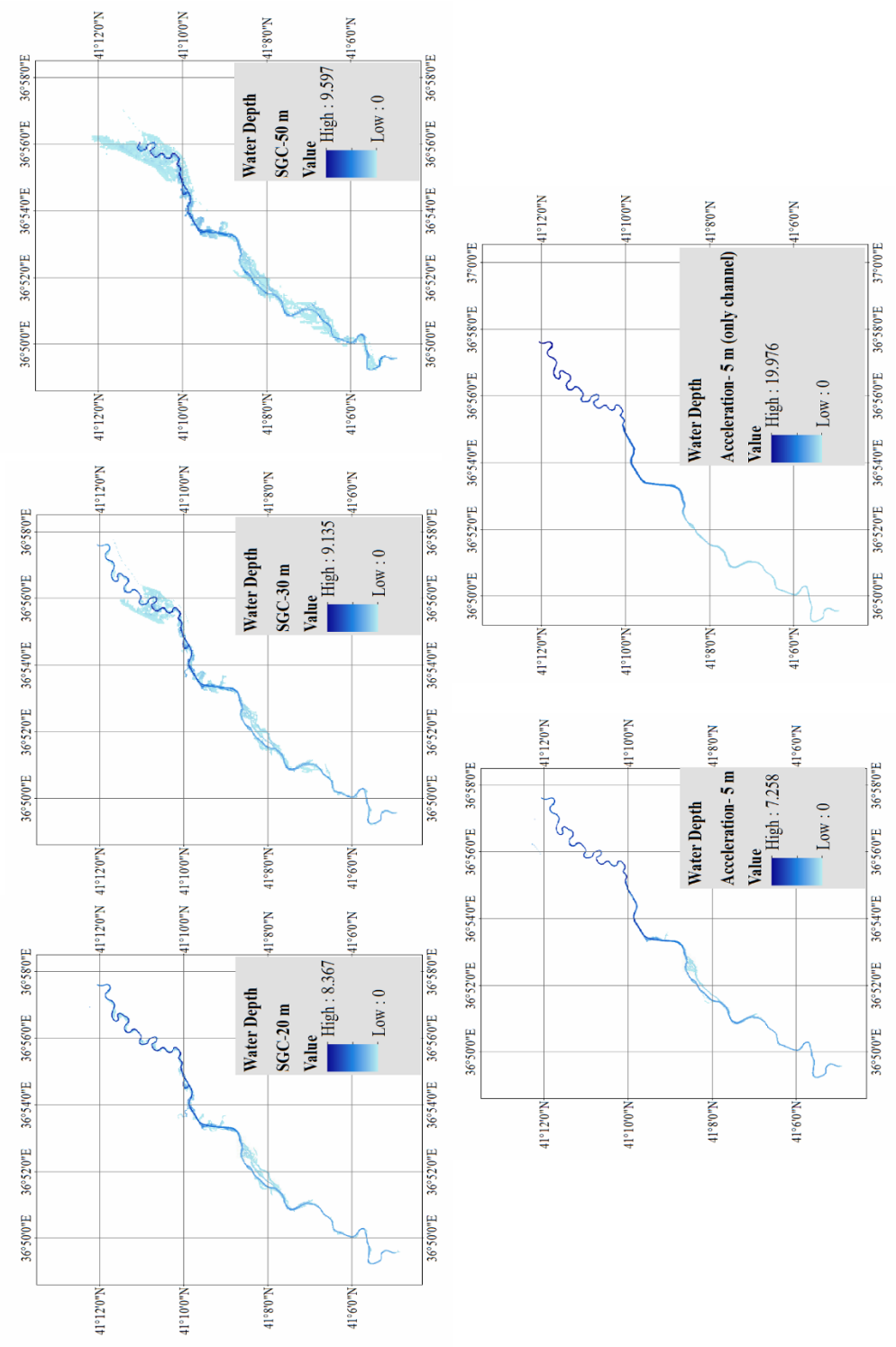

Figure 4-33 Subgrid Channel Solver and Acceleration Solver Results

The obtained flood extents show the effect of spatial resolution representing the flood inundation. As the resolution gets coarser, flood propagation increases most probably because of poor representation of the topography for the floodplain even though a fine resolution is used (5 m) for the channel. To show the difference between the flood extents, F-statistic values are calculated (Table 4-7). According to the F-statistic values, the closest result obtained for Acceleration Solver simulation with 5 m floodplain resolution is Subgrid Channel Solver simulation with 20 m floodplain and 5 m channel resolution.

In addition, Subgrid Channel Solver calculates the maximum water depth almost 15% higher (8,37 m) in comparison to Acceleration Solver (7,26 m). This result most likely stems from the use of different roughness coefficients for channel and floodplain as well as defining channel characteristics separately. The results on water depth also show that using coarse resolutions such as 20 m for the floodplain and a fine resolution 5 m for the channel on Subgrid Channel Solver gives better results than Acceleration Solver with 5 m floodplain resolution. On the other hand, considering computational costs, the use of the Acceleration Solver would be for the benefit of the user since it decreases the runtimes especially for fine resolutions depending on the strength of the processor of the computer.

Along with all these evaluations, the obtained results especially for the simulations run by fine resolutions are quite reasonable considering the information available in DSI report which indicates that the study area could pass a discharge of Q=510 m^3/s through the Terme Bridge without overflow.

To make a further investigation for the difference between the use of the Subgrid Channel Solver and the Acceleration Solver in terms of local water depths, the water depth at the x-sections obtained from the DEM are also presented (Figure 4-34 to 4-43).

Table 4-7 F-statistic values calculated by taking the Acceleration Solver result as base

LISFLOOD-FP Solver	Spatial Resolution	F-statistic (base 5 m acceleration solver)
Acceleration Solver	5 m	-
	5 m (only channel)	0,011
Subgrid Channel Solver	20 m	0,680
	30 m	0,570
	50 m	0,299

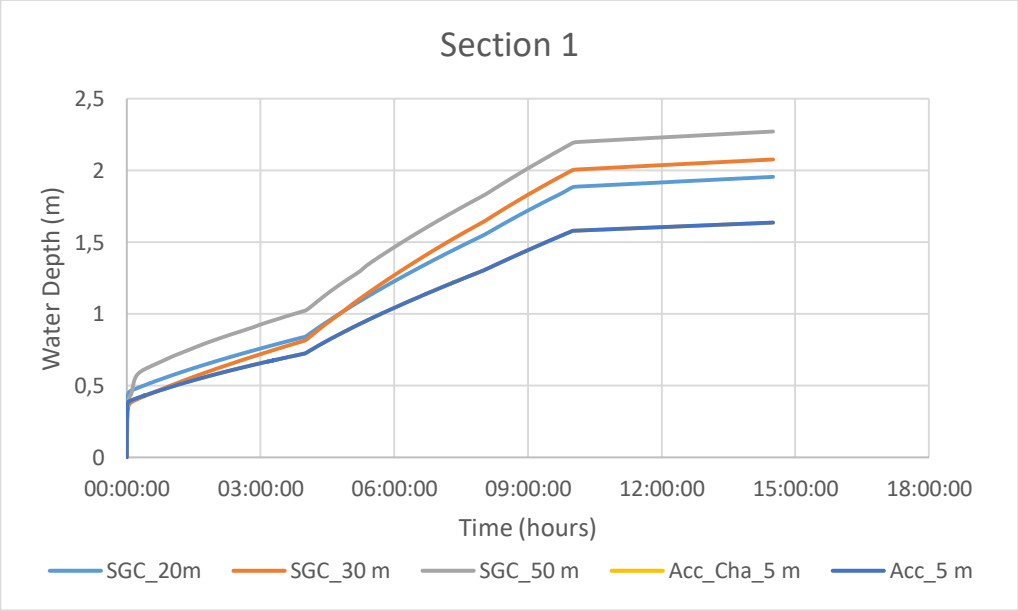

Figure 4-34 Local Water Depth Change for Subgrid Channel and Acceleration Solvers at Section 1

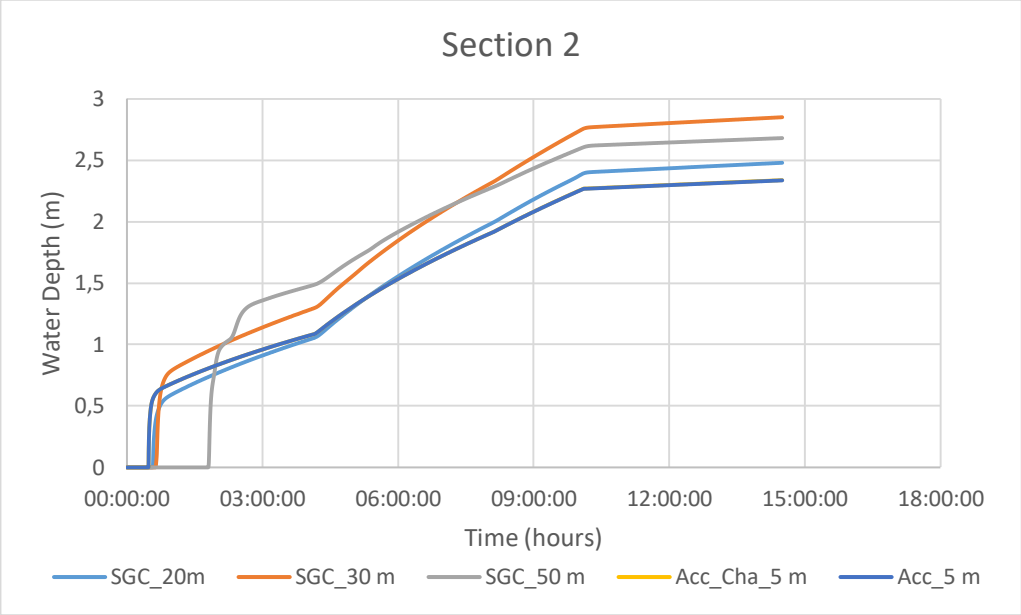

Figure 4-35 Local Water Depth Change for Subgrid Channel and Acceleration Solvers at Section 2

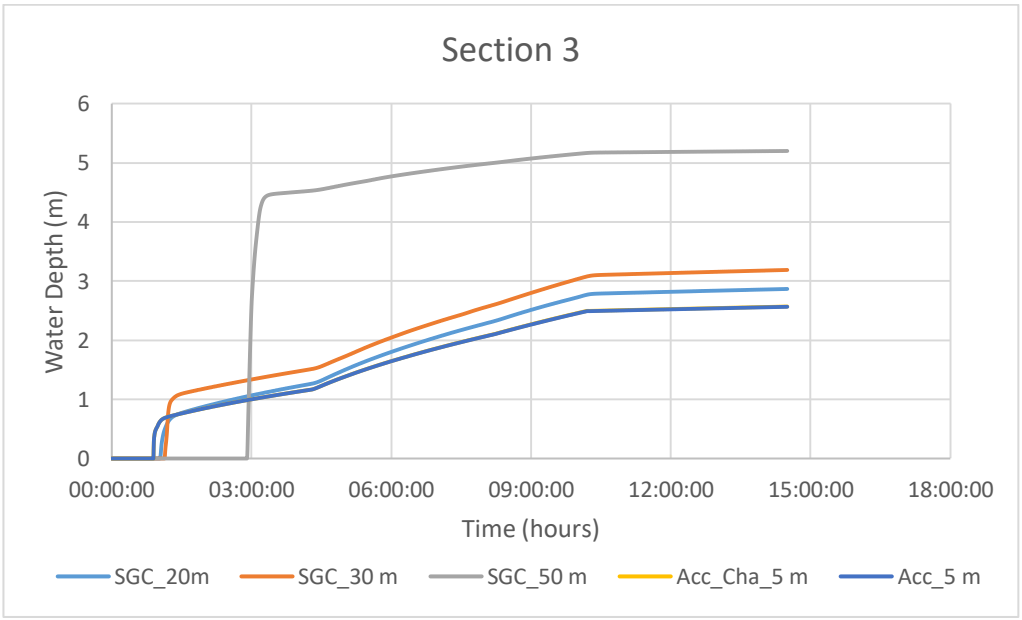

Figure 4-36 Local Water Depth Change for Subgrid Channel and Acceleration Solvers at Section 3

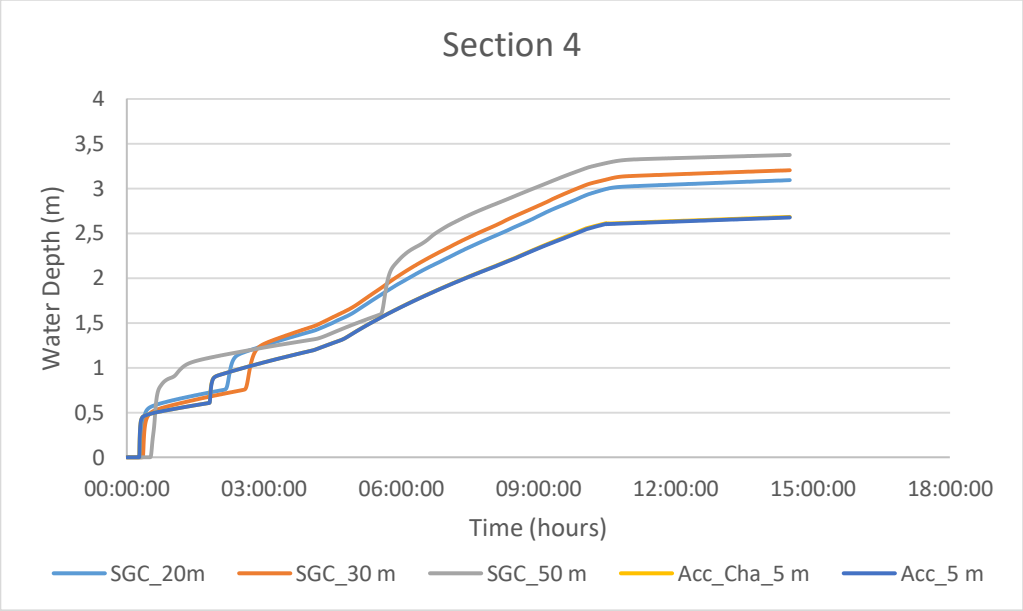

Figure 4-37 Local Water Depth Change for Subgrid Channel and Acceleration Solvers at Section 4

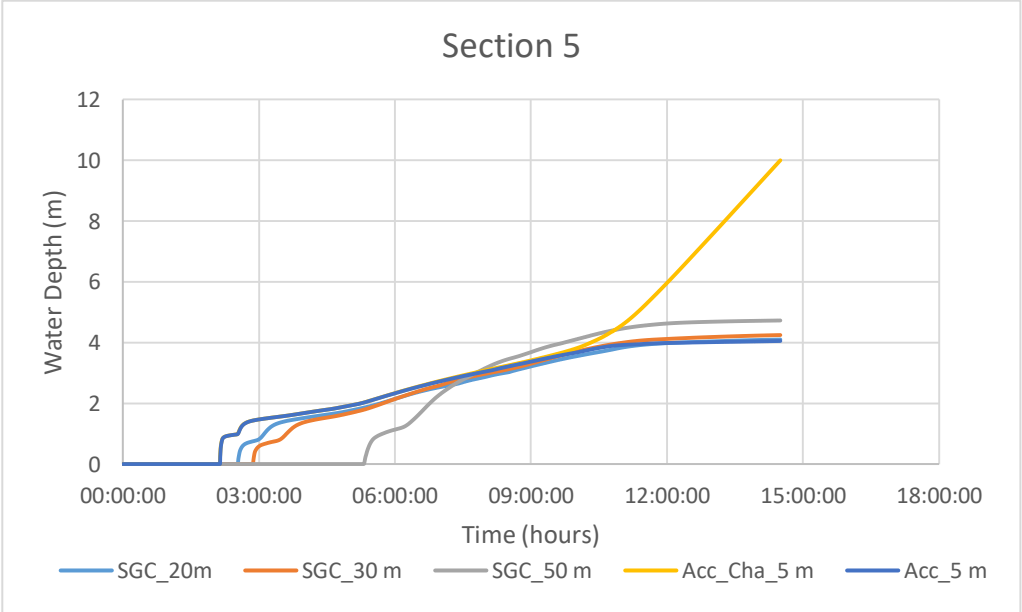

Figure 4-38 Local Water Depth Change for Subgrid Channel and Acceleration Solvers at Section 5

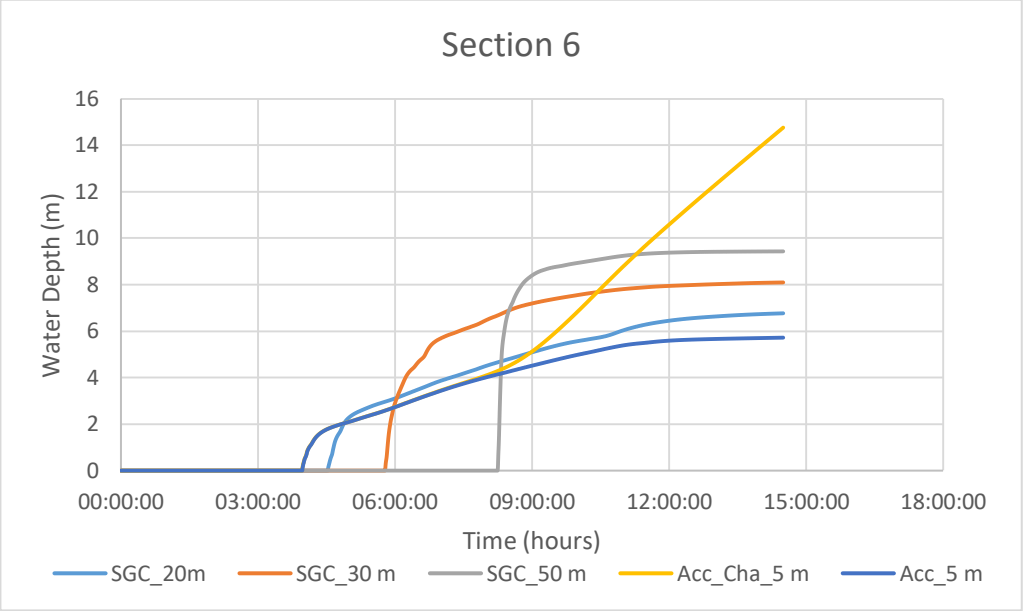

Figure 4-39 Local Water Depth Change for Subgrid Channel and Acceleration Solvers at Section 6

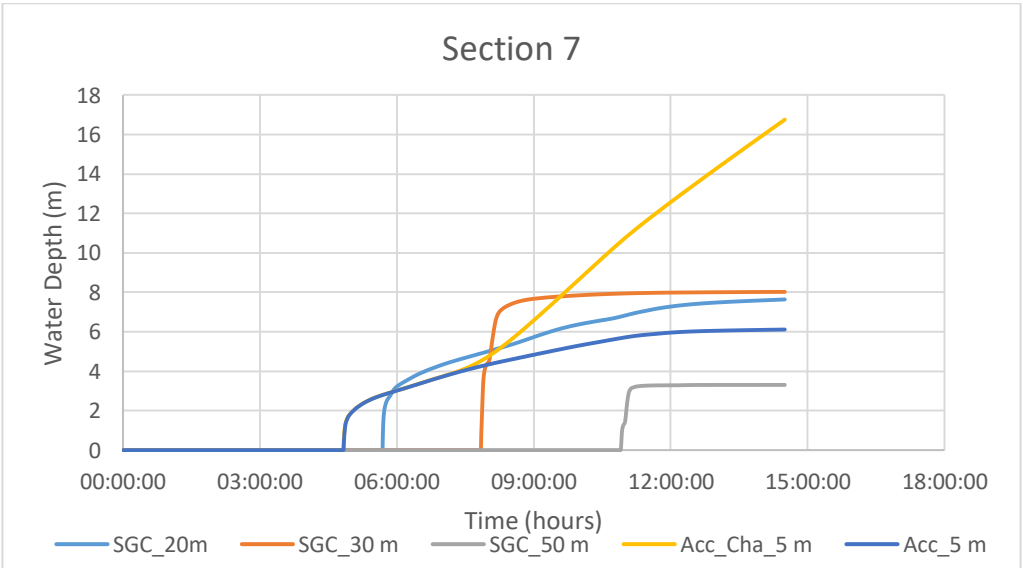

Figure 4-40 Local Water Depth Change for Subgrid Channel and Acceleration Solvers at Section 7

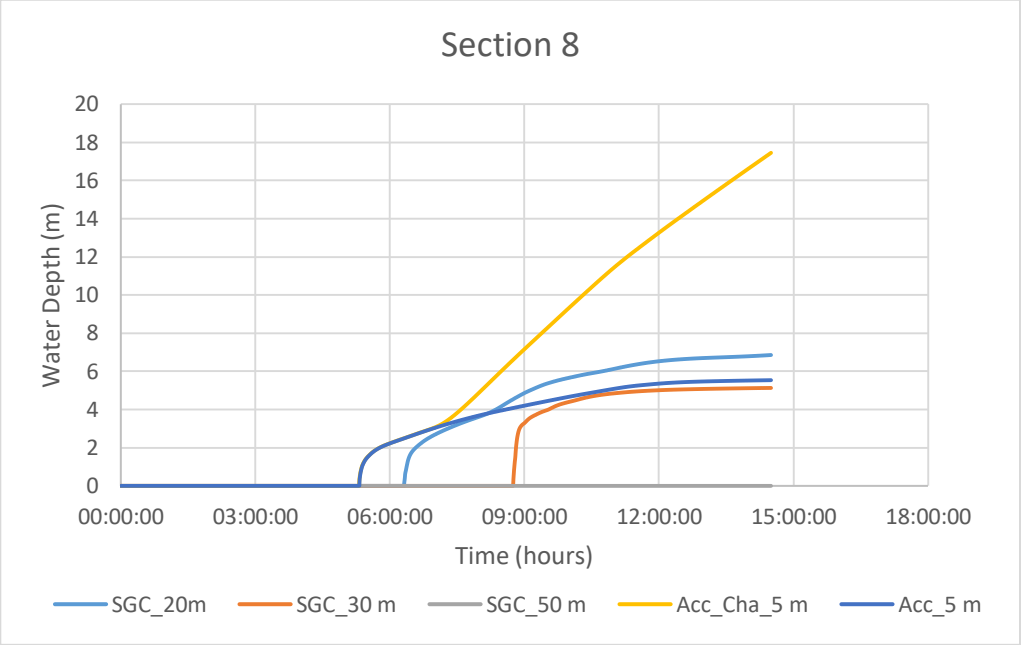

Figure 4-41 Local Water Depth Change for Subgrid Channel and Acceleration Solvers at Section 8

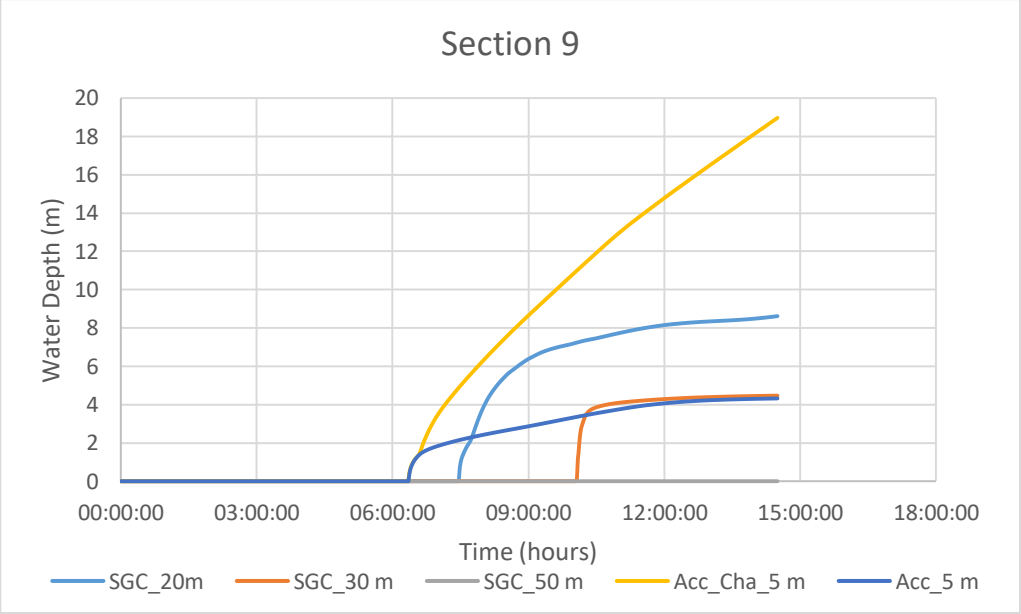

Figure 4-42 Local Water Depth Change for Subgrid Channel and Acceleration Solvers at Section 9

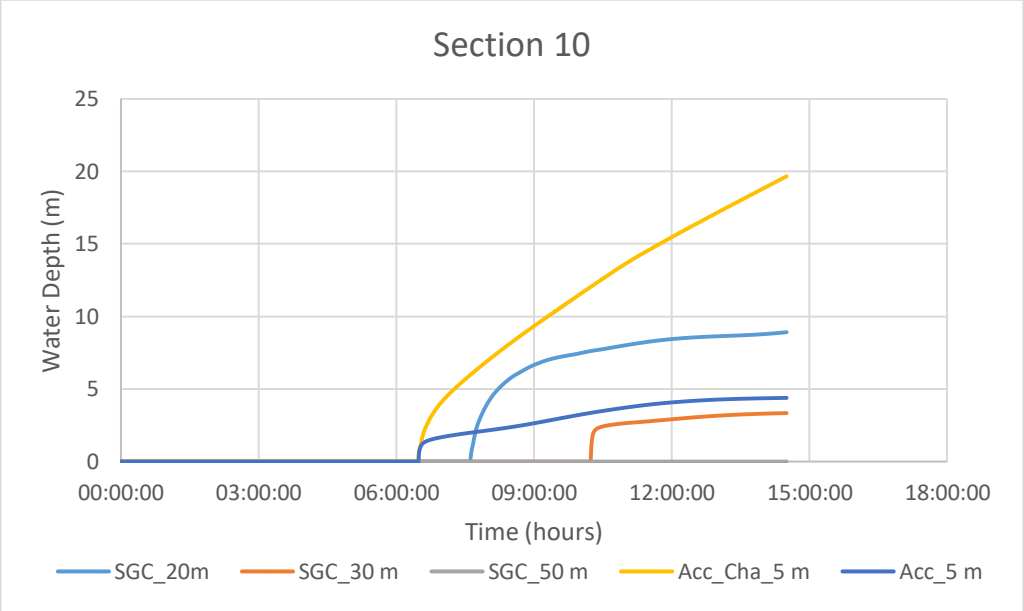

Figure 4-43 Local Water Depth Change for Subgrid Channel and Acceleration Solvers at Section 10

The graphs show that the Acceleration Solver generally makes underestimations in terms of local water depths compared to the Subgrid Channel Solver results. The flow reaches early to the x-sections especially taken after the braided end of the DEM which means the Acceleration Solver calculates the water speed higher in meandered parts. Since both solvers use the same formula while solving flood hydraulics, this difference likely to stem from the use of roughness parameter. Considering the change of the calculated velocities and the time of flow reaching to the meandered sections it can be said that the model is also sensitive to the topographical formations.

The Acceleration Solver simulation run by using only the channel extracted from tachometer DEM gives consistent results with the simulation run by using whole DEM in terms of local water depths until water reaches the Section 5 which is the braided part of the floodplain. After that section, channel simulation calculates the water depth

higher than the others. This result most likely stems from the considerable effect of the meandered parts on the hydraulic model.

Regarding the Subgrid Channel Solver results, resolutions coarser than 20 m causes over/under estimations in local water depths especially for the meandering parts of the DEM. For the simulation run by 50 m spatial resolution these over/under estimations can be observed significantly. The lag of flow reaching to the sections is also significant for the coarser resolutions due to the loss of topographical information while resampling.

The RMSE values are calculated regarding the local water depth changes to show how the meandered and braided sections are affected by the grid resolution and the selected solver (Table 4-8 and Figure 4-44). The table for RMSE of the water depths shows that the errors are calculated higher especially for the meandered parts which means the model is sensitive for the changes in topographical features.

Table 4-8 The RMSE values calculated by taking the 5 m resolution Acceleration Solver simulation results

Sections	Water Depth RMSE				
	5 m DEM	5 m Channel	SGC-20 m	SGC-30 m	SGC-50 m
Section 1	-	0,0005	0,2296	0,3072	0,4807
Section 2	-	0,0011	0,1035	0,3785	0,3968
Section 3	-	0,0031	0,2166	0,4783	2,6128
Section 4	-	0,0051	0,3134	0,4029	0,5543
Section 5	-	1,7467	0,2392	0,3449	0,9147
Section 6	-	3,2501	0,6274	1,9486	2,9251
Section 7	-	4,1483	1,0070	2,1330	3,0777
Section 8	-	4,9151	0,8897	1,5227	3,5455
Section 9	-	6,6988	2,6275	1,2850	2,5645
Section 10	-	7,1860	2,8461	1,3661	2,5236

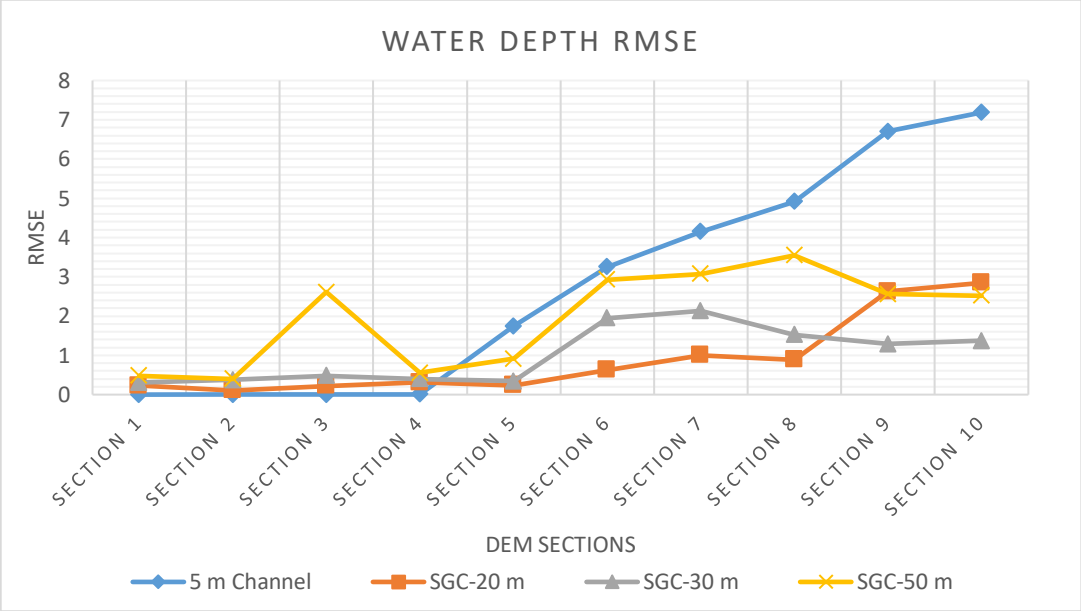

Figure 4-44 The RMSE trend according to local water depth section

RMSE values in terms of local water depth obtained, where Acceleration Solver results having 5 m spatial resolution is taken as base, is given in Figure 4-44. The lowest RMSE values are obtained for the Subgrid Channel Solver result which is run with 20 m floodplain and 5 m channel spatial resolution. Regarding to the coarser resolutions of the Subgrid Channel Solver, the RMSE values increased especially for the sections obtained at meandered part of the DEM. The increase in these errors likely to stem from poor representation of the topographical features. The simulation run by taking the channel only, gives the highest errors and shows an increase due to the strong effect of topographical conditions.

4.4. Flood Simulations for Q_{100} and Q_{500}

In this study, all simulations were run by using Q_{10}=446,74 m^3/s to test the results since it is known that "Q=510 m^3/s is passed through the Terme Bridge without overflow" and the obtained results were found reasonable. It is believed that LISFLOOD-FP can be used to obtain flood extent due to larger flood events.

Therefore, to see the consequences of a larger flood event in terms of water depth and flood propagation, Q_{100}=792,41 m^3/s and Q_{500}=1041,34 m^3/s discharge hydrographs were used as input. For the simulations 5 m spatial resolution DEM (Figure 3-2) was used while roughness coefficient was selected as n=0,040. In this part of the study, only the Acceleration Solver simulations were run because of the high computational cost of Subgrid Channel Solver simulations with these discharge values. In addition, the channel extracted from the DEM involving bathymetry data does not provide the appropriate data for Subgrid Channel Solver since it has limited extent compared to the DEM used in previous research carried out by using MIKE21 (Bozoğlu, 2015). The results are presented in Figure 4-45 and Figure 4-46 for Q_{100} and Q_{500} respectively. Figure 4-45 shows that the flood hydrograph having peak value as Q_{100}=792,41 m^3/s overflows with a 9,004 m maximum water depth and expands the inundated area as well as creating a slit in the pond towards the upstream. For hydrograph of Q_{500} having the peak values as 1041,34 m^3/s, the ponding area got larger and propagated to both sides of the river with a maximum water depth of 9,924 m. The flood extend values in terms of area is presented in Table 4-9.

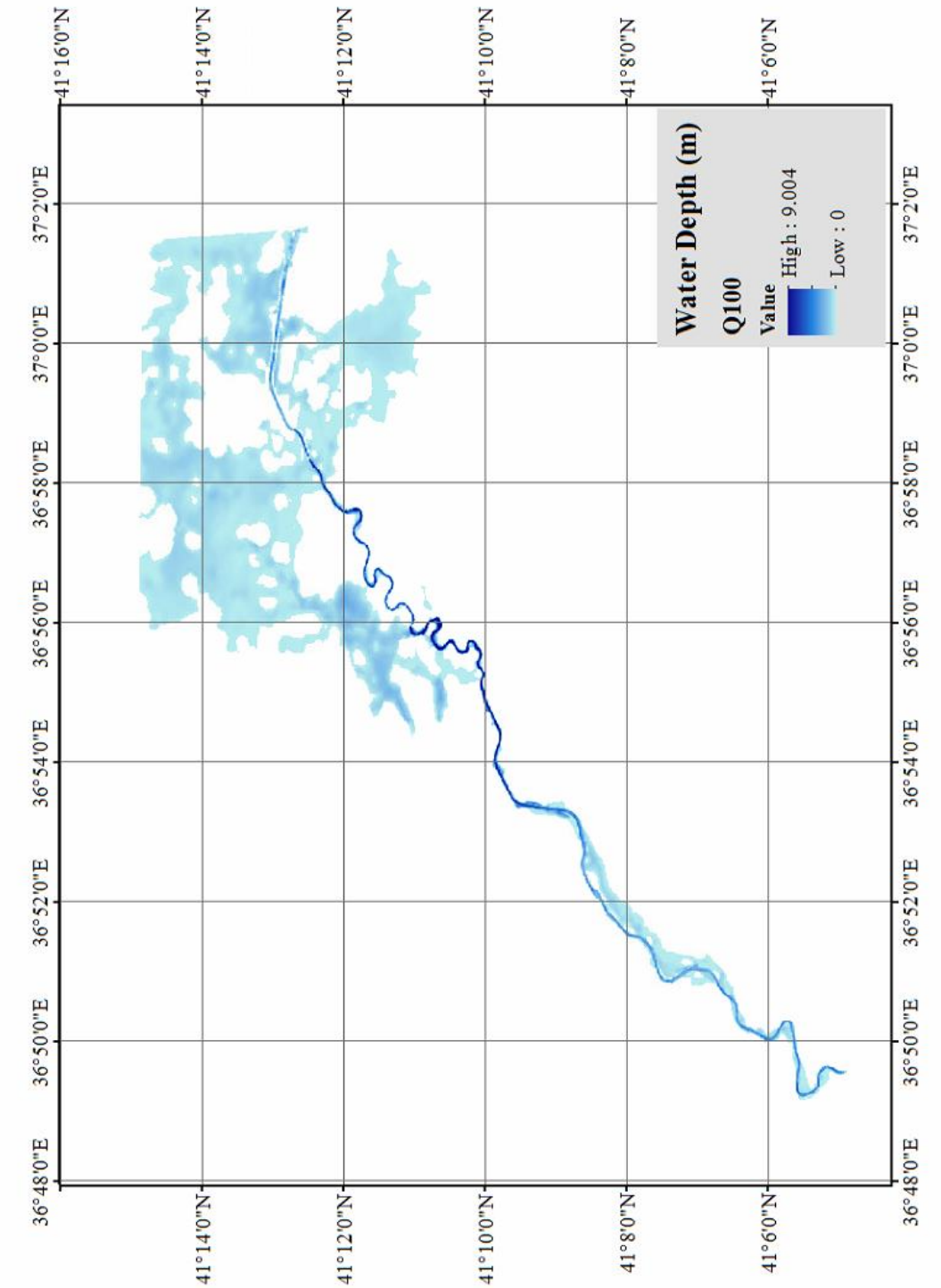

Figure 4-45 The resulting flood extent of Q_{100}= 792,41 m^3/s discharge hydrograph with n=0,040 and 5 m spatial resolution

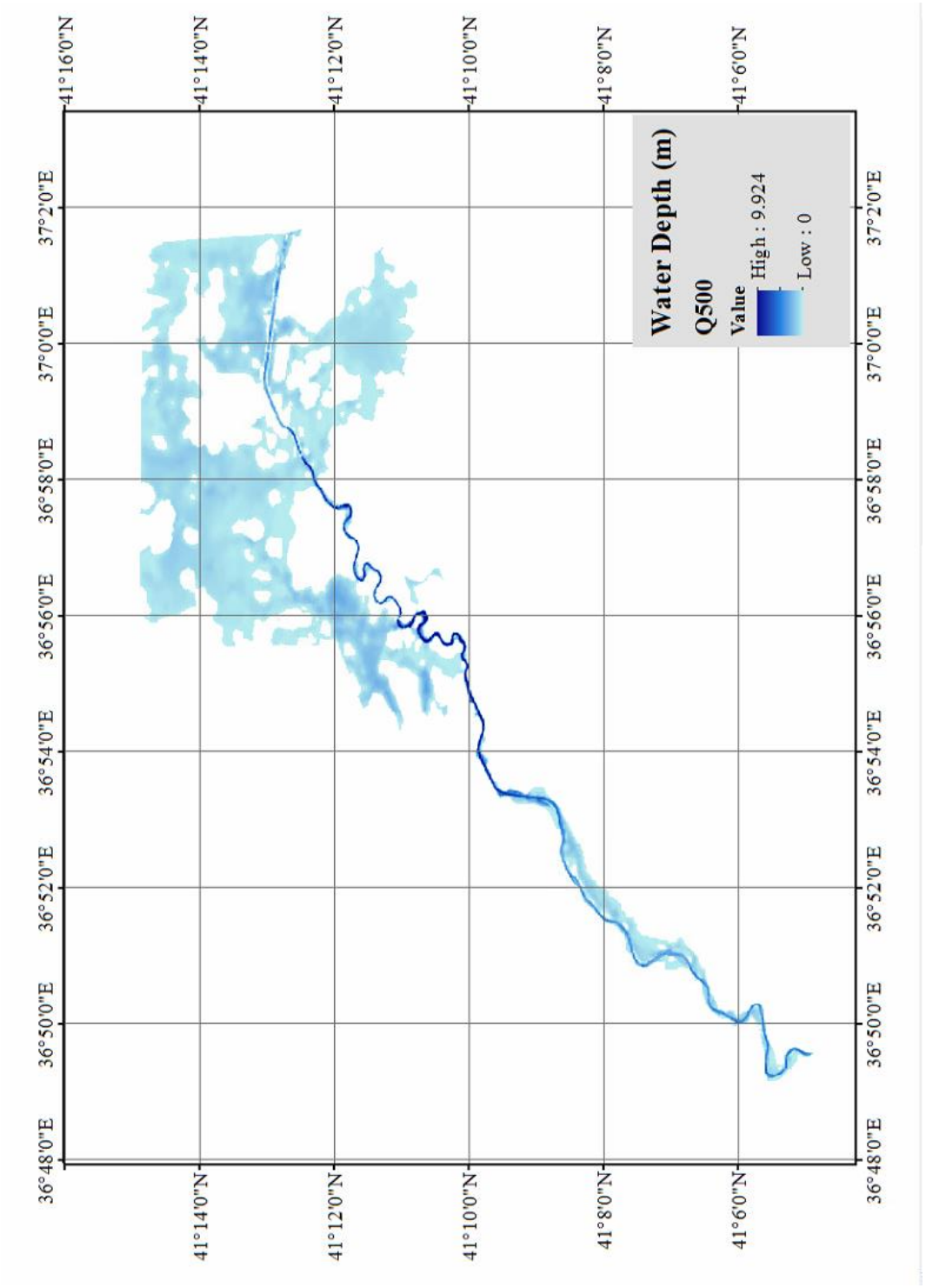

Figure 4-46 The resulting flood extent of Q_{500}= 1041,34 m^3/s discharge hydrograph with n=0,040 and 5 m spatial resolution

Table 4-9 Inundated Areas for three flood events

Discharge	Q_{10}	Q_{100}	Q_{500}
Inundated Area (km^2)	29,9438	36,2304	38,6790

CHAPTER 5

DISCUSSION OF THE RESULTS AND CONCLUSIONS

5.1. Results of Benchmark Study

In comparison part, the differences and similarities between two hydraulic models LISFLOOD-FP-Acceleration Solver and MIKE21, are investigated. The benchmark study is done with a 5 m resolution DEM by using MIKE21. Resulting flood propagations are compatible with each other. However, this compatibility is provided by using different distribution of roughness parameter. For MIKE21 simulation, varying roughness coefficients were applied to the floodplain (Demir, 2016). Regarding LISFLOOD-FP-Acceleration Solver, roughness coefficient is assigned to whole floodplain uniformly to obtain similar flood propagation compared to MIKE21. The results show that the neglected convective acceleration term has an effect on the flood propagation speed and surface area calculations of the flood inundation model. In addition, it is observed that the topographical formations such as meanders and braided parts of the DEM cause differences in terms of local water depths in LISFLOOD-FP hydraulic model results as well as MIKE21 results.

As it is mentioned before, MIKE21 and LISFLOOD-FP simulation results are similar, but the calculated area of the flood extent has difference. Resulting surface areas show that MIKE21 simulates the flood extent about 3% larger compared to the simulated area by LISFLOOD-FP. This small difference could be due to the selected lower simulation time in LISFLOOD-FP model as well as using different roughness coefficients. As for the water depths, LISFLOOD-FP calculates the maximum water depth as 8,61 m. This depth is almost 8% more than the result of MIKE21. These differences likely to stem from neglected acceleration term in the LISFLOOD-FP

hydraulic model as well as the distribution of the roughness coefficient on the floodplain.

Nimaev (2015) conducted a study with LISFLOOD-FP on a smaller area having spatial resolution of 1 m. In that study, MIKE21 also predicted the inundated area 10% more than LISFLOOD-FP. Considering the size of the study area and the magnitude of the event it can be said that MIKE21 makes larger predictions in terms of inundated areas and these estimations become more significant on local basis. He also found that there is a resemblance between MIKE21 and LISFLOOD-FP results in terms of water depth. However, LISFLOOD-FP calculated higher water depths for the ponding areas. In the present study, LISFLOOD-FP calculated the maximum water depth about 8% larger than MIKE21 simulations so that the results are consistent with Nimaev (2015).

The resulting hydrographs show that, flood routing in LISFLOOD-FP outputs is consistent with MIKE21 on the braided part of the DEM, except for the time of water entrance to the section. While the water reaching to the braided part about 2 hours in LISFLOOD-FP simulation, this duration extends to almost 4 hours for MIKE21. The lag between entrance and exit sections of the braided part for LISFLOOD-FP is almost 45 minutes and for MIKE21 this period is calculated as 35 minutes. As for the meandered part, a minor stabilization error is observed in LISFLOOD-FP results. This error most likely stems from the topographical formation. Since the LISFLOOD-FP may show system instabilities due to the use of low roughness coefficient, this error may be eliminated by assigning a higher roughness value to the model. The duration for water entrance to the meandered part is calculated as almost 6.5 hours for MIKE21 while it is calculated as about 4 hours for LISFLOOD-FP. Again, two-hour lag is calculated between two hydraulic models. The exit of the water from the meandered part lasts for about 3.5 hours in MIKE21 results in return, LISFLOOD-FP holds water for about 5 hours due to the ponding in that region. According to these results, it can be said that LISFLOOD-FP calculates the water velocity faster than MIKE21. The reason for that prediction may stem from assuming convective acceleration as

negligible. That means including this term to the formula may cause slowing down the fluid particle from one field to another therefore, a lag occurs in terms of water propagation speed in MIKE21.

5.2. Results of Sensitivity Analysis

In the sensitivity analysis part, the effect of spatial resolution and roughness parameter on flood hydraulics with use of LISFLOOD-FP is investigated by taking the benchmark study as a basis. The results show the importance of spatial resolution for the representation of flood propagation. However, the use of fine resolutions for the simulation introduces longer simulation times due to the detailed representation of topography. Therefore, it would be beneficial to choose the resolution considering the extent of the study site and the magnitude of the event as well as the strength of the computer processor. As for the effect of the roughness coefficient, it is observed that the use of small values causes system instabilities. Also, flood extent and water depth of the inundation changes when different values assigned to the floodplain. These results show that the choice of roughness parameter and spatial resolution has an important influence on model accuracy.

For the coarse resolutions (50 m and 100 m), flood propagation is represented in a poor way in contrast to fine resolutions (5 m and 10 m). In this study, for the same simulation time and constant roughness value, fine resolutions give better results regarding flood propagation. Obtained F-statistic values show that the DEM which has 10 m spatial resolution gives the closest result to 5 m resolution base map on the flood extent basis.

For local depth results, the lowest RMSE is obtained for 10 m resolution. Also, the graphs show that coarser resolutions make over/under estimations in water depths, especially for the meandered parts of the DEM. These results are compatible with previous studies conducted such as Hunter et al. (2008), who also observed these kinds

of over/under estimations. Hunter et al. (2008) stated that the reason for these estimations is reduced definition of the topography while resampling procedure and flow paths. The results of sensitivity analysis, which was conducted by Nimaev (2015) on a local urban area are also compatible with the present study results. Nimaev (2015) made his analyses in centimeter scales and found that fine resolutions provide more detailed representation of the topography.

In addition to the results above, spatial resolution also affects the computational cost. For fine resolutions the runtime of LISFLOOD-FP takes longer. Decreasing the spatial resolution results in shortened runtime. Therefore, it may be useful to choose an optimal spatial resolution considering the size of the study area and magnitude of the event for flood inundation model as mentioned in Hunter et al. (2005)'s research.

As for the roughness coefficient, stabilization errors occur for the values less than n=0,035. Therefore, smaller values are not used in this study. As it would be expected, increasing roughness value effects flood propagation. Greater roughness coefficients decelerate the water flow in the upstream part. As a result, calculated water depths are higher. F-statistic values are calculated by taking the simulation results for n=0,040 roughness value as base map, the highest value is obtained for n=0,050 in terms of flood extent. These results are also consistent with Nimaev (2015). His study showed that lower roughness coefficients result in more rapid flow propagation causing varying water depths.

As for the local water depths, the results show a stationary response due to roughness coefficient change. In this regard, the results are compatible with Hunter et al. (2008). Other studies conducted with LISFLOOD-FP such as Savage et al. (2016) and Fernández et al. (2016) state that setting roughness coefficient in a plausible range gives more accurate results which supports the present study results on roughness.

As well as the grid resolution and roughness coefficient, the use of a different DEM which contains tachometer data affected the resulting flood propagation in this study because the maps have different extents. While ponding could be observed on the north-west side of the DEM which is obtained from orthophotos, no ponding occurred for the DEM which contains tachometer data. It's presented that the extent of DEM used in flood modeling is important to obtain dependable results.

5.3. Results of Subgrid Channel Solver

The most recently developed solver of LISFLOOD-FP, Subgrid Channel Solver is also included in this study to understand the effects of defining the channel and the floodplain characteristics separately and compared with the Acceleration Solver. Also, it is investigated that how this solver copes with the use of different spatial resolutions for channel and floodplain and resolves the flood hydraulics. The results show that Subgrid Channel Solver gives better results than Acceleration Solver even for coarse resolutions since it allows the use of fine resolutions to define the channel, so that eliminates the negative effects of resampling techniques. On the other hand, computation times for Subgrid Channel Solver takes longer than the Acceleration Solver. Therefore, while deciding which solver to use, it would be useful to take into consideration the size of the study area, magnitude of the event and the DEM resolution together.

Since the model allows defining the channel characteristics and floodplain in detail, for the fine resolutions, the computational cost is considerably high in comparison to Acceleration Solver. Therefore, the Subgrid Channel Solver simulations are run for 20 m, 30 m and 50 m spatial resolutions for the floodplain allowing the loss of information in the topographical features to decrease the runtime and channel resolution is chosen as 5 m to preserve the channel characteristics. Roughness coefficients are set as n=0,035 for the channel and n=0,045 for the floodplain. As for the Acceleration Solver, 5 m resolution for the whole domain including the channel is

chosen while setting roughness value as n=0,040. The resulting flood extents and water depths show that Subgrid Channel Solver gives better results with coarser resolutions such as 20 m in comparison to Acceleration Solver. Instead of using one roughness parameter for the whole domain, the capability of choosing different values for channel and floodplain separately provides reasonable results with use of lower roughness values such as n=0,035 for the channel.

Even though both solvers use the same formula while calculating flood hydraulics, the ability of assigning different values of roughness parameter and spatial resolution to the channel and floodplain makes a significant change in water depth results while causing a slight difference in flood propagations. Considering the results and runtimes of both solvers, especially for the large areas and coarse resolutions the use of Subgrid Channel Solver would be favorable. On the other hand, for the fine resolutions such as the resolutions below 10 m, the use of Acceleration Solver can be beneficial considering the computation cost especially for the small areas.

5.4. Conclusions

In this study, sensitivity of LISFLOOD-FP is investigated according to roughness and spatial resolution parameters since it is proven that the accuracy of a hydraulic model strongly depends on model calibration.

"Samsun Terme District, Terme River Hazard Map Designation Report" published by DSI (2013), calculated roughness coefficient for Terme Bridge as n=0,029 and for upstream part of the river as n=0,045 with Cowan's method. Generally, the obtained model roughness values are higher than empirically derived values as it is stated in Hunter et al. (2008). In the present study, LISFLOOD-FP shows a good performance and gives reasonable results with close roughness values to those calculated values in DSI report.

In this study the aim is to analyze the use of simple inertial formulation of the shallow water equations in 2-D flood inundation modeling considering the convective acceleration term as negligible. It has been shown that the LISFLOOD-FP model works well for the small scaled areas (Nimaev, 2015). For the current study it is demonstrated that even though the acceleration term is neglected LISFLOOD-FP gives quite resembling results with the previous study conducted in the same area (Bozoğlu, 2015) and the model is also suitable to be used in large areas.

The objective of this study is also to show the sensitivity of the hydraulic model according to the roughness parameter and spatial resolution by using two different approaches while solving an inundation problem. Generally, roughness parameter is not used for calibration since every surface has its own specific roughness coefficient. However, the results of LISFLOOD-FP give a stationary response to roughness parameter. The use of small roughness values causes stabilization errors in results. Also, to obtain a reasonable flood extent the choice of the roughness coefficient is important since it can alter the resulting flood propagation. For that reason, it would be beneficial to have the data of a previous flood event (e.g. aerial photographs) as well as keeping the roughness parameter in a plausible range to make the model calibration.

In addition, the results show that also spatial resolution of the DEM is important whilst modeling with LISFLOOD-FP. Especially the simulation time is strongly affected by the resolution changes. Acceleration Solver has reasonable runtimes for fine resolutions such as 5 m (for the 1/1000 scaled DEM with bathymetry data) and 10 m (for the 1/5000 scaled DEM), it takes quite long time to run Subgrid Solver with these resolutions. Besides, Subgrid Solver provides better representation of the flood propagation even in relatively coarse resolutions such as 20 m. This is because of the possibility to define channel characteristics more detailed by assigning a different resolution to the channel. The use of coarse resolutions distorts the representation of

the flood propagation in Acceleration Solver results even though it provides considerably low computational costs.

It has been shown in the previous study conducted for a small scaled area (Nimaev, 2015) that Acceleration Solver gives better results compared to LISFLOOD-FP solvers (Flow-limited solver, Adaptive Solver, Roe Solver). In this study, the comparison results of the Acceleration Solver and the most recent Subgrid Solver show that both solvers give reasonable results. However, the size of the area and magnitude of the event should be considered while deciding which solver to use because of the high computational costs. The use of Subgrid Solver would be favorable in large areas and big flood events since it gives better results for coarse resolutions. For the studies carried out with fine resolutions the use of Acceleration Solver would be beneficial since the computational cost of Subgrid Solver will be higher.

Following all these considerations, it can be said that LISFLOOD-FP which is a noncommercial hydraulic model has the same capability to dissolve flood hydraulics like the MIKE21, which is a commercial hydraulic model, even though the neglected acceleration term. The model can be used both in small and large scaled areas since it provides acceptable results in terms of flood propagation and water depth calculations.

In this study the structures like bridges, culverts are not included in the modeling. The land surface information is considered linked to the DEM obtained by tachometer. In future studies the effect of structures in flood modeling must be considered especially for local studies.

REFERENCES

De Almeida, Gustavo A. M., Bates, P., (2013). Applicability of the local inertial approximation of the shallow water equations to flood modeling. Water *Resources Research, Vol. 49*, 4833-4844

Amponsah, W., Borga, M., Marchi, L., Boni, G., Cavalli, M., Comiti, F., Crema, S., Ana, L., Marra, F., Zoccatelli, D. (2014). The flash flood of October 2011 in the Magra River basin (Italy): rainstorm characterization and flood response analysis. *Journal of Hydrometeorology*

Aronica, G., Bates, P. D., and Horritt, M. S., (2002). Assessing the uncertainty in distributed model predictions using observed binary pattern information within GLUE, *Hydrological Processes, 16*, 2001-2016.

Bates, P. D., Horritt, M. S., Fewtrell, T. J., (2010). A simple inertial formulation of the shallow water equations for efficient two-dimensional flood inundation modeling. *Journal of Hydrology, 387*, 33-45.

Bates, P. D., Trigg, M., and Dabrowa, A. (2013). *Lisflood-FP User manual*. School of Geographical Sciences, University of Bristol.

Blösch, G., Nester, T., Komma, J., Parajka J., Perdigão, R. A. P., (2013). The June 2013 flood in the Upper Danube Basin, and comparisons with the 2002, 1954 and 1899 floods, *Hydrology and Earth System Sciences, Vol.17,* 5197-5212

Bozoğlu, B., (2015). *1-D and 2-D Flood Modeling Studies and Upstream Structural Measures for Samsun City Terme District*. The Graduate School of Natural and Applied Sciences of Middle East Technical University.

Chow, V. T., (1959). Open-Channel Hydraulics, 680 pp., Mc-Graw-Hill, New York

DSI. (2013). Samsun Terme District, Terme River Flood Hazard Map Designation Project. Retrieved from Samsun 7th Regional Directory.

Demir, G., Akyürek, Z., (2016). The İmportance of Digital Elevation Models (DEM) for Hydraulic Modeling. *4. National Flood Symposium*.

European Parliament (2007) Directive 2007/60/EC of the European Parliament and of the Council of 23 October 2007 on the assessment and management of flood risks.

Fewtrell, T. J., Bates, P. D., Horritt, M., Hunter, N. M., (2008). Evaluating the effect of scale in flood inundation modeling in urban environments. *Hydrological Processes, 22,* 5107-5118.

Fernández, A., Najafi, M. R., Durand, M., Mark, B. G., Moritz, M., Jung, H. C., Neal, J., Shastry, A., Laborde, S., Phang, S. C., Hamilton, I. M., Xiao, N., (2016). Testing the skill of numerical hydraulic modeling to simulate spatiotemporal flooding patterns in the Logone floodplain, Cameroon. *Journal of Hydrology, 539,* 265-280.

General Directorate of Meteorology. (2017). *Natural Disasters with Meteorological Characteristic 2016 Evaluation Report.* Retrieved from Ministry of Forestry and Water Management. URL1

General Directorate of Meteorology. (2018). *A Brief Assessment of the Natural Disasters with Meteorological Characteristic in 2017 in Turkey.* Retrieved from Ministry of Forestry and Water Management. URL2

Haider, S., Paquier, A., Morel, R., Champagne, J. Y., (2003). Urban flood modeling using computational fluid dynamics. *In proceedings of the Institution of Civil Engineers- Water and Maritime Engineering, 156(2),* 129-135

Hall, J., Arheimer, B., Borga, M., Brázdil, R., Claps, P., Kiss, A., Kjeldsen, T. R., Kriaučiūnienė, J., Kundzewicz, Z. W., Lang, M., Llasat, M. C., Macdonald, N., McIntyre, N., Mediero, L., Merz, B., Merz, R., Molnar, P., Montanari, A., Neuhold, C., Parajka, J., Perdiãgo, R. A. P, Plavcová, L., Rogger, M., Salinas, J. L., Sauquet, E., Schär, C., Szolgay, J., Viglione, A., Blöschl, G., (2014). Understanding flood regime changes in Europe: a state-of-the-art assessment. *Hydrology and Earth System Sciences, Vol.18,* 2735-2772

Haltaş, I., Tayfur, G., and Elçi, Ş., (2013). *Bararj Yıkılması Sonrasında Taşkın Yayılımının İki Boyutlu Saysısal Simülasyonu: Ürkmez Barajı Örneği.* Paper presented at meeting of the 3th National Flood Symposium, İstanbul, TURKEY

Hunter, Neil M., Horritt, Matthew S., Bates, Paul D., Wilson, Matthew D., Werner, Micha G. F. (2005). An adaptive time step solution for raster-based storage cell modeling of floodplain inundation. *Advances in Water Resources, 28,* 975-991.

Hunter, Neil M., Bates, Paul D., Horritt, Matthew S., Wilson, Matthew D. (2007). Simple spatially-distributed models for predicting flood inundation: A Review. *Geomorphology 90,* 208-225.

Hunter, N. M., Bates, P. D., Neelz, S., Pender, G., Villanuaeva, I., Wright, N. G., Liang, D., Facloner, R. A., Lin, B., Waller, S., Crossley, A. J., Mason, D. C. (2008). Benchmarking 2D hydraulic models for urban flooding. *Proceedings of the Institution of Civil Engineers – Water Management* 161, 13-30

Horritt, M. S., and Bates, P. D., (2001), Effects of spatial resolution on a raster-based model of flood flow, *Journal of Hydrology, 253,* 239-249

Marsh, T., (2008). A hydrological overview of the summer 2007 floods in England and Wales. *Weather, Vol. 63,* 274-279

Mignot, E., Paquier, A., Haider, S., (2006). Modeling floods in a dense urban area using 2D shallow water equations, Journal of Hydrology, 90(3-4), 226-243

Ministry of Agriculture of Forestry General Directorate of Water Management website URL3, URL4, URL5, URL6, URL7

De Moel, H., Van Alphen, J., Aerts, J.C.J.H., (2009). Flood Maps in Europe – methods, availability and use. *Natural Hazards and Earth System Science, Vol.9,* 289-301

Neal, J., Schumann, G., Bates, P., (2012). A subgrid channel model for simulating river hydraulics and floodplain inundation over large and data sparse areas, *Water Resources Research, Vol.48*

Nimaev, A., (2015). *The use of simple inertial formulation of the shallow water equations in 2-D flood inundation modeling.* The Graduate School of Natural and Applied Sciences of Middle East Technical University.

Özdemir, H., Neal, J.,Bates, P., and Döker, F. (2013). 1-D and 2-D urban dam-break flood modeling in İstanbul, Turkey. *Geophysical Research Abstracts Vol.16,* EGU2014-218, EGU General Assembly

Özdemir, H., Bates, P.D., de Almeida, G. A. M. (2018). Modeling urban floods at submeter resolution: challenges or opportunities for flood risk management? *Flood risk management,* 855-865

Sanyal, J., Carbonneau, P., Densmore, A. L., (2014). Low-cost inundation modeling at the reach scale with sparse data in the Lower Damodar River basin, India. *Hydrological Sciences Journal, Vol. 59*

Savage, T. S. J., Pianosi, F., Bates, P., Freer, J., Wagener, T., (2016). Quantifying the importance of spatial resolution and other factors through global sensitivity analysis of a flood inundation model. *Water Resources Research.*

Şahin, E., Akıntuğ, B., Yanmaz, A. M., (2013). Modeling of Morphou (Güzelyurt) Flood and Remedial Measures. *Teknik Dergi, 24, (3),* 6447-6462

Tarrant, O., Todd, M., Ramsbottom, D., Wicks, J., (2005). 2D floodplain modeling in the tidal thames – addressing the residual risk. *Water and Environment Journal 19(2),* 125-134

Ulbrich, U., Brücher, T., Fink, A. H., Leckebusch, G. C., Krüger, A., Pinto, J. G., (2003). The central European floods on August 2002: Part 1-Rainfall periods and flood development. *Weather, Vol. 58,* 371-377

Wood, M., Hostache, R., Neal, J., Wagener, T., Giustarini, L., Chini, M., Corato, G., Matgen, P., Bates, P., (2016). Calibration of channel depth and friction parameters in the LISFLOOD-FP hydraulic model using medium-resolution SAR data and identifiability techniques. *Hydrology Erath System Sciences, Vol.20,* 4983-4997

Yu, D., Lane, SN., (2006). Urban fluvial modeling using a two-dimensional diffusion-wave treatment, part 1. Mesh resolution effects. *Hydrological Processes 20(7),* 1541-1565.

URL1: https://www.mgm.gov.tr/FILES/genel/kitaplar/dogalafet-2016.pdf,last visited on December 2018

URL2: https://www.mgm.gov.tr/FILES/Haberler/2018/2017AfetDegerlendirme.pdf, last visited on December 2018

URL3:https://www.tarimorman.gov.tr/SYGM/Belgeler/Devam+eden+projeler+(5).pdf, last visited on March 2019

URL4:https://www.tarimorman.gov.tr/SYGM/Belgeler/PROJELER/Tamamlanan%20projeleri%20(3)-converted%20(1).pdf, last visited on March 2019

URL5:https://www.tarimorman.gov.tr/SYGM/Belgeler/Ta%C5%9Fk%C4%B1n%20Dairesi%20Sunum/17.11.2015_TA%C5%9EKIN%20Y%C3%96NET%C4%B0M%C4%B0NDE%20MODELLEME%20%C3%87ALI%C5%9EMALARI.pdf, last visited on March 2019

URL6:https://www.tarimorman.gov.tr/SYGM/Belgeler/Ta%C5%9Fk%C4%B1n%20Dairesi%20Sunum/Flood%20Management%20in%20Turkey.pdf, last visited on March 2019

URL7:https://www.tarimorman.gov.tr/SYGM/Belgeler/Ta%C5%9Fk%C4%B1n%20Dairesi%20Sunum/WWF7_Presentation_isakin.pdf, last visited on March 2019

APPENDICES

A. SIMULATION RESULTS FOR DIFFERENT SPATIAL RESOLUTIONS

5 m, 10 m, 50 m and 100 m DEM resolutions are used. The explanations are given in Section 4.2.1 and the resulting flood extents are presented in Figure 0-1 to Figure 0-4.

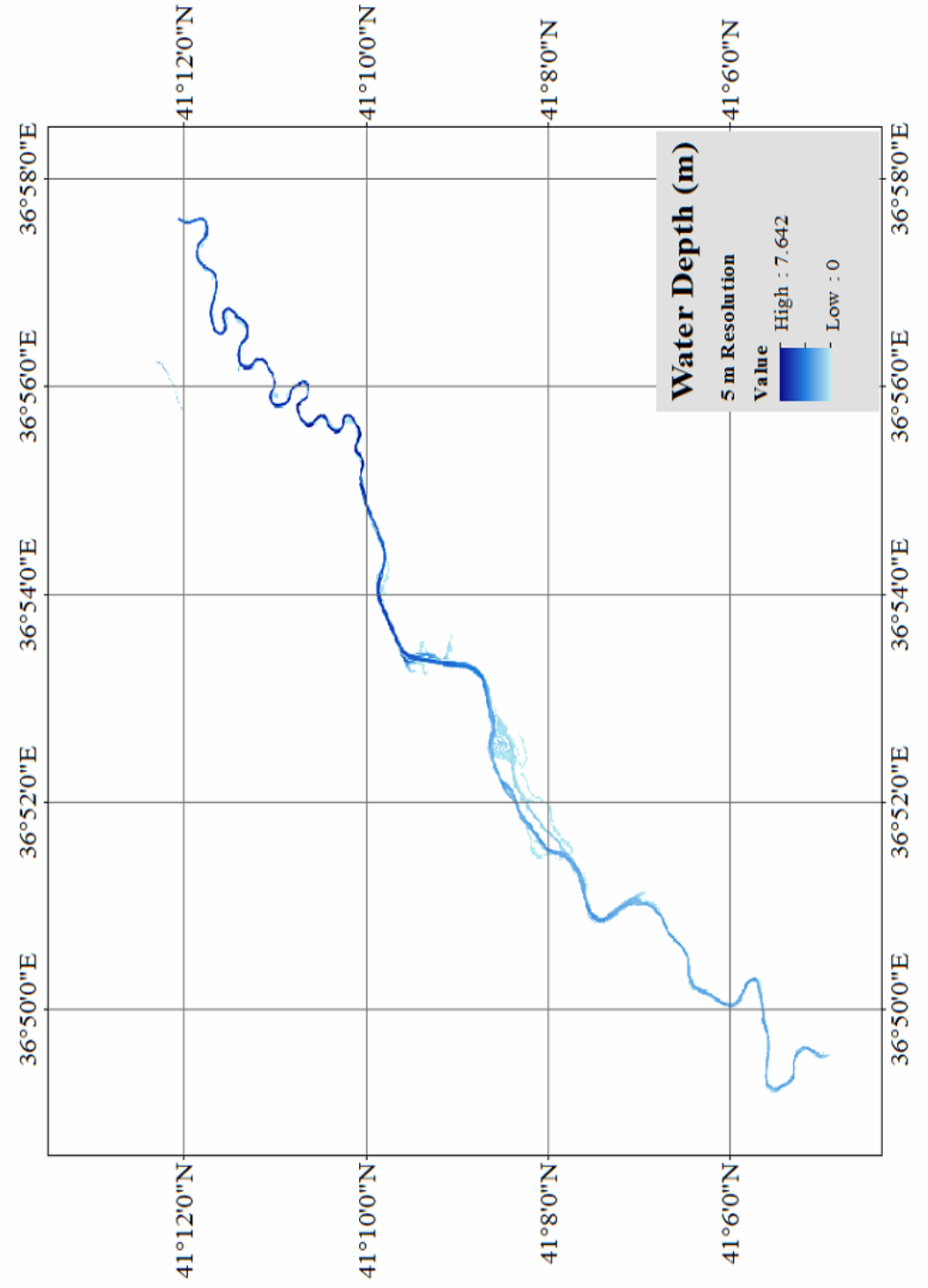

Figure 0-1 Flood extent for n=0,040 and 14,5 hours simulation time for 5 m DEM resolution

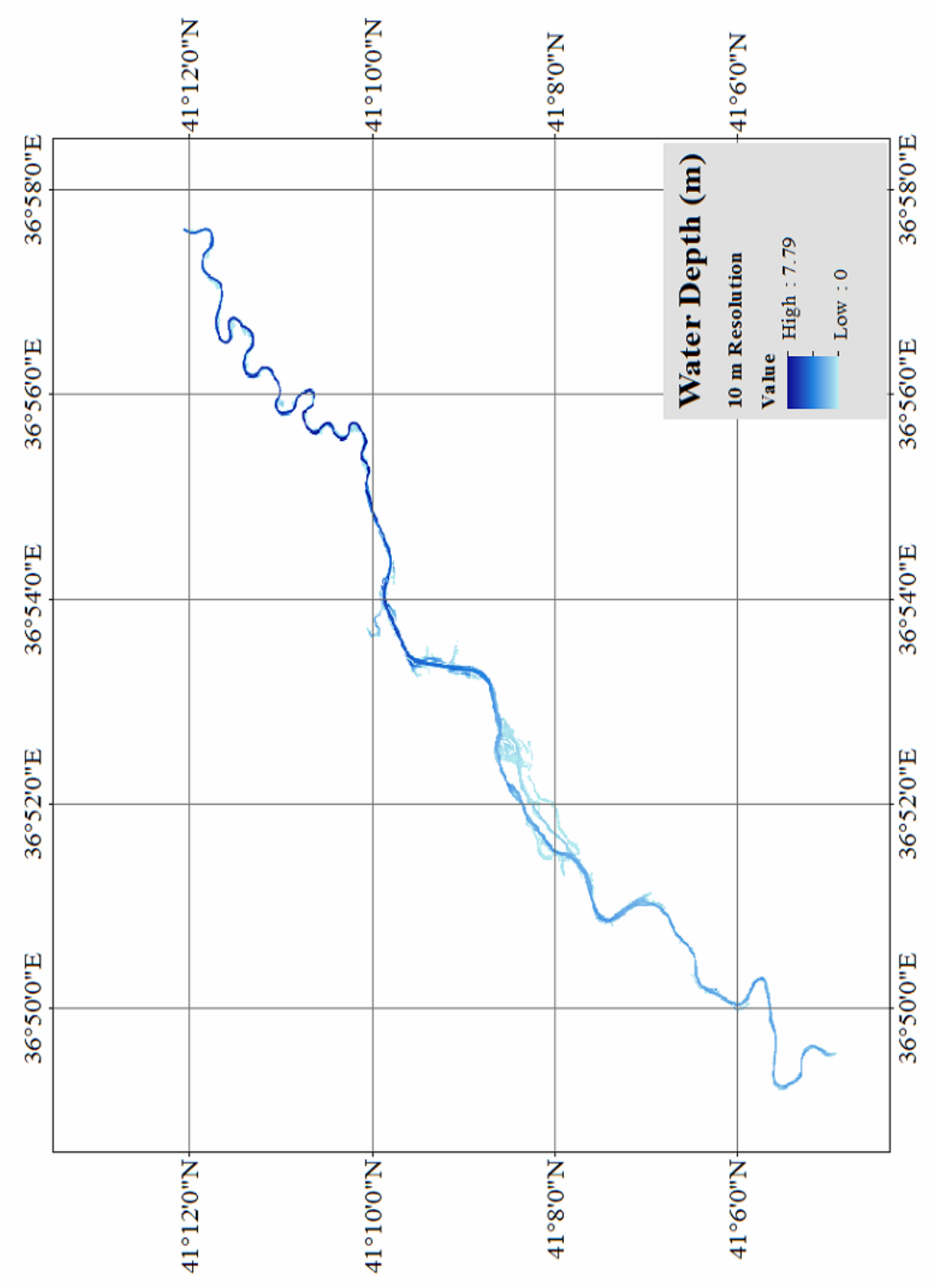

Figure 0-2 Flood extent for n=0,040 and 14,5 hours simulation time for 10 m DEM resolution

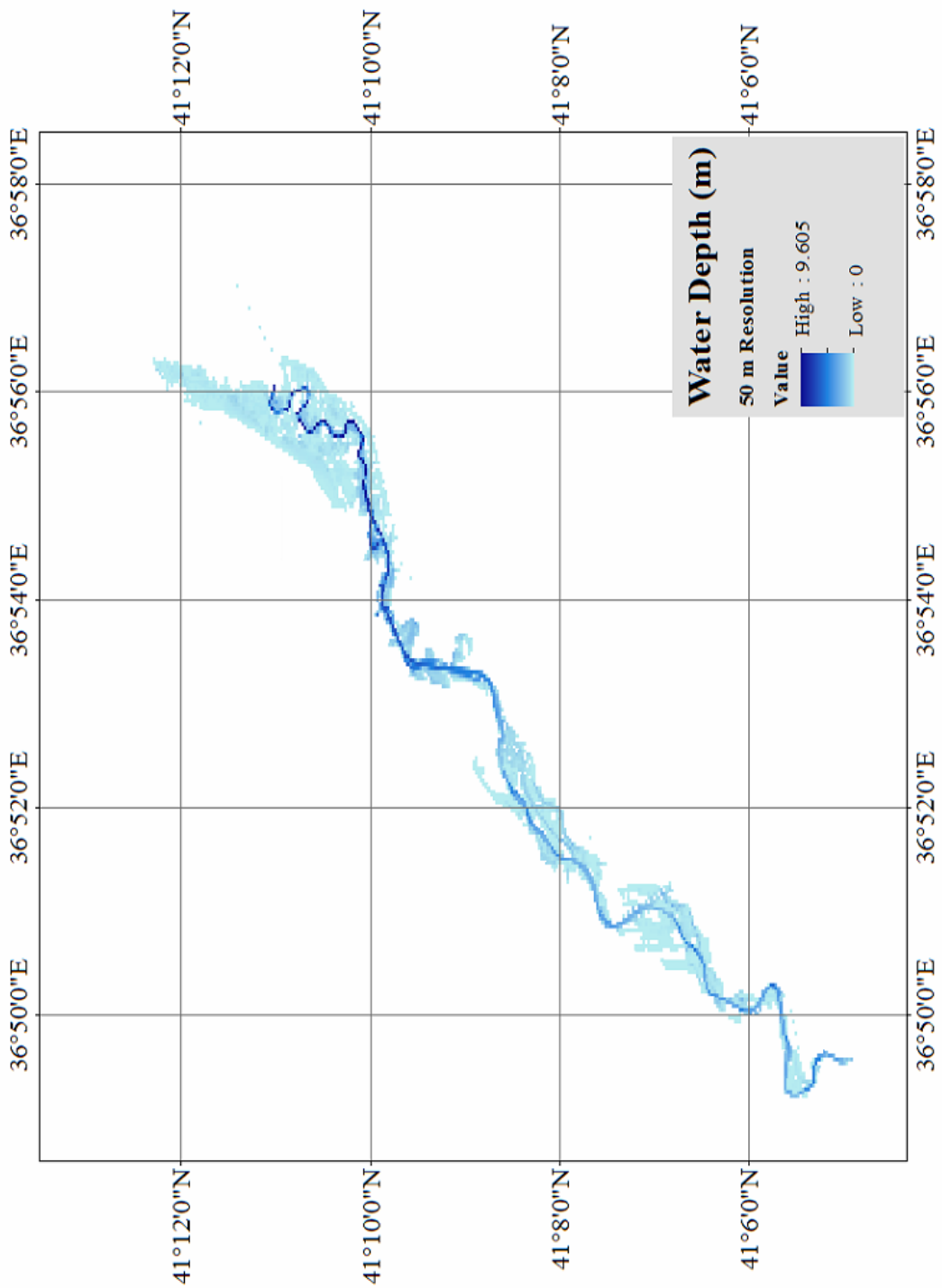

Figure 0-3 Flood extent for n=0,040 and 14,5 hours simulation time for 50 m DEM resolution

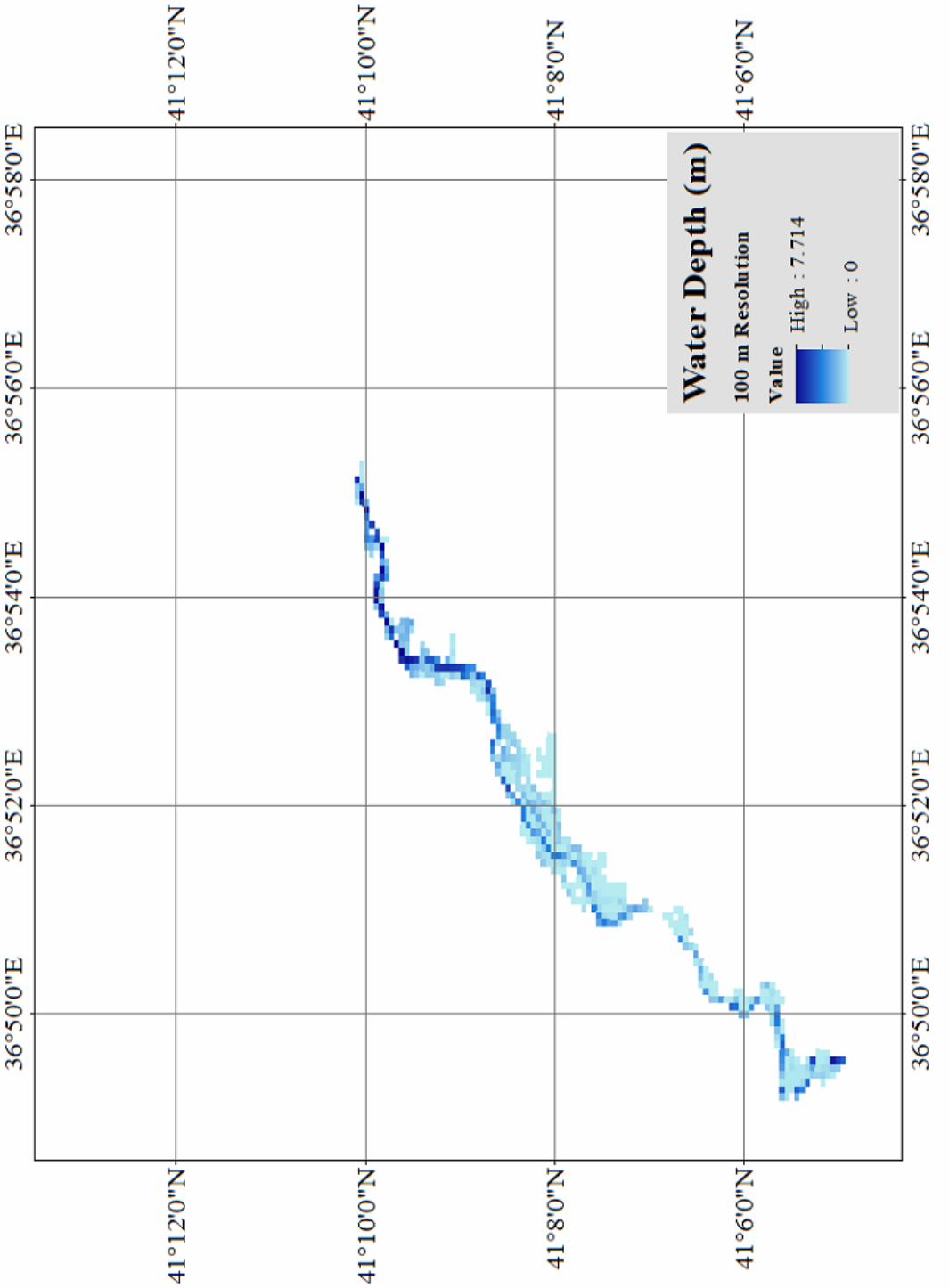

Figure 0-4 Flood extent for n=0,040 and 14,5 hours simulation time for 100 m DEM resolution

B. SIMULATION RESULTS FOR DIFFERENT ROUGHNESS VALUES

Roughness coefficients are altered between 0,040-0,10 and the details are presented in Section 4.2.2. Simulation results are given in Figure 0-9 to Figure 0-15.

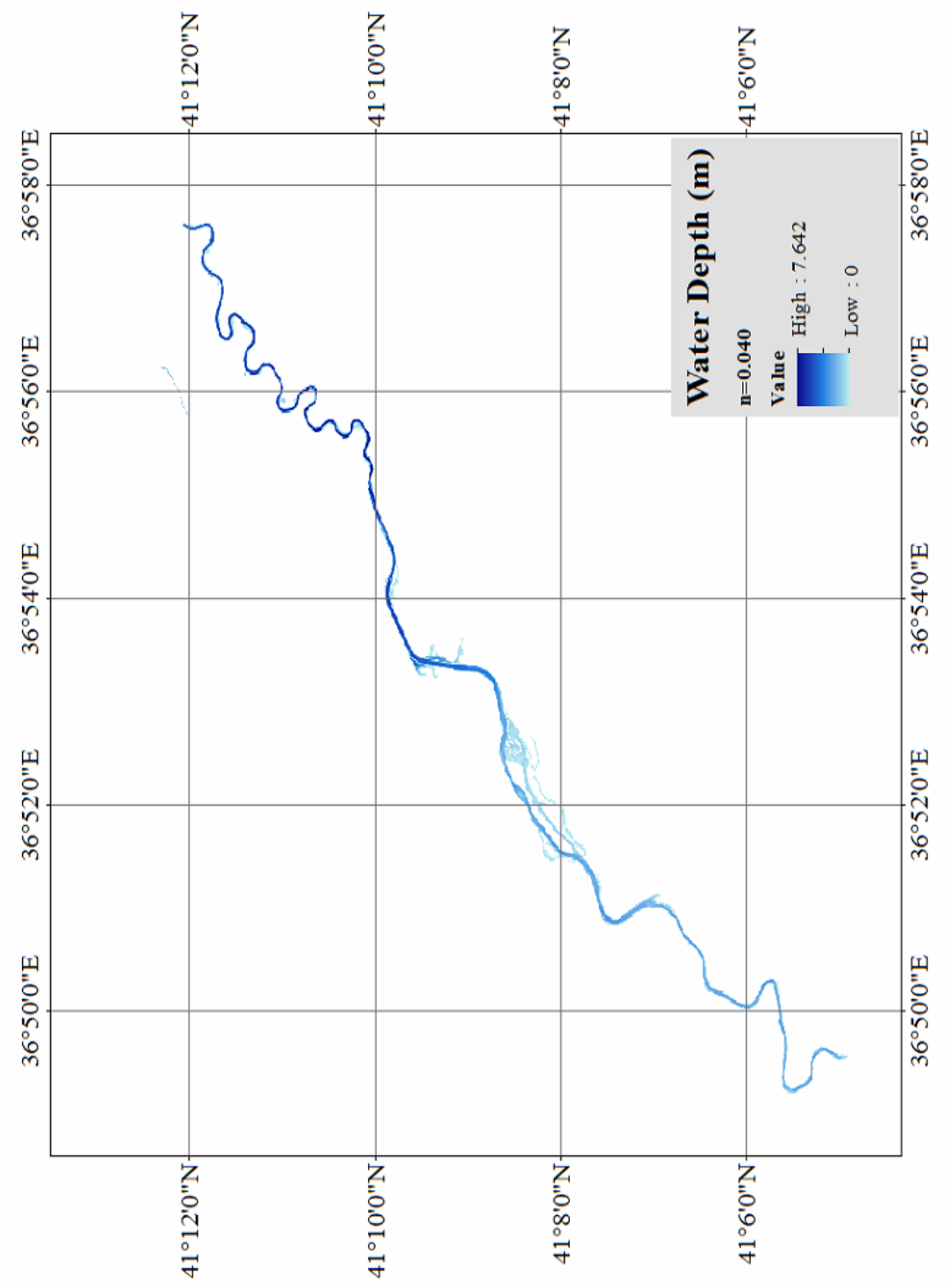

Figure 0-5 Flood extent for 5 m resolution and 14.5 hours simulation time by taking n= 0,040

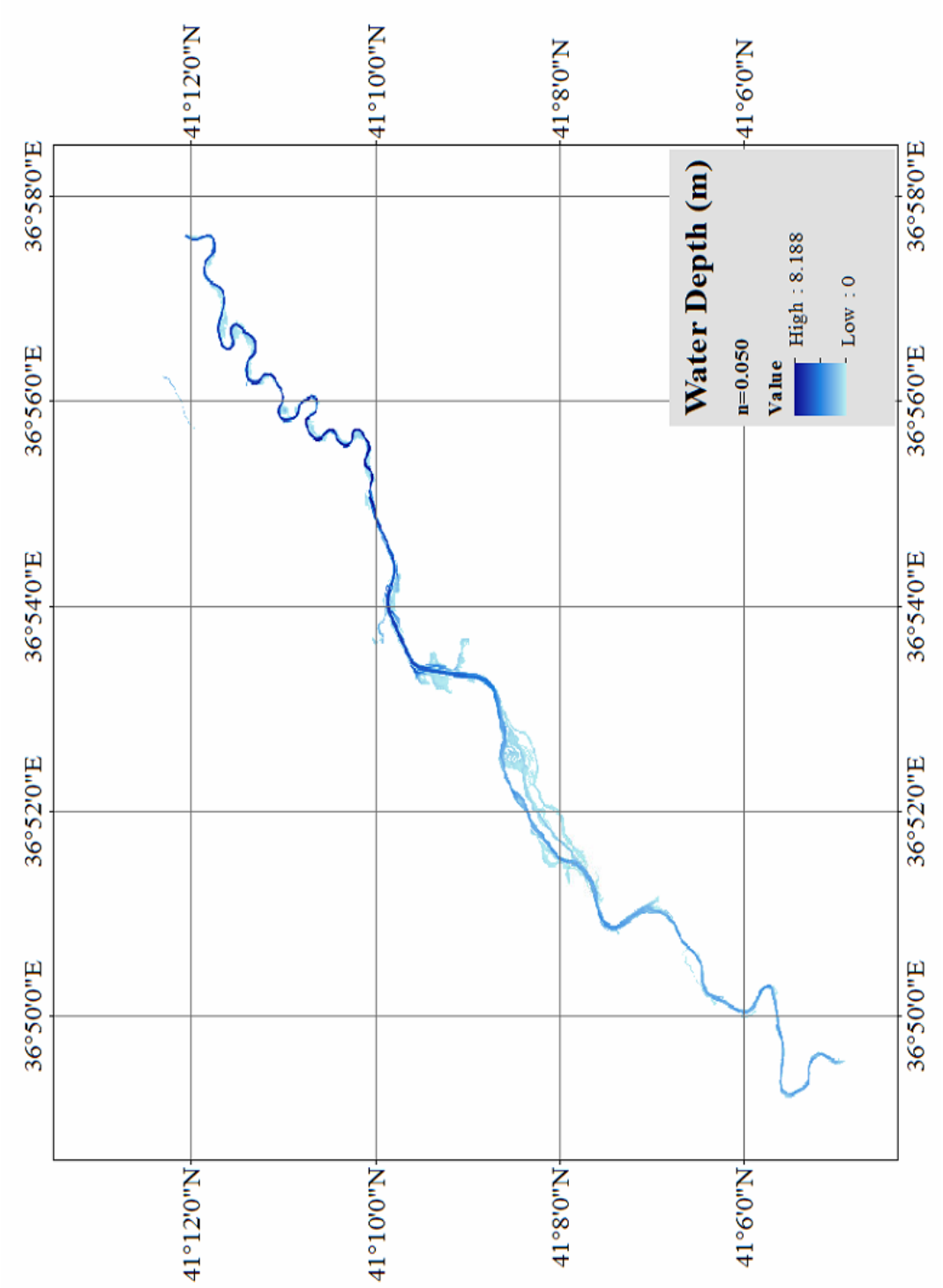

Figure 0-6 Flood extent for 5 m resolution and 14.5 hours simulation time by taking n= 0,050

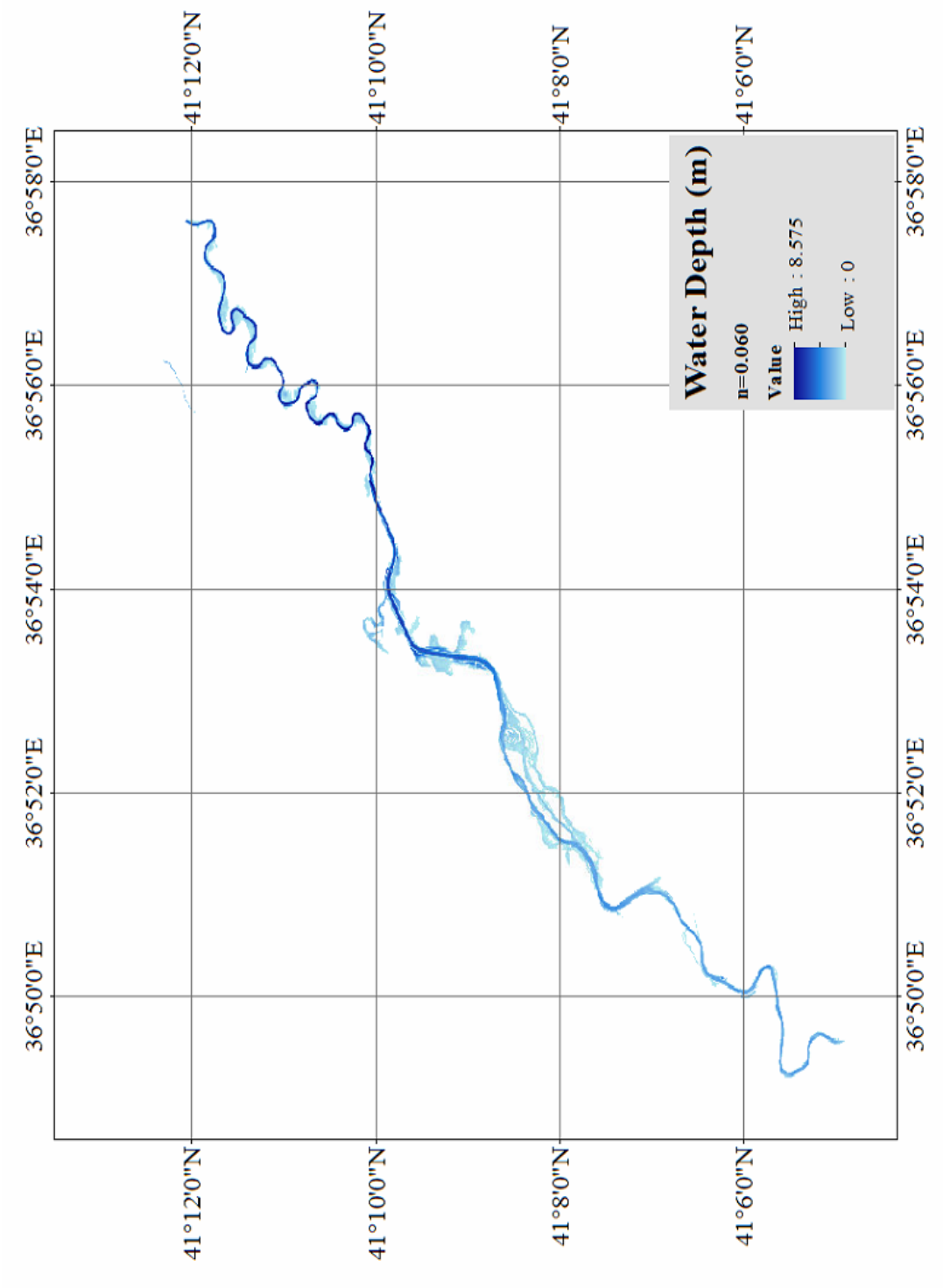

Figure 0-7 Flood extent for 5 m resolution and 14.5 hours simulation time by taking n= 0,060

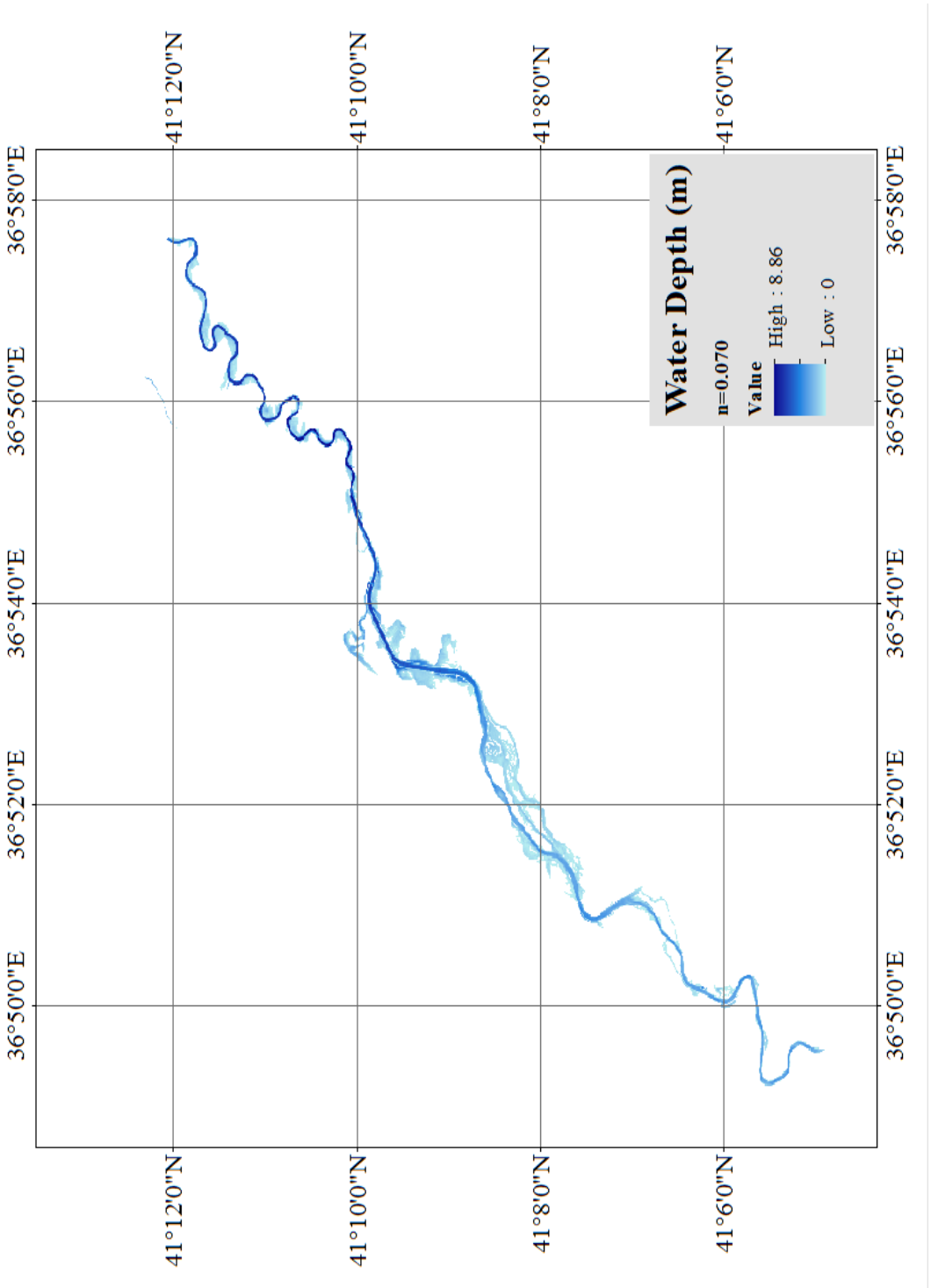

Figure 0-8 Flood extent for 5 m resolution and 14.5 hours simulation time by taking n= 0,070

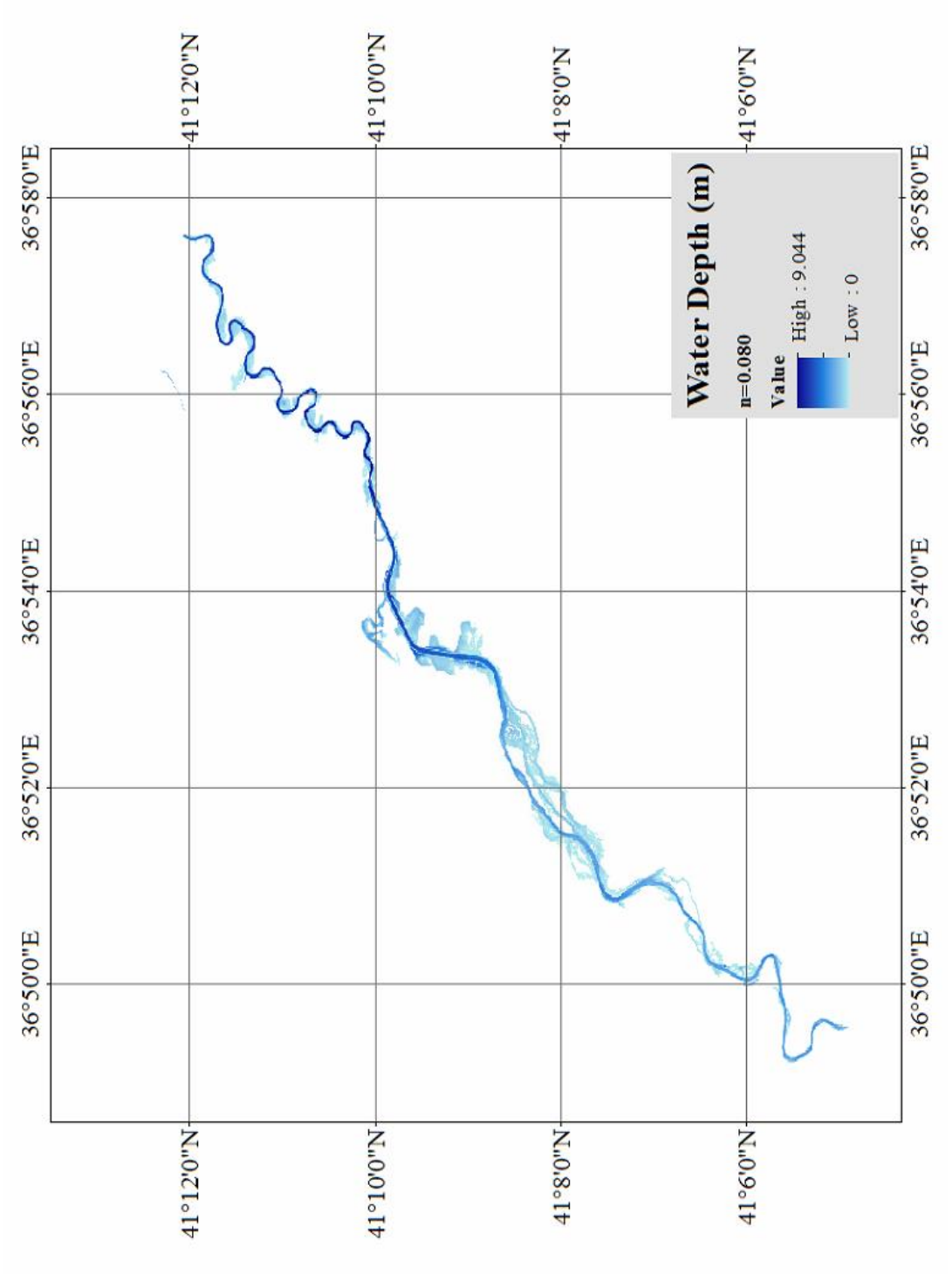

Figure 0-9 Flood extent for 5 m resolution and 14.5 hours simulation time by taking n= 0,080

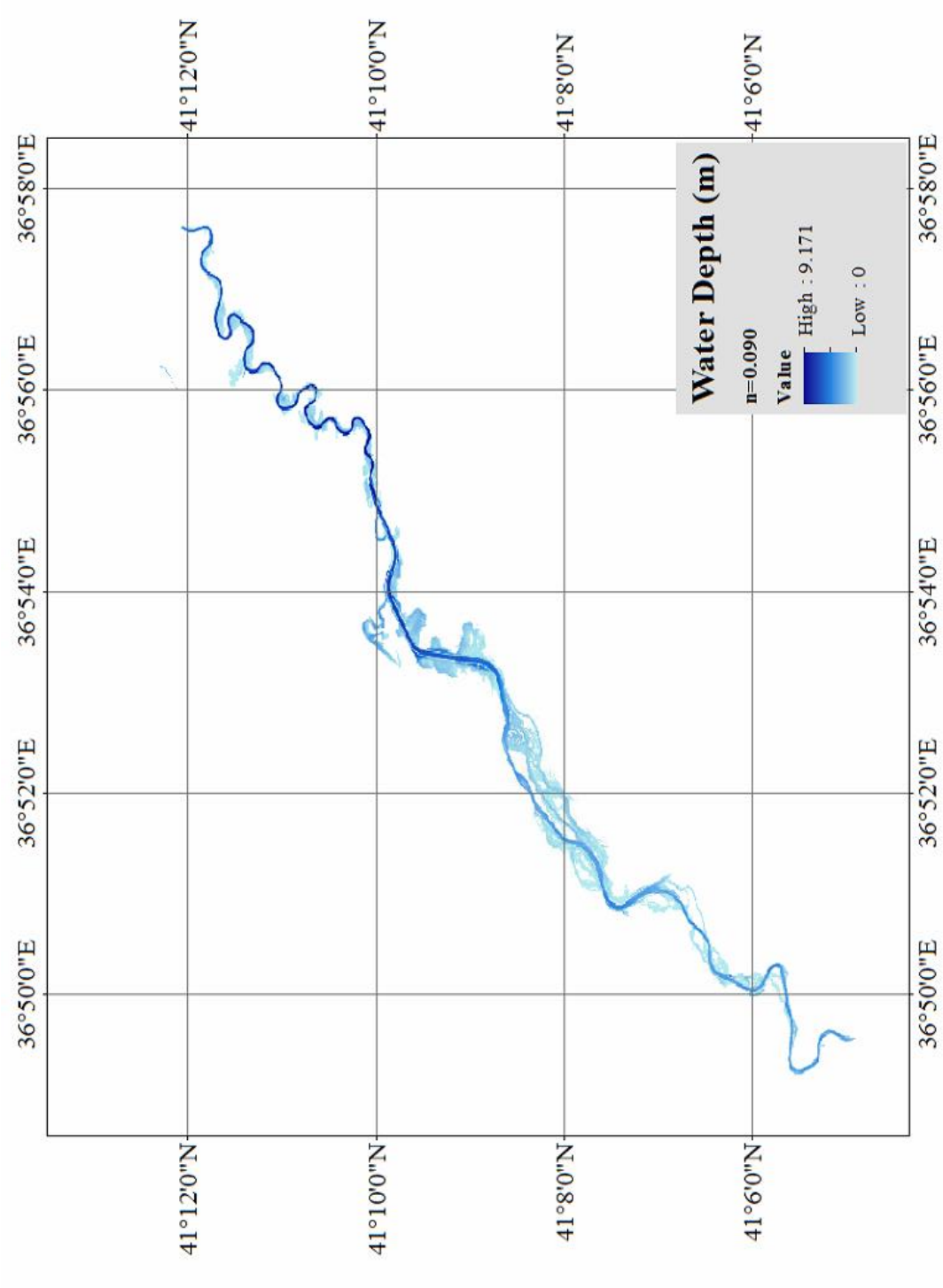

Figure 0-10 Flood extent for 5 m resolution and 14.5 hours simulation time by taking n= 0,090

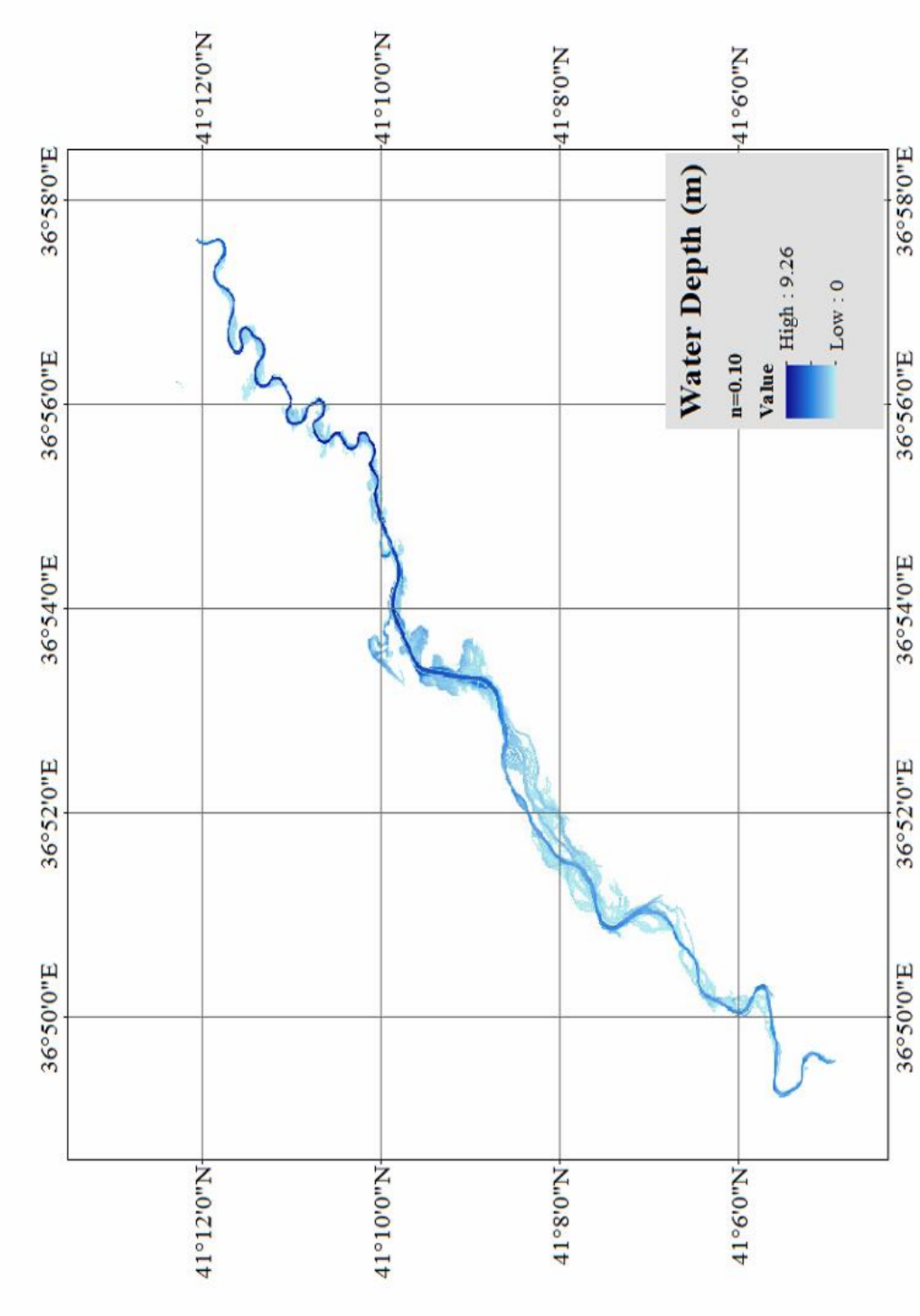

Figure 0-11 Flood extent for 5 m resolution and 14.5 hours simulation time by taking n= 0,10

C. SIMULATION RESULT COMPARISON OF SUBGRID CHANNEL SOLVER AND ACCELERATION SOLVER

For Subgrid Channel Solver the roughness coefficient is picked as n=0,035 for the channel and n=0,045 for the floodplain while it is set as n=0,040 for Acceleration Solver. Spatial resolution of the Subgrid Channel Solver is altered between 20 m and 50 m for the floodplain and remained constant for channel as 5 m and the results are compared with the 5 m Acceleration Solver simulation results. The explanations and details are presented in Section 4.3. Simulation results are given in Figure 0-16 to Figure 0-20.

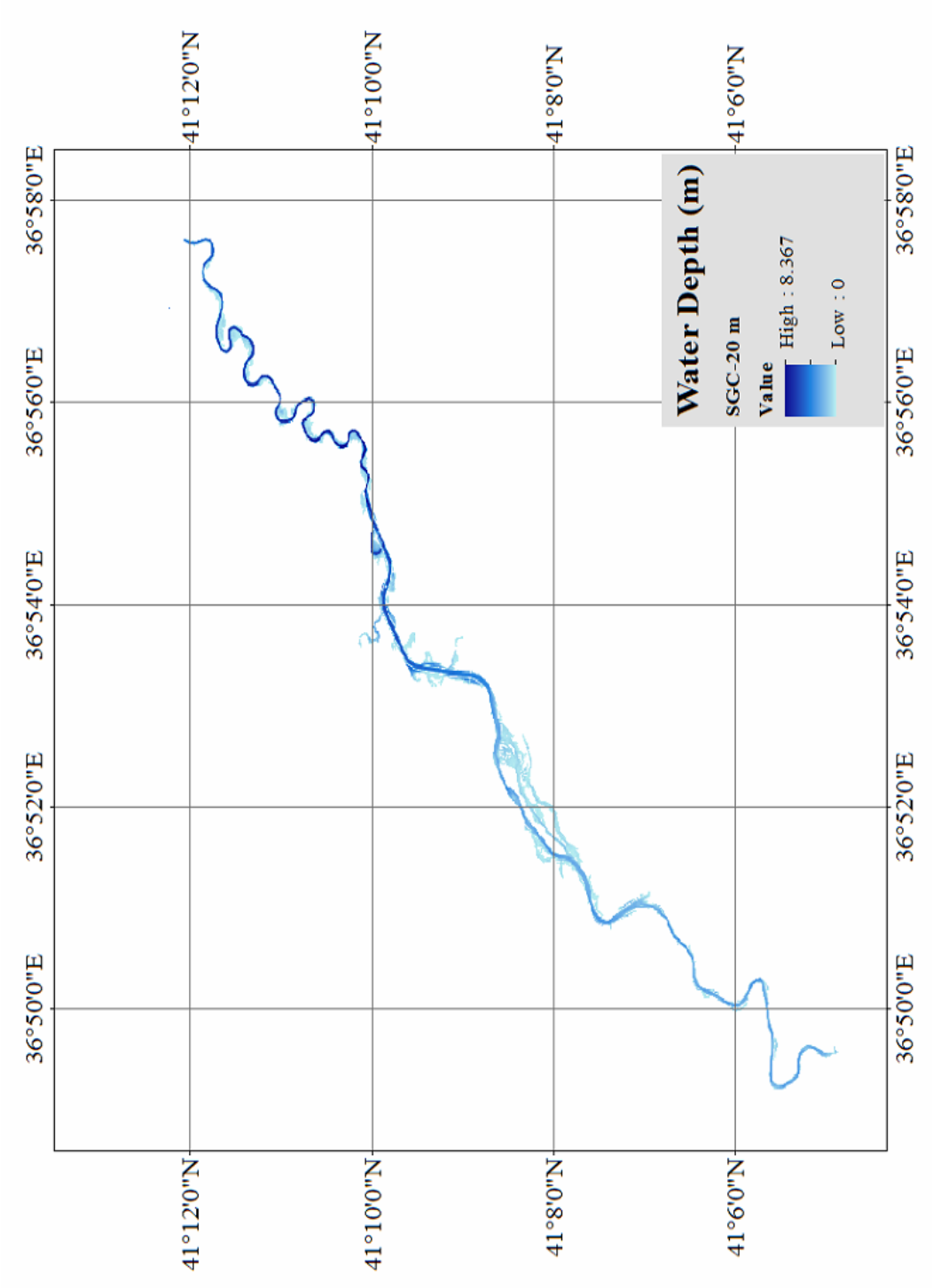

Figure 0-12 Subgrid Channel Solver Results with $n_{channel}$=0,035 and $n_{floodplain}$=0,045 for 20 m spatial resolution

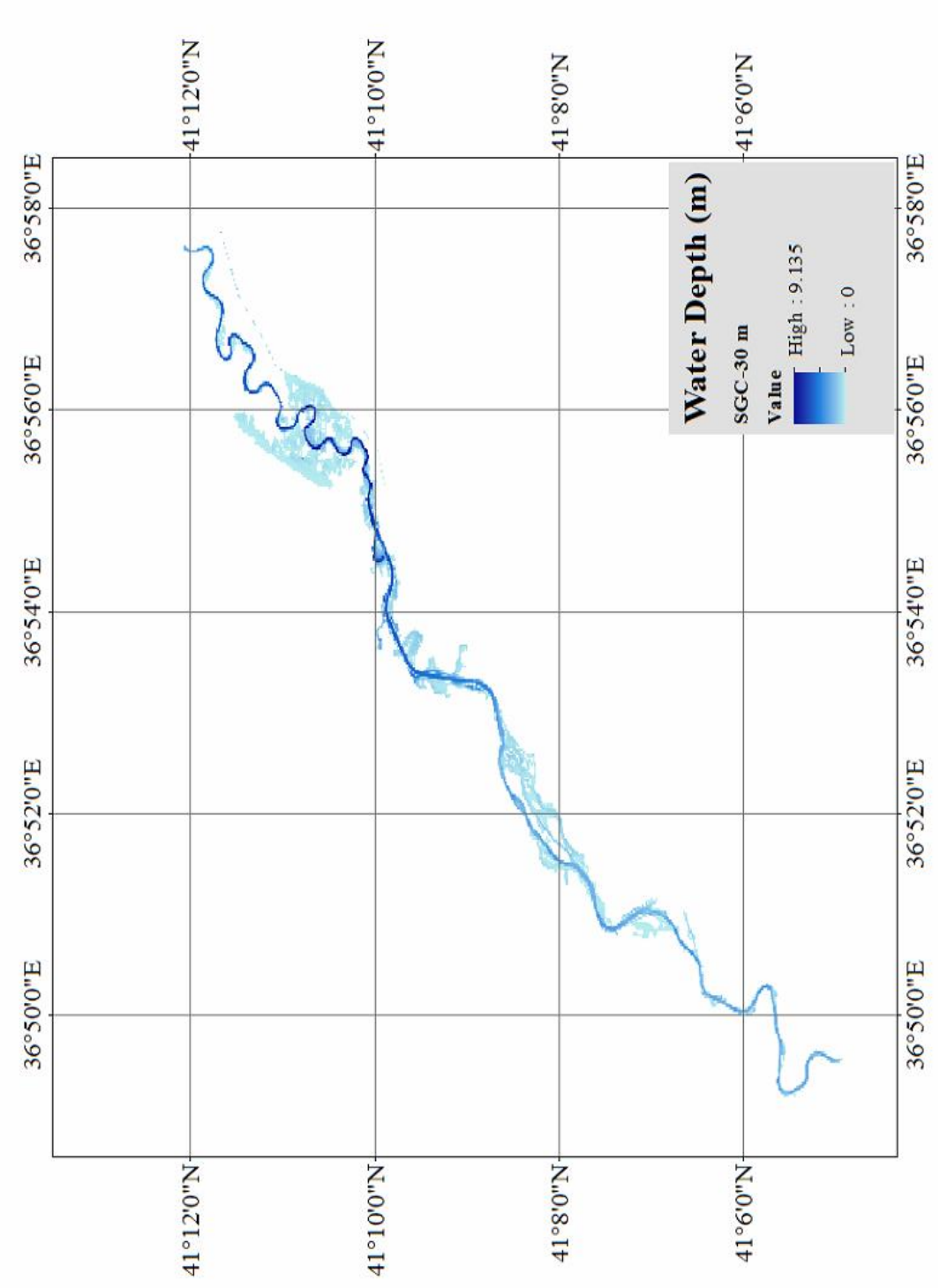

Figure 0-13 Subgrid Channel Solver Results with $n_{channel}$=0,035 and $n_{floodplain}$=0,045 for 30 m spatial resolution

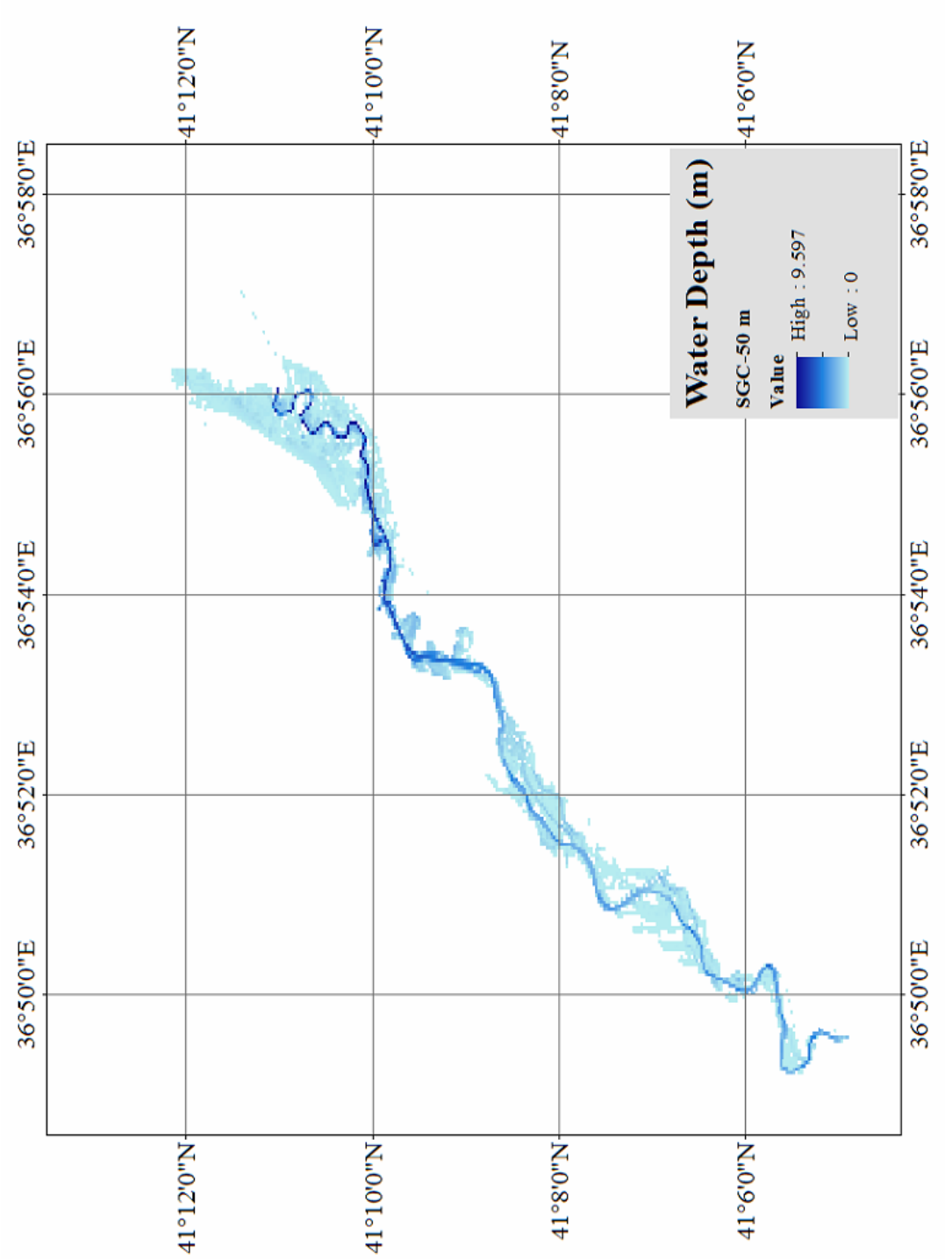

Figure 0-14 Subgrid Channel Solver Results with $n_{channel}$=0,035 and $n_{floodplain}$=0,045 for 50 m spatial resolution

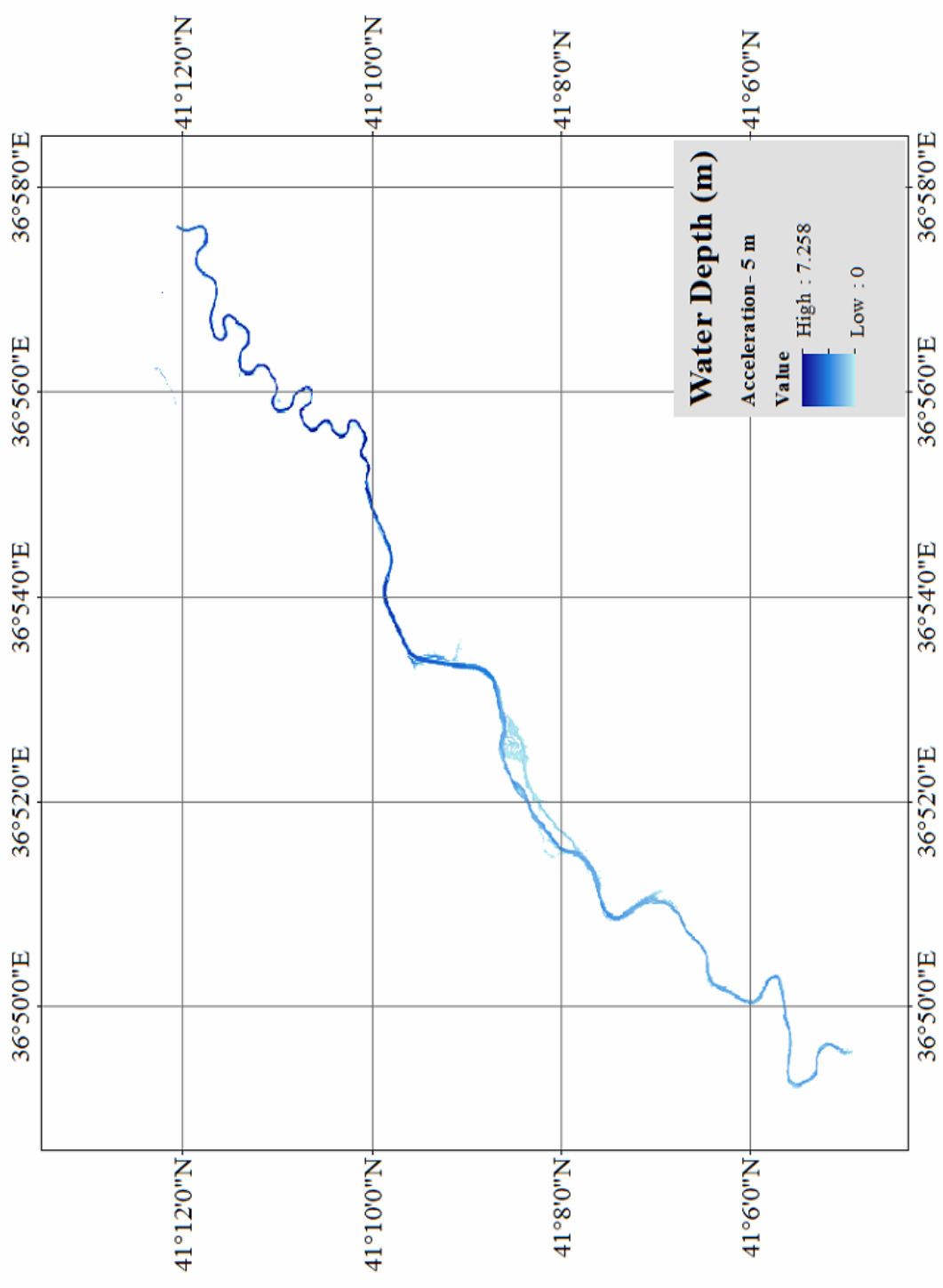

Figure 0-15 Acceleration Solver Results for n=0,035 on whole domain with 5 m spatial resolution

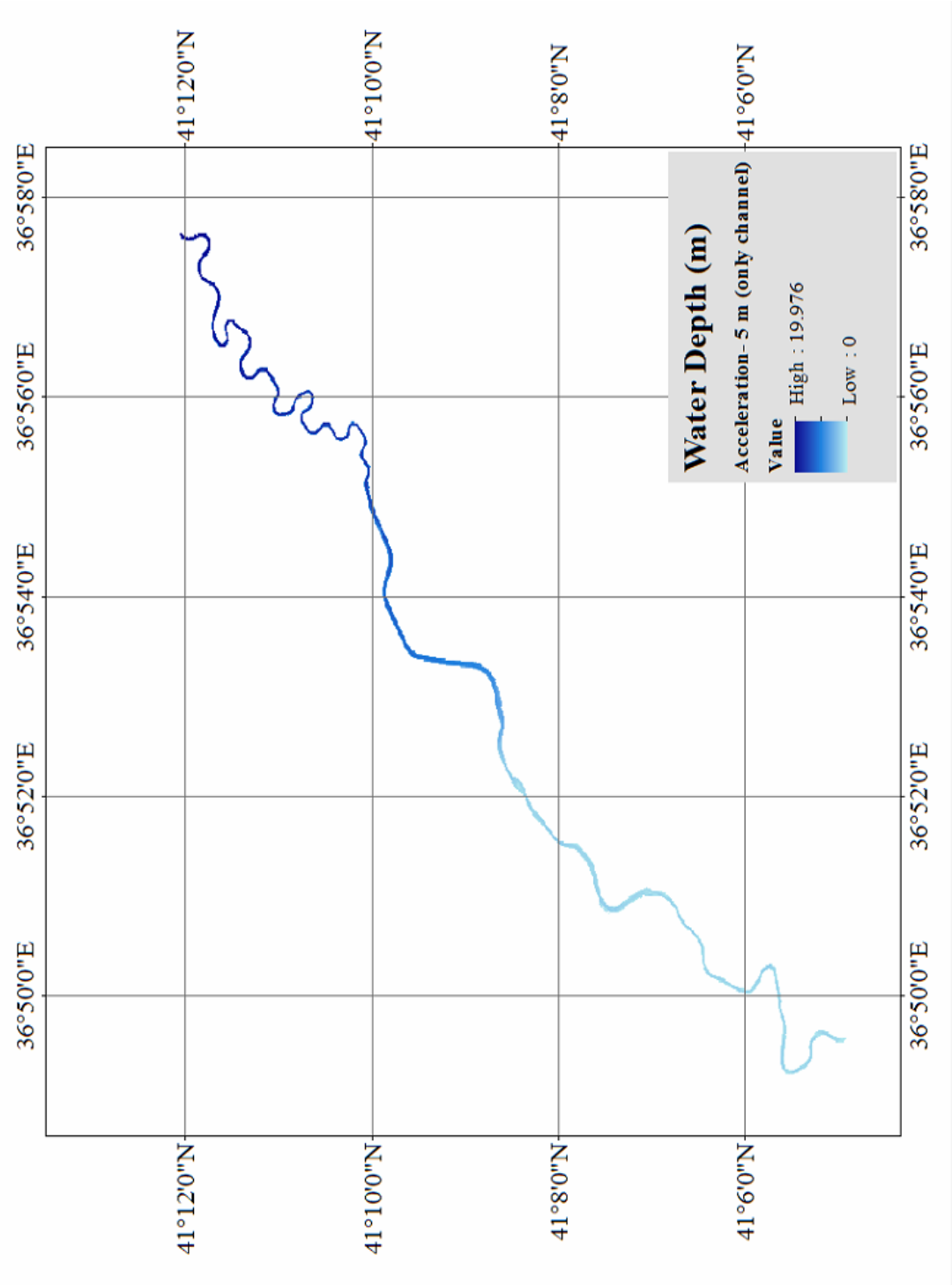

Figure 0-16 Acceleration Solver Results for only channel for n=0,035 with 5 m spatial resolution